

THE UNIVERSITY OF MICHIGAN
INDUSTRY PROGRAM OF THE COLLEGE OF ENGINEERING

A BOUNDARY-LAYER ANALYSIS OF HEAT AND MASS TRANSFER
IN FREE CONVECTION AROUND HORIZONTAL, CYLINDRICAL BODIES

Dudley A. Saville

A dissertation submitted in partial fulfillment
of the requirements for the degree of
Doctor of Philosophy in the
University of Michigan
Department of Chemical and Metallurgical Engineering
1965

January, 1966
IP-725

Doctoral Committee:

Professor Stuart W. Churchill, Chairman
Assistant Professor Brice Carnahan
Assistant Professor Joe D. Goddard
Associate Professor William P. Graebel
Assistant Professor James O. Wilkes

To My Wife and Parents

"Enfin, lorsque la chaleur pénètre les masses fluides et y détermine des mouvements intérieurs, par les changements continuels de température et de densité de chaque molécule, peut-on encore exprimer par des équations différentielles les lois d'un effect aussi composé; et quel changement en résulte-t-il dans les équations généraux de l'Hydro-dynamique?"

J. B. J. Fourier, "Theorie Analytique de la Chaleur",
"Oeuvres de Fourier", Tome Premier, ed. Gaston Darboux,
Gauthier-Villars et Fils, Paris (1888)

ACKNOWLEDGEMENTS

The author takes this opportunity to thank the members of his Doctoral Committee and its Chairman, Professor S. W. Churchill, for their encouragement and assistance throughout the course of this research. Thanks are also due to the Diamond Alkali Company for financial assistance, in the form of a fellowship, during the summer of 1965.

TABLE OF CONTENTS

	<u>Page</u>
ACKNOWLEDGMENT	iv
LIST OF TABLES	vii
LIST OF FIGURES	viii
LIST OF APPENDICES	ix
NOMENCLATURE	x
ABSTRACT	xvi
CHAPTER	
1. Introduction	1
2. Mathematical Models	4
2.1 Problem Statement	4
2.2 Mathematical Model of Free Convection in Curvilinear Coordinates	13
2.3 A Boundary-Layer Model	21
2.4 The Boundary-Layer Model in Series Form	28
2.5 Special Cases of the Principal Function	36
2.6 Behavior of Dependent Variables Near Stagnation Points	39
3. Numerical Solutions	43
3.1 Comparison of Theoretical and Experimental Results	43
3.2 The Effects of Schmidt and Prandtl Numbers, the First-Order Terms, the Body Class	53
3.3 Simultaneous Heat and Mass Transfer and the Effects of Interfacial Velocity and Heat Capacity (Ackermann Effect)	60
4. Asymptotic Solutions	63
4.1 General Observations	63
4.2 Asymptotic Solutions for Lewis Number = 1	65
4.3 Asymptotic Solutions for Large Schmidt Numbers and Small Prandtl Numbers	79
4.4 Asymptotic Solutions for Large Schmidt and Prandtl Numbers	82

TABLE OF CONTENTS (Cont'd)

	<u>Page</u>
5. Final Remarks	89
APPENDICES	92
BIBLIOGRAPHY	118

LIST OF TABLES

<u>Table</u>		<u>Page</u>
I	Comparison of Average Nusselt Numbers Determined by Jodlbauer with the Predictions of Boundary-Layer Theory, ($Pr = .7$)	51
II	Comparison of Local Sherwood Numbers Determined by Schütz with the Predictions of Boundary-Layer Theory, ($Sc = 1763$)	52
III	Derivatives of the Stream and Temperature Functions at the Surface for Temperature-Driven Free Convection Around Blunt-Nosed Objects	54
IV	"First Order Corrections" to the Nusselt Number and Surface Shear Stress (Circular Cylinder)	58
V	The Effects of the Body-Shape Class	60
VI	The Effects of the Interfacial Velocity Parameter, B, and the Ackermann Parameter, A, for Free Convection Around Blunt-Nosed Bodies ($Pr = Sc$).....	61
VII	Approximate Solutions for Large Schmidt and Prandtl Numbers	85
VIII	Functional Behavior of the Shear Stress, \mathcal{T} , the Nusselt Number, Nu , and the Sherwood Number, Sh	86
IX	Scaled Tangential Coordinate, ξ , for $S(x) = \sin(x)$	99
X	The Effects of Step Size and "Infinity" on the Characteristic Values for the Zero-Order Terms	110
XI	Summary of the Parameters in the Tabulated Results	111

LIST OF FIGURES

<u>Figure</u>		<u>Page</u>
1	Arc Length Parameters and Body-Force Components: Bodies with Convex Surfaces.....	15
2	Arc Length Parameters and Body-Force Components: Bodies with Concave Surfaces.....	16
3	Expansion Coefficient/Characteristic Driving Force Sign Combinations.....	20
4	Dependent Variable Behavior Near a Sharp Nose.....	40
5	Temperature-Driven Free Convection Around a Horizontal, Circular Cylinder. Dimensionless Tangential Velocity - Dimensionless Normal Distance at 30° from the Lower Stagnation Point.....	45
6	Temperature-Driven Free Convection Around a Horizontal, Circular Cylinder. Dimensionless Temperature - Dimensionless Normal Distance at 30° from the Lower Stagnation Point.....	46
7	Temperature-Driven Free Convection Around a Horizontal, Circular Cylinder. Dimensionless Tangential Velocity - Dimensionless Normal Distance at 90° from the Lower Stagnation Point.....	47
8	Temperature-Driven Free Convection Around a Horizontal, Circular Cylinder. Dimensionless Temperature - Dimensionless Normal Distance at 90° from the Lower Stagnation Point.....	48
9	Temperature-Driven Free Convection Around a Horizontal, Circular Cylinder. Dimensionless Tangential Velocity - Dimensionless Normal Distance at 150° from the Lower Stagnation Point.....	49
10	Temperature-Driven Free Convection Around a Horizontal, Circular Cylinder. Dimensionless Temperature - Dimensionless Normal Distance at 150° from the Lower Stagnation Point.....	50
11	Derivatives of the Zero- and First-Order Stream Functions: Blunt-Nosed Bodies.....	55
12	Zero- and First-Order Temperature Functions: Blunt-Nosed Bodies.....	56

LIST OF APPENDICES

<u>Appendix</u>		<u>Page</u>
A	Expansions for the Scaled Tangential Coordinate and the Principal Function	93
B	Numerical Techniques and Computer Programs	100
C	Numerical Results	109

NOMENCLATURE

The principal symbols are defined in this table. All of the symbols are defined in the text. Those symbols having only temporary significance are not given here. The equation numbers refer either to the definition of the term or to the first instance of its use.

<u>English Letters</u>	<u>Definition</u>
A	Ackermann coefficient, Eqn. (2.36) $= (C_{PA\infty} - C_{PB\infty}) \Delta\omega / C_{P\infty}$
B	Interfacial velocity parameter, Eqn. (2.36) $= \Delta\omega / (1 - \omega_s)$
$C_{P\infty}$	Characteristic heat capacity of fluid, Eqn. (2.5)
$C_{PA\infty}$	Heat capacity of the species undergoing transfer, Eqn. (2.5)
$C_{PB\infty}$	Heat capacity of the "stagnant" species, Eqn. (2.5)
D_{∞}	Mass diffusivity characteristic of the fluid
F	Stream function in the "transformed" coordinate system, Eqns. (2.67)
F_0, F_1	Zero and first order stream functions Eqns. (2.75) and (2.76)
ψ_i, ψ_o	"Inner" and "outer" stream functions, Secs. 4.2 and 4.3
G	Large Parameter, Eqn. (2.42) $= gL^3 / \nu_{\infty}^2$

English LettersDefinition

G_r	Grashof number, Eqns. (2.56) and (2.57), $= G\beta \Delta Q$ for $ \beta \Delta Q \geq \gamma \Delta \omega $, otherwise $= G\gamma \Delta \omega$
\vec{g}, g	Body force vector (gravity in the usual case) and the magnitude of \vec{g} , Eqn. (2.4)
\bar{H}_A, \bar{H}_B	Partial specific enthalpies of the species being transferred and the "stagnant" species, Eqns. (2.5) and (2.6)
\vec{J}_A	Mass flux density vector, Eqn. (2.17)
\tilde{K}, K	Curvature and dimensionless curvature, Eqn. (2.21)
L, \tilde{L}	Reference length, Eqn. (2.25); length, Eqn. (2.61)
M	Dimensionless mass concentration function, Eqn. (2.67) $= (\omega - \omega_\infty) / (\omega_s - \omega_\infty)$
M_0, M_1	Zero and first order mass concentration functions, Eqns. (2.75) and (2.76)
\tilde{m}_i, \tilde{m}_o	"Inner" and "outer" mass concentration functions, Secs. 4.2 and 4.3
Nu, \bar{Nu}	Local and mean Nusselt numbers, Eqns. (2.60) and (2.61)
O	Order symbol, See Sec. 4.1
p, p'	Local pressure, Eqn. (2.4), "dynamic pressure," Eqn. (2.10)
Pr	Prandtl number, Eqn. (2.35) $= \nu_\infty / \alpha_\infty$

English LettersDefinition

Sc	Schmidt number, Eqn. (2.35) $= \nu_{\infty} / D_{\infty}$
Sh, \bar{Sh}	Local and mean Sherwood numbers, Eqns. (2.62) and (2.63)
$S(x)$	Sine of the angle between the normal to the surface and the body force vector, Eqn. (2.49)
T	Dimensionless temperature, Eqn. (2.67) $= (\theta - \theta_{\infty}) / (\theta_s - \theta_{\infty})$
T_0, T_1	Zero and first order temperature functions, Eqns. (2.75) and (2.76)
$t_i^{\omega}, t_o^{\omega}$	"Inner" and "outer" temperature functions, Secs. 4.2 and 4.3
\tilde{U}	Local velocity in the tangential direction, Eqn. (2.26)
\vec{V}	Local velocity vector, Eqn. (2.1)
\vec{V}_A, \vec{V}_B	Local velocities of species "A" and "B" Eqn. (2.16)
\tilde{V}	Local velocity in the normal direction, Eqn. (2.26)
\vec{W}	Vector defined by Eqn. (2.28)
\tilde{x}, x	Distance tangent to the surface, Figs. 1 and 2, dimensionless distance, Eqn. (2.25), ($x = \tilde{x} / L$)
\tilde{y}, y'	Distance normal to the surface, Figs. 1 and 2, dimensionless distance, Eqn. (2.25), ($y' = \tilde{y} / L$)

English LettersDefinition

y Stretched boundary layer coordinate, Eqn. (2.45)
 $y = y' G^{1/4}$

\bar{z} A complex variable, Eqn. (A1)

Greek Letters

α_∞ Thermal diffusivity of the fluid, Eqn. (2.3)

β Temperature coefficient of expansion of the fluid
 Eqn. (2.8)

δ Concentration coefficient of expansion of the
 fluid, Eqn. (2.9)

$\Delta\theta, \Delta\omega$ Characteristic temperature difference, $(\theta_s - \theta_\infty)$,
 Eqn. (2.34), characteristic concentration dif-
 ference, $(\omega_s - \omega_\infty)$, Eqn. (2.34)

Θ Dimensionless temperature, Eqn. (2.32)
 $= (\theta - \theta_\infty) / (\theta_s - \theta_\infty)$

$\theta, \theta_s, \theta_\infty$ Local temperature, surface temperature,
 temperature far from the object, Eqns. (2.3) and
 (2.7)

η Transformed normal distance, Eqn. (2.66)

$K(\xi), K_0, K_1$ Principal function, Eqn. (2.71), first and second
 coefficients in the expansion of the principal
 function; (see Appendix A).

μ_∞ Viscosity of the fluid, Eqn. (2.64)

Greek LettersDefinition

ξ	Transformed tangential distance, Eqn. (2.66)
π	"Pi" 3.14159...
ρ, ρ_∞	Local density of the fluid, density of the fluid far from the object, Eqns. (2.4) and (2.7)
σ, σ_m	Ratios defined by Eqns. (2.56) and (2.57)
$\tau, \bar{\tau}$	Local dimensionless shear stress and average dimensionless shear stress, Eqns. (2.64) and (2.65)
ϕ	Angle between a horizontal line and a line tangent to the surface, Eqn. (2.21)
Ψ	Stream function, Eqn. (2.26)
ψ	Boundary layer stream function, Eqn. (2.42)
Ω	Dimensionless mass concentration function, Eqn. (2.33) $= (\omega - \omega_\infty) / (\omega_s - \omega_\infty)$
$\omega, \omega_s, \omega_\infty$	Local mass fraction variable, mass fraction variable at the surface, mass fraction variable far from the surface, Eqns. (2.3) and (2.17)

Operators and other Symbols

$\tilde{\nabla}$	Gradient operator
$\tilde{\nabla} \cdot$	Divergence operator
$\tilde{\nabla}^2$	Laplacian operator
$\tilde{\nabla} \times$	Curl operator
$(\vec{\tau}) \cdot (\vec{\tau})$	Scalar or "dot" product

Operators and
other Symbols

Definition

$(\vec{}) \times (\vec{})$

Vector or "cross" product

$\stackrel{d}{=}$

means "is defined as"

\sim

means "...is asymptotic to..."

\rightarrow

means "...approaches..."

ABSTRACT

The laminar boundary-layer description of planar, free-convection around cylindrical bodies is examined for arbitrary body contours. The flow is a result of temperature and/or concentration differences between the surface of the object and the fluid. Dilute, binary systems are studied. For a body with an outer surface maintained at a uniform temperature and a uniform concentration of the species undergoing transfer, it is possible to treat a number of combinations of the "driving forces" and coefficients of expansion. With transformations suggested by analogy with the work of Goertler on forced convection, new series representations of the dependent boundary-layer variables, viz., temperature, concentration and velocity, are developed. The ordinary differential equations which determine the functions in these series are independent of the body contour. Instead, some of the numerical coefficients in the differential equations are fixed by the class of the body shape; e.g., sharp-nosed, blunt-nosed, or flat-nosed. Hence, the solutions for a particular class of body shapes may be obtained once and for all for fixed values of the dimensionless parameters appearing in the problem. The body contour enters the problem only when the series are assembled. The series are found to converge rapidly for the class of blunt-nosed bodies, one term in each series (the zero-order term), being sufficient to represent the heat-flux density at the surface. The accuracies of the one-term representations are determined by

comparing the numerical solutions with experimental data and by calculating the corrections given by the first-order terms.

Free convection around blunt-nosed bodies is described for several Prandtl numbers between .01 and 1763. by the numerical solutions to the zero-order equations. The description of free convection around sharp-nosed bodies can be obtained from the numerical solutions of Ostrach for the vertical plate, when his results are interpreted in terms of the present theory.

The effects of the body-shape class are investigated at Prandtl numbers of .01, 1. and 1000. The differences due to class are found to be small. The effect of the normal velocity, which is due to mass transfer at the fluid-solid boundary, is investigated, as is the effect of a difference between the heat capacity of the species undergoing transfer and the heat capacity of the fluid.

Asymptotic forms of the differential equations are used to find the flux densities and the shear stress at the surface for:

(i) equal Prandtl and Schmidt numbers, (ii) low Prandtl but high Schmidt numbers, and (iii) high Schmidt and Prandtl numbers, for free convection driven by both temperature and concentration differences. Explicit formulae are given for the determination of the heat- and mass-flux densities and the shear stress at the surface of the object.

CHAPTER 1

Introduction

A fluid motion is termed free or natural convection when the motion is due solely to the interaction between body forces (such as that of gravity) and local density variations in the fluid. These local density variations may be the result of temperature and/or composition variations. The study of transport processes in such a flow field is naturally complicated by interactions between the transport processes. This situation is in sharp contrast to the study of heat and/or mass transport in forced convection. There, the flow field is usually known a priori and interactions are frequently negligible.

Much of the study of thermal, free-convection phenomena has been directed towards describing flow and heat transfer near vertical plates and cylinders, horizontal cylinders, and spheres. Some recent work has also been done towards finding body shapes for which the differential equations describing the phenomena can be reduced to ordinary differential equations (Ostrach⁽²³⁾). This naturally results in a considerable reduction in the effort required to obtain relations between the quantities of interest. The use of boundary-layer theory, in connection with laminar, free convection around submerged objects, leads to the very useful result (which may be obtained without actually solving the equations), that for a given body and fluid the rate of heat transfer is proportional to the Grashof number raised to the quarter power. Inspection of asymptotic

forms of the boundary-layer description also leads to the conclusion that the proportionality factor, which depends on the body shape and the properties of the fluid as characterized by the Prandtl number, varies as the square root of the Prandtl number as the Prandtl number tends to zero. On the other hand, the proportionality factor varies as the quarter power of the Prandtl number as the Prandtl number tends to an infinitely large value. Concentration-driven free convection differs from its temperature-driven counterpart mainly due to the presence of an interfacial velocity at the solid-fluid boundary. This velocity destroys the similarity between these two flows. Acrivos⁽¹⁾ has recently analyzed the effect of this condition on the rate of mass transfer.

In view of the previous discussion, it is apparent that there are two general areas wherein a lack of understanding and description exists. They are in the areas of: (i) effects due to body shape, and (ii) effects due to interaction between the heat- and mass-transfer processes. Some work has been done in both these areas and will be mentioned later.

This research is directed towards a description of free convection driven by both temperature and concentration, with particular attention to the problem of body shape. The boundary-layer description of two-dimensional, planar flows around solid objects is developed in Chapter 2. The submerged object has a temperature and/or concentration differing from that of the fluid far from the object.

Dilute, two-component fluids are considered. The motion is assumed to be steady. A transformation, similar to that used by Goertler⁽¹²⁾ for studies of two-dimensional, forced convection, boundary layers, is used to develop series expansions for the stream, temperature and concentration functions. In Chapter 3 some numerical solutions for the first two terms in the expansions are given. These results are compared with experimental data taken from the literature. It is shown that the use of the transformation essentially eliminates the body shape variable from direct consideration in the solution of the differential equations. Chapter 4 is devoted to some asymptotic solutions for extreme values of the Schmidt and Prandtl numbers, which appear as parameters in the differential equations. The final chapter, number 5, summarizes the research and suggests possible extensions.

CHAPTER 2

Mathematical Models

2.1 Problem Statement

Free convection, resulting from temperature-induced density differences, has been the subject of theoretical and experimental studies for over a century. Two early investigators were Dulong and Petit (as cited by Ede⁽⁹⁾), who studied the cooling of spheres in 1817. A comprehensive survey of research on free convection near vertical surfaces has been made by Ede⁽⁹⁾. A flow driven by concentration-induced density differences is mentioned in a review by Schmidt⁽²⁷⁾. Ostrach⁽²³⁾ has recently presented an extensive summary of free-convection research. These reviews obviate the need for a general review of free convection here, so reference to reports in the literature will be made only in connection with specific aspects of the work.

Somers⁽²⁹⁾ studied free convection near a vertical plate when the density of the fluid depended on temperature and concentration. However, his theory is limited by restricting the Schmidt and Prandtl numbers to be almost equal. Furthermore, the so-called integral forms of the boundary-layer equations were used with assumed velocity, temperature and concentration profiles. Somers indicated that concentration and temperature effects are not strictly additive.

Gil, del Casal and Zeh⁽¹¹⁾ and Sparrow, Minkowycz and Eckert⁽³⁰⁾ report theoretical work on free convection due to the

combined effects of temperature and concentration. Gill et al studied the effects due to temperature- and concentration-dependent physical properties for hydrogen-air, helium-air, water vapor-air, and carbon dioxide-air mixtures. The flow was that near a vertical plate. For the carbon dioxide-air system fluid-property effects were almost absent. By way of contrast, in hydrogen-air and helium-air systems the assumption of constant physical properties resulted in errors of about 10 per cent, while for the water vapor-air system the error was about 50 per cent. All of these discrepancies depended on the concentration of the "diffusing species" and diminished with decreasing concentration. Sparrow, et al studied free convection near a stagnation point on a curved surface in the helium-air system. In addition to accounting for property changes due to temperature and composition, both the Dufour effect (transport of energy due to composition gradients) and the Soret effect (transport of mass due to temperature gradients) were included. Their conclusion was that these "coupling effects" may be appreciable for low molecular weight materials when the concentration of the diffusing species is high.

These investigations point out, via the "case study method," that property variations and coupling can be important factors in particular situations. However, the studies do not, due to their nature, furnish information about the effects of changes in the average fluid properties, as characterized by the Schmidt and Prandtl numbers.

In the present study a description of free convection will be developed which accounts for the effects of body shape, average fluid properties and interactions between the heat and mass transport processes as they affect the density of the fluid. Such a description, in which the major features of the phenomena are retained, while local property variations and coupling are suppressed, is felt to be of value. Firstly, because these latter effects are of secondary importance in many instances. Secondly, such an idealized model can be used as a basis for comparison. Finally, because of its simplicity such a model enables one to study free convection without the restriction of a particular type of fluid property behavior.

Two main classes of planar, free convection will be examined. The two classes represent flows around two types of symmetrical bodies, "sharp-" and "blunt-nosed"; e.g., wedges and parabolae. By considering these classes of body shapes it will prove possible to develop rather general methods for describing the flow, within the framework of boundary-layer theory.

In each instance the body is assumed to be immersed in a large body of fluid, which is taken to be of infinite extent, and which has no motion imposed on it except that brought on by the non-uniform density field. The surface of the object is kept at a temperature level different from that in the fluid far from the object - the object is a source or sink for thermal energy. Similar boundary conditions are imposed on the concentration of a single chemical species. Hence, the surface of the body either loses or gains energy

and/or material by transfer to or from the fluid. It is further specified that there is no forced injection or removal of material through the surface of the object. Since the surface of the object and the fluid far from the object are at different levels of temperature and concentration, transport causes temperature and concentration variations throughout the fluid which give rise to spatial density variations. In each class of flows the axis of symmetry of the object is assumed to be parallel to the "body force" vector. Hereafter the use of "body force" will refer to volumetric forces acting on the fluid. Gravity will be the only body force considered but the results can easily be extended to any body force which can be expressed in terms of a linear potential function.

Now, the interaction between gravity and density causes the fluid to move. Hence, the transport processes within the fluid are convection (bulk transport) and diffusion (molecular transport). The motion is assumed to be in a steady state. This latter restriction rules out any consideration of turbulent motions. The problem now is to describe this flow, in particular the local velocity, temperature and concentration, from which the rates of transport between the object and the fluid can be determined.

In the following chapters certain simplifying assumptions will be made. In general, these assumptions will be noted but in the interest of brevity certain obvious ones will not be mentioned. Furthermore, the description will not be developed from first principles. Rather, a familiar description will be selected as a starting

point. For a detailed development of the equations of change the reader is referred to the treatise of Bird, Stewart and Lightfoot⁽³⁾ or a paper by Merk.⁽²⁰⁾ The model is based on a Newtonian fluid, with Fourier's and Fick's laws governing the molecular fluxes of heat and mass. The couplings between temperature and concentration gradients, in the forms of the Dufor and Soret effects, are neglected. Within the framework of the theory to be presented, which requires small "driving forces," these effects are expected to be small. The effects of composition, temperature and pressure on the properties of the fluid, excepting density in the body force terms in the equations of motion, viscous dissipation of energy, and compression are all neglected. The assumption of constant properties has been formally justified by Ostrach⁽²²⁾ and by Hellums and Churchill⁽¹³⁾ for the case of temperature-driven free convection. In this latter instance the justification is based on the fact that the product of the coefficient of thermal expansion, β , and the characteristic temperature difference, , is small. The results of the constant property assumption may be viewed as the zeroth approximation in a parameter perturbation in the quantity $\beta\Delta\Theta$. Ostrach also shows that, within the framework of this approximation, viscous dissipation of energy may be neglected. Hence, for flows driven by temperature and composition effects both $\beta\Delta\Theta$ and $\delta\Delta\omega$, where δ is the coefficient of expansion due to concentration changes and $\Delta\omega$ is the characteristic concentration difference, must be small. For the very low speeds found in free convection the effects of compression in the energy equation can be neglected (Schlichting⁽²⁵⁾, p. 292).

These assumptions lead to the following mathematical model for free convection in a two-component, non-reacting system. The continuity equation,

$$\tilde{\nabla} \cdot \vec{V} = 0 \quad (2.1).$$

The conservation equation for one of the two species present,

$$\vec{\nabla} \cdot \vec{\nabla} \omega = \mathcal{D}_\infty \nabla^2 \omega \quad (2.2).$$

The conservation equation for thermal energy,

$$\vec{\nabla} \cdot \vec{\nabla} \Theta = \alpha_\infty \nabla^2 \Theta - \frac{\mathcal{D}_\infty}{C_{P_\infty}} \vec{\nabla} \omega \cdot \vec{\nabla} (\bar{H}_A - \bar{H}_B) \quad (2.3).$$

The equation of motion,

$$\vec{\nabla} \cdot \vec{\nabla} \vec{V} = - \frac{1}{\rho_\infty} \vec{\nabla} P + \frac{\rho}{\rho_\infty} \vec{g} + \nu_\infty \nabla^2 \vec{V} \quad (2.4).$$

The operators have their usual meanings; the tilde implies that the operator is not dimensionless. \mathcal{D}_∞ , α_∞ , C_{P_∞} , ρ_∞ , ν_∞ are, respectively, the mass diffusivity, thermal diffusivity, heat capacity, density and kinematic viscosity, which are characteristic of the fluid. \vec{V} is the local velocity vector, ω , the local mass fraction of the species which is being transferred to or from the solid (A, say), Θ , the local temperature, P , the local pressure, ρ , the local density and \vec{g} , the body force vector (gravity). The second term on the right-hand side of equation (2.3) represents the so-called Ackermann effect (Merk⁽²⁰⁾), which is an energy transport effect due to diffusion. \bar{H}_A and \bar{H}_B are the partial specific enthalpies (units of energy per unit mass) of species A and the "stagnant" species (B, say). For

"perfect" or more generally "athermal" solutions, wherein there are no heat effects due to mixing, \bar{H}_A and \bar{H}_B are independent of composition (Denbigh⁽⁸⁾). This is the type of solution considered in this research.

Now, over small temperature ranges it can further be assumed that $\bar{H}_A = C_{PA\infty} (\Theta - \Theta_\infty)$ and $\bar{H}_B = C_{PB\infty} (\Theta - \Theta_\infty)$, where $C_{PA\infty}$ and $C_{PB\infty}$ are the heat capacities per unit mass for species A and B at the temperature Θ_∞ , a reference temperature. Hence,

$$\bar{H}_A - \bar{H}_B = (C_{PA\infty} - C_{PB\infty}) (\Theta - \Theta_\infty) \quad (2.5),$$

and

$$\tilde{\nabla} (\bar{H}_A - \bar{H}_B) = (C_{PA\infty} - C_{PB\infty}) \tilde{\nabla} \Theta \quad (2.6).$$

The model is as yet incomplete, there are four equations and five unknowns. The final relation is the equation of state, which, under the restrictions previously noted, takes the following form:

$$P = P_\infty [1 - \beta (\Theta - \Theta_\infty) - \gamma (\omega - \omega_\infty)] \quad (2.7).$$

Here, β and γ are:

$$\beta \doteq -\frac{1}{P_\infty} \left[\frac{\partial P}{\partial \Theta} \right]_{\substack{\Theta = \Theta_\infty \\ \omega = \omega_\infty}} \quad (2.8),$$

and

$$\gamma \doteq -\frac{1}{P_\infty} \left[\frac{\partial P}{\partial \omega} \right]_{\substack{\Theta = \Theta_\infty \\ \omega = \omega_\infty}} \quad (2.9).$$

The coefficients β and γ are treated as constants, and ω_∞ is a reference concentration.

It is convenient to introduce a dynamic pressure, P' , defined as

$$\tilde{\nabla} P = \rho_\infty \vec{g} + \tilde{\nabla} P' \quad (2.10).$$

The dynamic pressure relation and the equation of state are now substituted into the equations of motion to yield

$$\tilde{\nabla} \cdot \tilde{\nabla} \vec{V} = -\frac{1}{\rho_\infty} \tilde{\nabla} P' - \beta(\theta - \theta_\infty) \vec{g} - \gamma(\omega - \omega_\infty) \vec{g} + \nu_\infty \tilde{\nabla}^2 \vec{V} \quad (2.11).$$

Using the identity

$$\tilde{\nabla} \cdot \tilde{\nabla} \vec{V} = \frac{1}{2} \tilde{\nabla}(\tilde{\nabla} \cdot \vec{V}) - \tilde{\nabla}_x \tilde{\nabla}_x \vec{V} \quad (2.12),$$

one finds

$$\frac{1}{2} \tilde{\nabla}(\tilde{\nabla} \cdot \vec{V}) - \tilde{\nabla}_x \tilde{\nabla}_x \vec{V} = -\frac{1}{\rho_\infty} \tilde{\nabla} P' - \beta(\theta - \theta_\infty) \vec{g} - \gamma(\omega - \omega_\infty) \vec{g} + \nu_\infty \tilde{\nabla}^2 \vec{V} \quad (2.13).$$

Subsequent application of the "curl operator," $\tilde{\nabla}_x$, to Equation (2.13) results in

$$\tilde{\nabla} \cdot \tilde{\nabla} \vec{W} = -\beta \tilde{\nabla} \theta_x \vec{g} - \gamma \tilde{\nabla} \omega_x \vec{g} + \nu_\infty \tilde{\nabla}^2 \vec{W} \quad (2.14),$$

where

$$\vec{W} = \tilde{\nabla}_x \vec{V} \quad (2.15).$$

Note that the various mathematical operations which have been used to remove the pressure variable have increased the order of the system.

The boundary conditions are taken as follows.

(a) At the interface between the surface of the object and the fluid, the temperature is constant at Θ_s and the mass fraction of the species undergoing transfer is constant at ω_s . The velocity in the direction tangent to the surface is zero. However, the velocity in the direction normal to the surface is not zero due to a flux of species A. To develop a condition for the normal component of velocity let the mass flux density (mass/area/time) of A relative to the mass average velocity be \vec{J}_A . Now the mass average velocity is defined by

$$\vec{V} = \omega \vec{V}_A + (1 - \omega) \vec{V}_B \quad (2.16),$$

where \vec{V}_A and \vec{V}_B are the velocities of species A and B, and ω is the mass fraction of A. From Fick's law

$$\vec{J}_A = -\rho \mathcal{D}_\infty \vec{\nabla} \omega \quad (2.17),$$

where \mathcal{D}_∞ is the diffusion coefficient. Now,

$$\vec{J}_A = \rho \omega (\vec{V}_A - \vec{V}) \quad (2.18)$$

and at the surface $\vec{V}_B = 0$, so that

$$\vec{J}_A = \rho \vec{V} (1 - \omega_s) \quad (2.19).$$

Hence, at the surface,

$$\vec{V} = -\frac{1}{1 - \omega_s} \mathcal{D}_\infty \vec{\nabla} \omega \quad (2.20).$$

Along the extension of the plane of symmetry of the body, parallel to the body force vector, the velocity normal to the extension is zero and the gradients of temperature and concentration normal to the extension are zero; i.e., symmetry extends into the fluid.

(b) Far from the object and the plane of symmetry, temperature and concentration approach the values Θ_∞ and ω_∞ . Hence, the reference state is that of the fluid far from the object. The condition placed on the velocity far from the object has been inferred from the experimental data of Schmidt and Beckmann⁽²⁶⁾ and Jodlbauer⁽¹⁵⁾. It is that the velocity parallel to a tangent to the body is zero. This condition will suffice for the boundary-layer theory that will follow.

It is to be noted that for closed bodies, e.g., cylinders, nothing has been said about the plume (a column of fluid) which rises above or falls below the object. In what follows the plume is to be completely ignored and, as a result, the theory may be invalid in the region of the plume. Furthermore, since the plume may affect the rest of the flow, the theory must be substantiated by appeals to experiments or to a more complete theory.

2.2 Mathematical Model of Free Convection in Curvilinear Coordinates

The mathematical model described in the previous section is specialized by choosing a particular coordinate system, which is intimately connected with the geometry of the immersed object. The coordinate system is an orthogonal, curvilinear system based on distances measured along the surface from an intersection of the plane

of symmetry with the surface of the body and on distances measured normal to the surface. The curvilinear coordinate system, the various operators, the body force vector, and the velocity vector are developed next in terms of this coordinate system. The geometries for each of the two classes of flows to be studied are given in Figures 1 and 2.

Let \tilde{x} and \tilde{y} be the distances along and normal to the surface and ϕ the angle, measured in the clockwise direction, between a horizontal plane and the line tangent to the surface at \tilde{x}, \tilde{y} . The local curvature, \tilde{K} , is defined as

$$\tilde{K} \triangleq \frac{d\phi}{d\tilde{y}} \quad (2.21).$$

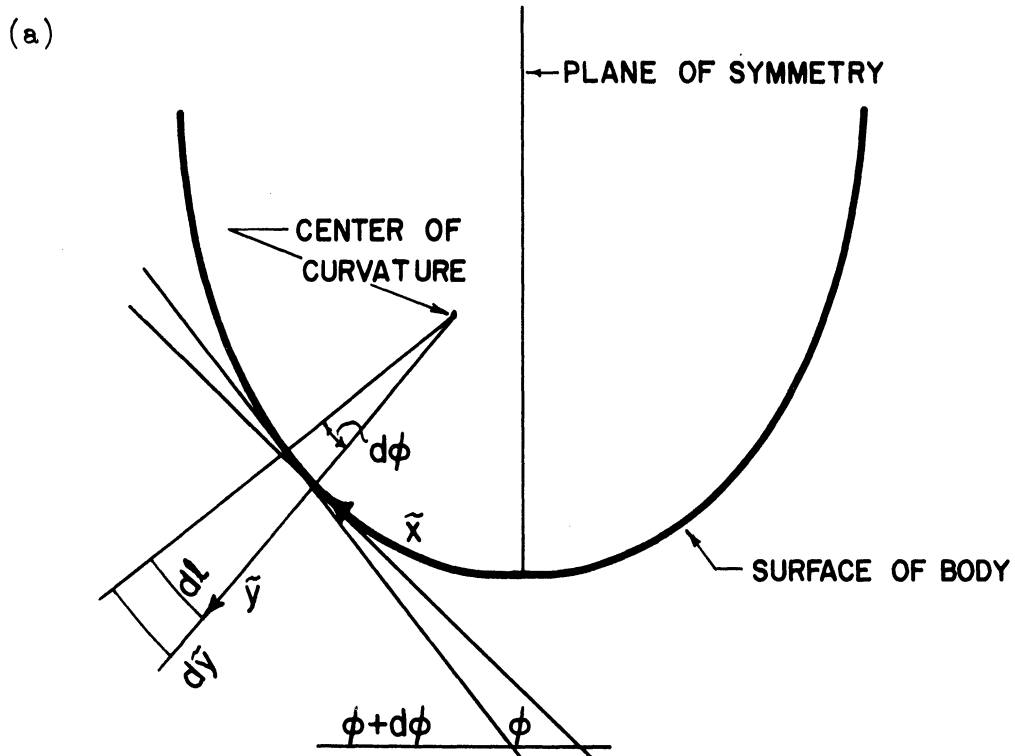
A differential area in the plane of \tilde{x} and \tilde{y} is then

$$dA = (1 + \tilde{K}\tilde{y}) d\tilde{x} d\tilde{y} \quad (2.22).$$

Hence, the arc length parameters or metrical coefficients are

$$h_{\tilde{x}} = 1 + \tilde{K}\tilde{y}, \quad h_{\tilde{y}} = 1 \quad (2.23).$$

For cusped-nosed bodies or for any concave body a unique coordinate system is defined only for points (\tilde{x}, \tilde{y}) within the region defined by the evolute (a curve traced by the center of curvature) and the surface of the body. Furthermore, it is apparent that for wedge-nosed bodies such a coordinate system is not defined upstream from the body, except in the case of a flat plate.



$$dl = (1/\tilde{K} + \tilde{y})d\phi = (1 + \tilde{K}\tilde{y})d\tilde{x} \quad , \quad dA = (1 + \tilde{K}\tilde{y})d\tilde{x}d\tilde{y} \quad , \quad h_x = 1 + \tilde{K}\tilde{y} \quad , \quad h_y = 1$$

(b)

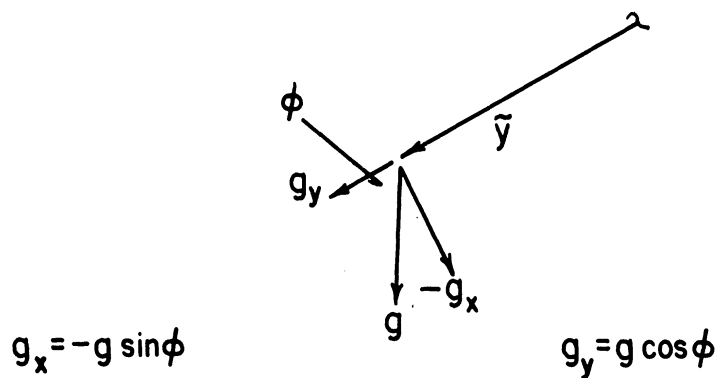
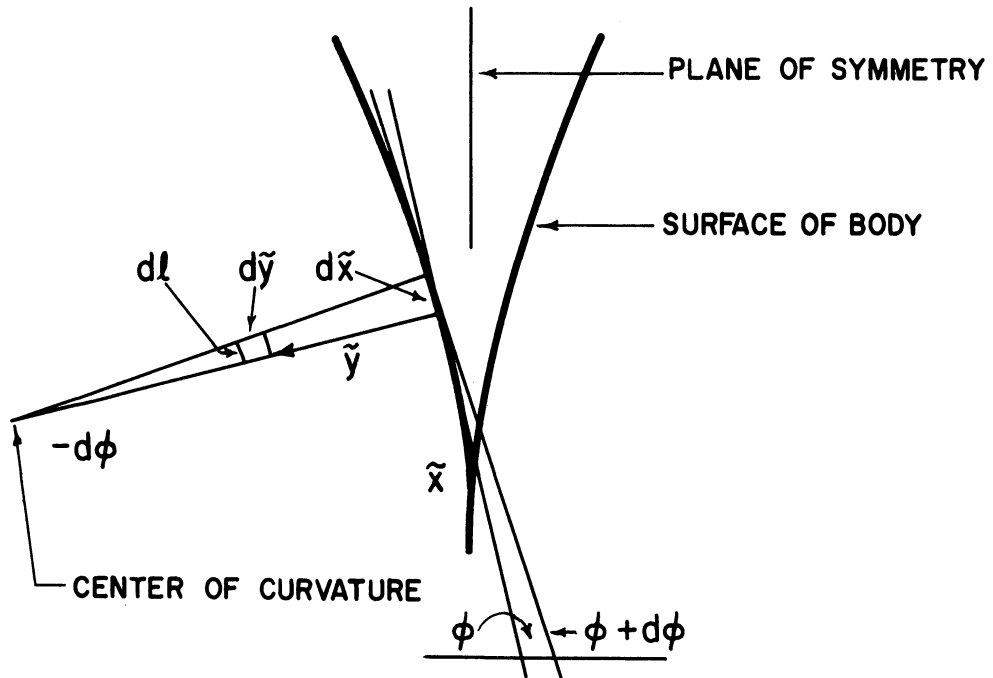


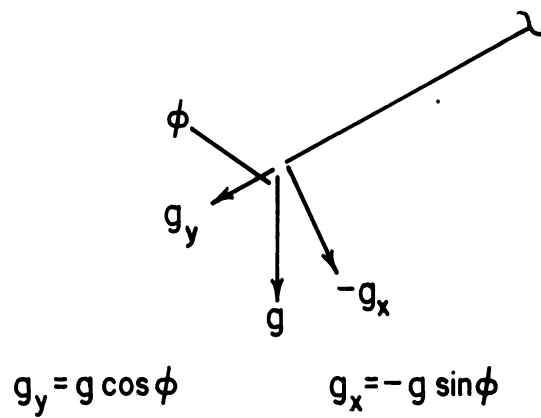
Figure 1. (a) Arc Length Parameters and (b) Body Force Components for Bodies with Convex Surfaces

(a)



$$dl = (1/\tilde{K} + \tilde{y})d\phi = (1 + \tilde{K}\tilde{y})d\tilde{x}, \quad dA = (1 + \tilde{K}\tilde{y})d\tilde{x}d\tilde{y}, \quad h_x = 1 + \tilde{K}\tilde{y}, \quad h_y = 1$$

(b)



$$g_y = g \cos \phi \qquad g_x = -g \sin \phi$$

Figure 2. (a) Arc Length Parameters and (b) Body Force Components for Bodies with Concave Surfaces

In the two-dimensional, curvilinear coordinate system the equation of continuity is

$$\nabla \cdot \vec{V} = \frac{1}{1+\tilde{K}\tilde{y}} \left[\frac{\partial \tilde{U}}{\partial \tilde{x}} + \frac{\partial}{\partial \tilde{y}} [(1+\tilde{K}\tilde{y})\tilde{V}] \right] \quad (2.24),$$

where \tilde{U} and \tilde{V} are the dimensional velocities in the \tilde{x} and \tilde{y} directions. The dimensionless coordinates x and y' and the dimensionless curvature K , are introduced by

$$x = \frac{\tilde{x}}{L}, \quad y' = \frac{\tilde{y}}{L}, \quad K = \tilde{K}L \quad (2.25),$$

where L is a characteristic length. The dimensionless stream function, Ψ , is introduced with

$$\tilde{U} = \frac{v_\infty}{L} \frac{\partial \Psi}{\partial y'}, \quad \tilde{V} = -\frac{v_\infty}{L(1+Ky)} \frac{\partial \Psi}{\partial x} \quad (2.26).$$

Then

$$\vec{W} = -\vec{k} \frac{v_\infty}{L^2} \frac{1}{1+Ky'} \left[\frac{\partial}{\partial x} \left[\frac{1}{1+Ky'} \frac{\partial \Psi}{\partial x} \right] + \frac{\partial}{\partial y'} \left[(1+Ky') \frac{\partial \Psi}{\partial y'} \right] \right] \quad (2.27)$$

or

$$\vec{W} = -\vec{k} \frac{v_\infty}{L^2} \nabla^2 \Psi \quad (2.28),$$

where \vec{k} is a unit vector normal to the plane of the flow and

∇^2 is the dimensionless Laplacian. Furthermore,

$$\vec{\nabla} \cdot \vec{\nabla} = \frac{v_\infty}{L^2} \frac{1}{1+Ky'} \left[\frac{\partial \Psi}{\partial y'} \frac{\partial}{\partial x} - \frac{\partial \Psi}{\partial x} \frac{\partial}{\partial y'} \right] \quad (2.29),$$

$$L^2 \vec{\nabla}^2 = \frac{1}{1+Ky'} \left[\frac{\partial}{\partial x} \left[\frac{1}{1+Ky'} \frac{\partial}{\partial x} \right] + \frac{\partial}{\partial y'} \left[(1+Ky') \frac{\partial}{\partial y'} \right] \right] \quad (2.30),$$

and

$$L \tilde{\nabla} = \nabla = \frac{\vec{i}}{1+Ky'} \frac{\partial}{\partial x} + \vec{j} \frac{\partial}{\partial y'} \quad (2.31)$$

where \vec{i} and \vec{j} are unit vectors in the x and y' directions.

Hence,

$$\tilde{\nabla} \Theta_x \vec{g} = \frac{\vec{k}}{L} g \left[\frac{\cos \phi}{1+Ky'} \frac{\partial \Theta}{\partial x} + \sin \phi \frac{\partial \Theta}{\partial y'} \right] \quad (2.32),$$

and similarly for $\tilde{\nabla} \omega_x \vec{g}$. Here, "g" is the magnitude of the vector \vec{g} . Now the dimensionless concentration and temperature are introduced as

$$\Omega \triangleq \frac{\omega - \omega_\infty}{\Delta \omega}, \quad \Theta \triangleq \frac{\Theta - \Theta_\infty}{\Delta \Theta} \quad (2.33),$$

with

$$\Delta \omega \triangleq (\omega_s - \omega_\infty), \quad \Delta \Theta \triangleq (\Theta_s - \Theta_\infty) \quad (2.34).$$

The Prandtl and Schmidt numbers are defined as

$$Pr \triangleq \frac{\nu_\infty}{\alpha_\infty}, \quad Sc = \frac{\nu_\infty}{D_\infty} \quad (2.35),$$

and introducing A and B with

$$A \triangleq \frac{(C_{p\infty} - C_{p\infty s}) \Delta \omega}{C_{p\infty}}, \quad B \triangleq \frac{\Delta \omega}{1 - \omega_s} \quad (2.36),$$

the partial differential equations are now

$$\frac{1}{1+Ky'} \left[\frac{\partial \Psi}{\partial y'} \frac{\partial \Omega}{\partial x} - \frac{\partial \Psi}{\partial x} \frac{\partial \Omega}{\partial y'} \right] = Sc^{-1} \nabla^2 \Omega \quad (2.37),$$

$$\frac{1}{1+Ky'} \left[\frac{\partial \Psi}{\partial y'} \frac{\partial \Theta}{\partial x} - \frac{\partial \Psi}{\partial x} \frac{\partial \Theta}{\partial y'} \right] = Pr^{-1} \nabla^2 \Theta - A Sc^{-1} \nabla \Omega \cdot \nabla \Theta \quad (2.38),$$

$$\frac{1}{1+Ky'} \left[\frac{\partial \Psi}{\partial y'} \frac{\partial}{\partial x} \nabla^2 \Psi - \frac{\partial \Psi}{\partial x} \frac{\partial}{\partial y'} \nabla^2 \Psi \right] = \nabla^2 \nabla^2 \Psi + \left\{ \right. \quad (2.39).$$

$$\left\{ \right. = \frac{g\beta \Delta \Theta l^3}{\nu_\infty^2} \left[\frac{\cos \phi}{1+Ky'} \frac{\partial \Theta}{\partial x} - \sin \phi \frac{\partial \Theta}{\partial y'} \right]$$

$$- \frac{g\gamma \Delta \omega l^3}{\nu_\infty^2} \left[\frac{\cos \phi}{1+Ky'} \frac{\partial \Omega}{\partial x} - \sin \phi \frac{\partial \Omega}{\partial y'} \right]$$

Note that ϕ is the angle between the surface normal and the body force. The boundary conditions are:

(a) at the surface

$$\Theta = \Omega = 1, \quad \frac{\partial \Psi}{\partial y'} = 0, \quad \frac{\partial \Psi}{\partial x} = B Sc^{-1} \frac{\partial \Omega}{\partial y'} \quad (2.40),$$

(b) far from the surface

$$\Theta, \Omega, \frac{\partial \Psi}{\partial y'} \rightarrow 0 \quad (2.41).$$

The equation for the stream function, equation (2.39), contains the dimensionless parameters $\beta \Delta \Theta$ and $\gamma \Delta \omega$. In order to continue the development leading to a boundary-layer description both these parameters must have the same sign, if they are of the same order of magnitude. For example, suppose that the Schmidt and Prandtl numbers are approximately the same size and that the Ackermann effect

term is very small, then $\Theta \doteq \Omega$ and if $\beta \Delta\Theta = -\gamma \Delta\omega$ there will be no motion, and no boundary layer. If the signs of $\beta \Delta\Theta$ and $\gamma \Delta\omega$ are different and one parameter is much larger than the other it may be possible to treat the problem by considering one effect as a small perturbation on the other, depending, of course, on the other parameters in the problem.

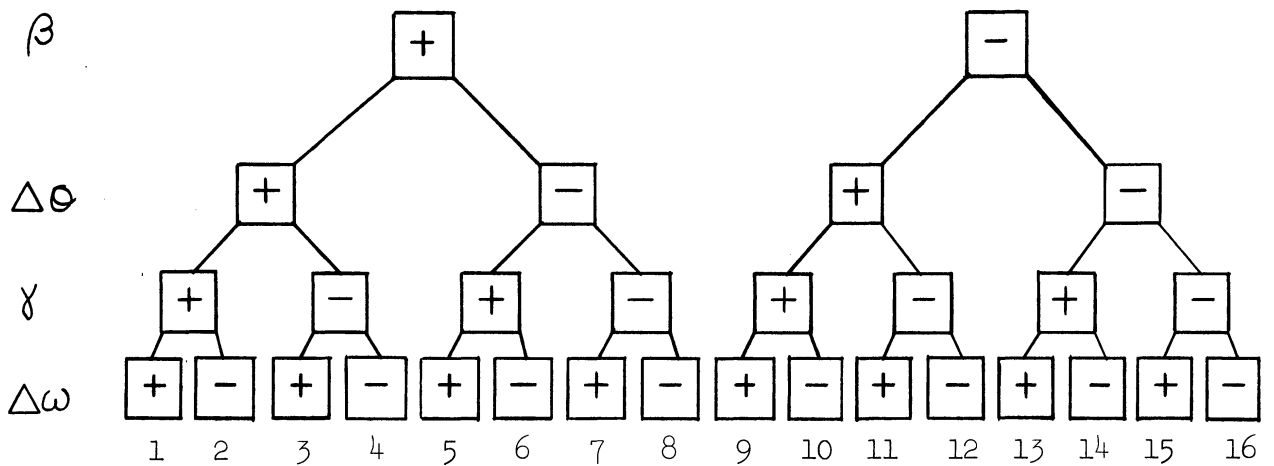


Figure 3. Expansion Coefficient/Characteristic Driving Force Sign Combinations

Of the sixteen possible cases (considering combinations of the signs of $\beta, \Delta\Theta, \gamma, \Delta\omega$) shown in Figure 3, eight have the same sign for $\beta \Delta\Theta$ and $\gamma \Delta\omega$. Four of these result in a flow counter to the direction of the body force, gravity, and the other four result in a flow in the direction of the body force. For example, consider the case of a body whose cross section is a closed curve. For cases 1, 4, 13 and 16, hereinafter called the "positive

condition," the flow develops in a direction counter to gravity and a plume rises above the cylinder. While for cases 6, 7, 10 and 11, the "negative condition," the situation is reversed. It is apparent that the differential equations are the same for both the positive and negative conditions if, for the latter, the symbol "g" is replaced with "-g" and the origin of the coordinate system is the upper intersection of the plane of symmetry with the body contour. For "open bodies" (e.g., a body cross-section with a parabolic contour, or a wedge) the positive condition can be treated only if the body opens upward and vice versa for the negative condition. With these restrictions in mind, the "eight possible cases" can be treated with the same system of differential equations. The only difference in the description of these eight cases is in the boundary condition for the stream function. The parameter B may be positive or negative, depending on the sign of $\Delta\omega$.

2.3 A Boundary-Layer Model

In what may be termed the classical boundary-layer theory, as explained by Schlichting⁽²⁵⁾, it is postulated that there exists a thin region near solid objects in which certain quantities describing the flow change very rapidly. One is led to consider the relative size of certain expressions in the differential equations describing the flow and discard some, due to their relative smallness. This leads to an impressive simplification of the differential equations. In forced-convection problems the validity of such approximations depends

on the size of the Reynolds number for the flow. The theory becomes a better approximation as the Reynolds number increases. The classical theory, however, lacks a systematic formulation which would allow one to find corrections to the theory for lower Reynolds numbers. Recently, boundary-layer theory, for forced-convection problems, has been put on a more formal and systematic basis by considering it as that which van Dyke⁽³¹⁾ calls a "singular perturbation problem." By means of methods developed to analyze this type of problem, corrections to the classical theory can, in principle, be derived. The quantities of interest are developed in two asymptotic expansions in the Reynolds number. These expansions are postulated to have overlapping regions of validity. In one of the regions, the "outer region," the flow is largely determined by the body shape and the upstream flow. The effects of viscosity are small in the outer region, which is "far" from the body. On the other hand, in the region near the body, the "inner region," the effects of viscosity are strong. The first term in the inner expansion is found by solving Prandtl's classical boundary-layer equations.

A corresponding theory for free convection around submerged objects has not been developed. One of the difficulties appears to be that the flow far from the object is completely determined by the inner flow, near the object, and cannot be specified a priori.

In this research, attention will be directed only to the first terms in "inner expansions" (as given by the usual boundary-layer theory), and neither the higher-order terms nor a description of the flow far from the object will be sought. The validity of the results will be justified, instead, by comparisons with experiments.

The differential equations describing the free-convection phenomena contain a parameter $g \ell^3 / \nu_\infty^2$, hereafter denoted by the symbol G . If the transformation $\Psi \rightarrow G^{1/2} \Psi'$ be made, then the equations become formally the same as those for forced convection, where $G^{1/2}$ plays the same role as the Reynolds number; i.e., in the equation for the stream function $G^{-1/2}$ appears as a coefficient of the highest derivatives. Hence, based on the corresponding development for forced convection, the following expansions may be expected to be valid near the object for large G :

$$\Psi G^{-1/2} = \Psi' = G^{-1/4} \overset{(0)}{\Psi}(x,y) + o(G^{-1/4}) \quad (2.42),$$

$$\Theta = \overset{(0)}{\Theta}(x,y) + o(G^{-1/4}) \quad (2.43),$$

$$\Omega = \overset{(0)}{\Omega}(x,y) + o(G^{-1/4}) \quad (2.44),$$

with

$$y = y' G^{1/4} \quad (2.45).$$

The order symbol, $o(\epsilon)$, means that succeeding terms are of an order smaller than ϵ ; e.g., $o(G^{-1/4})$ indicates, in Equation (2.42), that

$$\lim_{G \rightarrow 0} \left[\frac{\Psi' - G^{-1/4} \Psi^{(0)}}{G^{-1/4}} \right] = 0 \quad (2.46).$$

The orders of the succeeding terms in the expansions are based on a heuristic examination of the differential equations after substitution of the expansions.

The partial differential equations for the "zereth" approximations are

$$\Psi_y^{(0)} \Psi_{xx}^{(0)} - \Psi_x^{(0)} \Psi_{yy}^{(0)} = S C^{-1} \Psi_{yy}^{(0)} \quad (2.47),$$

$$\Psi_y^{(0)} \Theta_x^{(0)} - \Psi_x^{(0)} \Theta_y^{(0)} = R^{-1} \Theta_{yy}^{(0)} - A S C^{-1} \Psi_{yy}^{(0)} \Theta_y^{(0)} \quad (2.48),$$

$$\Psi_y^{(0)} \Psi_{xyy}^{(0)} - \Psi_x^{(0)} \Psi_{yyy}^{(0)} = \beta \Delta \Theta S(x) \Theta_y^{(0)} + \gamma \Delta \omega S(x) \Psi_{yy}^{(0)} + \Psi_{yyy}^{(0)} \quad (2.49),$$

where $S(x)$ is $\sin \phi$. The subscripts "x" and "y" denote partial differentiation. The equation for $\Psi^{(0)}$ can be integrated once, using the boundary conditions, to give

$$\Psi_y^{(0)} \Psi_{xy}^{(0)} - \Psi_x^{(0)} \Psi_{yy}^{(0)} = \beta \Delta \Theta S(x) \Theta_y^{(0)} + \gamma \Delta \omega S(x) \Psi_{yy}^{(0)} + \Psi_{yyy}^{(0)} \quad (2.50)$$

In the preceding development terms which vanish, supposedly, as $G \rightarrow \infty$, have been neglected. A further requirement is that the

curvature of the body, K , be small; this is to insure that $KyG^{-1/4}$ remains small. Consider, now, Equations (2.47), (2.48) and (2.50); the absence of second derivatives with respect to x indicates that in the "zeroth" approximation there is no mechanism whereby events downstream can affect the flow upstream. For closed bodies, where there is a plume, the applicability of this model must be established by experiment. This matter will be examined in Chapter 3.

A further simplification is still possible. When $|\beta \Delta \Theta| \geq |\gamma \Delta \omega|$ define

$$G_r \doteq G\beta \Delta \Theta \quad (2.51).$$

Now $\beta \Delta \Theta$ no longer appears as an explicit parameter but rather in the ratio σ_m , where

$$\sigma_m \doteq \frac{\gamma \Delta \omega}{\beta \Delta \Theta} \quad (2.52).$$

Conversely, when $|\beta \Delta \Theta| < |\gamma \Delta \omega|$

let $G_r \doteq G\gamma \Delta \omega \quad (2.53)$

and

$$\sigma_r \doteq \frac{\beta \Delta \Theta}{\gamma \Delta \omega} \quad (2.54).$$

In general, then, Equation (2.50) is written as

$$\Psi_y^{(0)} \Psi_{xy}^{(0)} - \Psi_x^{(0)} \Psi_{yy}^{(0)} = \sigma_r S(x) \Theta^{(0)} + \sigma_m S(x) \Omega^{(0)} + \Psi_{yyy}^{(0)} \quad (2.55),$$

where the symbol G is replaced by G_r in every instance, e.g., $y = y' G_r^{1/4}$.

Here, for $|\beta \Delta \Theta| \geq |\gamma \Delta \omega|$

$$\sigma_r \doteq 1, \sigma_m \doteq \frac{\gamma \Delta \omega}{\beta \Delta \Theta}, \quad Gr \doteq Gr \beta \Delta \Theta, \quad (2.56)$$

and for $|\beta \Delta \Theta| < |\gamma \Delta \omega|$

$$\sigma_r \doteq \frac{\beta \Delta \Theta}{\gamma \Delta \omega}, \sigma_m \doteq 1, \quad Gr \doteq Gr \gamma \Delta \omega \quad (2.57).$$

"Gr" is the familiar Grashof number for either a temperature "driving-force" or a concentration "driving-force."

The governing partial differential equations and boundary conditions in the model are then

$$\Psi_y^{(o)} \Omega_x^{(o)} - \Psi_x^{(o)} \Omega_y^{(o)} = Sc^{-1} \Omega_{yy}^{(o)} \quad (2.47),$$

$$\Psi_y^{(o)} \Theta_x^{(o)} - \Psi_x^{(o)} \Theta_y^{(o)} = Pr^{-1} \Theta_{yy}^{(o)} - A Sc^{-1} \Omega_y^{(o)} \Theta_y^{(o)} \quad (2.48),$$

$$\Psi_y^{(o)} \Psi_{xy}^{(o)} - \Psi_x^{(o)} \Psi_{yy}^{(o)} = \sigma_r S^{(x)} \Theta^{(o)} + \sigma_m S^{(x)} \Omega^{(o)} + \Psi_{yyy}^{(o)} \quad (2.55),$$

$$\Theta^{(o)}(x,0) = \Omega^{(o)}(x,0) = 1, \quad \Psi_y^{(o)}(x,0) = 0, \quad \Psi_x^{(o)}(x,0) = B Sc^{-1} \Omega_y^{(o)} \quad (2.58),$$

and

$$\Theta^{(o)}(x,y), \Omega^{(o)}(x,y), \Psi_y^{(o)}(x,y) \longrightarrow 0, \quad y \longrightarrow \infty \quad (2.59).$$

Before proceeding further with the development, the following quantities are defined for the boundary-layer model as applied to dilute mixtures ($\omega \ll 1$).

The Nusselt number, Nu , for the dimensionless heat-flux density at the surface

$$Nu \stackrel{d}{=} \frac{(\text{heat-flux density})(\text{characteristic length})}{(\text{thermal conductivity})(\text{temperature difference})}$$

or
$$Nu = -Gr^{+1/4} \left[\Theta_y^{(0)} + (A+B)PrSc^{-1} \Omega_y^{(0)} \right]_{y=0} \quad (2.60).$$

The second term on the right arises from mass transfer. The Nusselt number averaged over a length, \mathcal{L} , is

$$\bar{Nu} \stackrel{d}{=} \frac{1}{\mathcal{L}} \int_0^{\mathcal{L}} Nu(x) dx \quad (2.61).$$

The Sherwood number, for the dimensionless mass flux density at the surface,

$$Sh \stackrel{d}{=} \left[\frac{\rho \omega_s V_A (1 - \omega_s) L}{(\rho D_{\infty}) \Delta \omega} \right]_{y=0} = Gr^{+1/4} \left[\Omega_y^{(0)} \right]_{y=0} \quad (2.62).$$

The average Sherwood number

$$\bar{Sh} \stackrel{d}{=} \frac{1}{\mathcal{L}} \int_0^{\mathcal{L}} Sh(x) dx \quad (2.63).$$

The dimensionless shear stress at the surface

$$\mathcal{T} \stackrel{d}{=} \frac{\tau L^2}{V_{\infty} \mu_{\infty}} = Gr^{3/4} \left[\Psi_{yy}^{(0)} \right]_{y=0} \quad (2.64),$$

and the average stress

$$\bar{\mathcal{T}} \stackrel{d}{=} \frac{1}{\mathcal{L}} \int_0^{\mathcal{L}} \mathcal{T}(x) dx \quad (2.65).$$

2.4 The Boundary-Layer Model in Series Form

The body shape still remains in the problem in terms of the function $S(\alpha)$, representing the sine of the angle between the body force vector (gravity in the usual case) and the normal to the surface. In order to achieve a description in which the body shape is no longer an explicit variable, further work must be done.

One approach, at this stage, is to expand $S(\alpha)$ and the dependent variables $\overset{(0)}{\Omega}$, $\overset{(0)}{\Theta}$ and $\overset{(0)}{\Psi}$ as power series in α and then to solve the resulting equations for the coefficients of like powers of α , which depend on y . This is the basis for the Blasius series for forced convection past cylindrical objects (see Schlichting⁽²⁵⁾, p. 146). This technique, expansion of $S(\alpha)$ as a power series in α , was used by Chaing and Kaye⁽⁷⁾ for temperature-driven free convection around a circular, horizontal cylinder. It is possible to scale all of the coefficients resulting from the expansion for $S(\alpha)$ out of the problem, which Chaing and Kaye did not do. However, there are some questions about the ability of the resulting series to represent the dependent variables accurately with only a small number of terms. In fact, van Dyke indicates that the Blasius series (forced convection) actually diverges for $\alpha > .62$ in the case of the circular cylinder (see Schlichting, p. 154). Chaing and Kaye indicated that three terms are sufficient for temperature-driven free convection at a Prandtl number of .7. For the average heat-flux density over the whole circumference of the cylinder, Chaing and Kaye's one-term expansion gave a result 14 per cent higher than a two-term expansion,

and the two-term expansion was 0.3 per cent lower than a three-term expansion. In any case, a representation which requires as few terms as possible is desirable.

Hermann⁽¹⁴⁾ treated the problem of temperature-driven free convection around horizontal, circular cylinders using boundary-layer theory but assumed "similarity" so that the problem could be reduced to the solution of ordinary differential equations. The fact of the matter is that the flow does not possess the assumed similarity. Hermann realized this difficulty but expected that the error involved would not be serious. The agreement between the calculated temperature field and the experimental results of Jodlbauer⁽¹⁵⁾ was indeed good. However, for the velocity field the agreement was not as good. Hermann's method has two shortcomings in that there is no systematic way of improving his approximate solution to the boundary-layer equations and it is not readily apparent how other cylindrical objects are to be treated. Each object would have to be treated as a separate case.

Goertler⁽¹²⁾ attempted to generalize and improve the convergence of the stream-function series, for two-dimensional forced convection past submerged objects, by scaling both the x and y coordinates. His efforts were in part rewarded, for in the case of the circular cylinder the first term of the Goertler series differs from the "exact" solution by less than 4 per cent over 60 per cent of the distance from the stagnation point to the point of flow separation. Furthermore, in those cases where sufficient similarity

exists to enable one to transform the boundary-layer equations to ordinary differential equations, the Goertler series gives this result immediately.

The following transformations are now introduced for free-convection problems, the intent is to develop series representations for the concentration, temperature, and stream functions which converge rapidly and are universal as far as body shape is concerned "Universal" is here taken to mean that the body shape does not appear in any of the differential equations explicitly.

$$\left. \begin{aligned} \xi &= \int_0^x [S(x_1)]^{1/3} dx_1 \\ \eta &= \left(\frac{3}{4}\right)^{1/4} \frac{y [S(x)]^{1/3}}{\xi^{1/4}} \end{aligned} \right\} \quad (2.66)$$

$$\left. \begin{aligned} \Psi^{(0)}(x,y) &= \left(\frac{4}{3}\right)^{3/4} \xi^{3/4} F(\xi,\eta) \\ \Theta^{(0)}(x,y) &= T(\xi,\eta) \\ \Omega^{(0)}(x,y) &= M(\xi,\eta) \end{aligned} \right\} \quad (2.67)$$

It is understood that F , T and M still depend on the other dimensionless parameters Sc , Pr , σ_T , σ_M , A and B . Note that Acrivos⁽¹⁾ used essentially the transformations given for y and $\Psi^{(0)}$ to establish the form required for $S(x)$ which would enable one to transform the boundary-layer equations to ordinary differential

equations. With these transformations equations (2.47), (2.48) and (2.55) become

$$\frac{4}{3}\xi(F_\eta M_\xi - F_\xi M_\eta) - FM_\eta = Sc^{-1} M_{\eta\eta} \quad (2.68),$$

$$\frac{4}{3}\xi(F_\eta T_\xi - F_\xi T_\eta) - FT_\eta = Pr^{-1} T_{\eta\eta} - A Sc^{-1} M_\eta T_\eta \quad (2.69)$$

and

$$\frac{4}{3}\xi(F_\eta F_\xi - F_\xi F_\eta) - FF_{\eta\eta} + \frac{4}{3}K(\xi)F_\eta F_\eta = \alpha_r T + \sigma_m M + F_{\eta\eta\eta} \quad (2.70),$$

where

$$K(\xi) = \frac{1}{2} + \frac{1}{3}\xi[S(x)]^{-4/3} \frac{dS}{dx} \quad (2.71)$$

The boundary conditions are

$$\left. \begin{aligned} M(\xi,0) = T(\xi,0) = 1, F_\eta(\xi,0) = 0 \\ F(\xi,0) + \frac{4}{3}\xi F_\xi(\xi,0) = B Sc^{-1} M_\eta(\xi,0) \\ M(\xi,\infty) = T(\xi,\infty) = F_\eta(\xi,\infty) = 0 \end{aligned} \right\} \quad (2.72)$$

Goertler's⁽¹²⁾ terminology, of "principal function" for $K(\xi)$, will be employed here. The principal function depends on the body shape and at this point two classes of body shapes are introduced. For sharp-nosed bodies the series for $K(\xi)$ proceeds as (see Appendix A)

$$K(\xi) = \frac{1}{2} + K_1 \xi + \dots \quad (2.73)$$

where K_1 etc. are constants. For blunt-nosed bodies

$$K(\xi) = \frac{3}{4} + K_1 \xi^{3/2} + \dots \quad (2.74)$$

The variables M , T and F are represented as follows:

(a) for sharp-nosed bodies,

$$M(\xi, \eta) = \sum_{j=0}^{\infty} M_j(\eta) \xi^j, \quad T(\xi, \eta) = \sum_{j=0}^{\infty} T_j(\eta) \xi^j, \quad F(\xi, \eta) = \sum_{j=0}^{\infty} F_j(\eta) \xi^j \quad (2.75),$$

(b) for blunt-nosed bodies (where the curvature at the nose is not zero),

$$M(\xi, \eta) = \sum_{j=0}^{\infty} M_j(\eta) \xi^{3j/2}, \quad T(\xi, \eta) = \sum_{j=0}^{\infty} T_j(\eta) \xi^{3j/2}, \quad F(\xi, \eta) = \sum_{j=0}^{\infty} F_j(\eta) \xi^{3j/2} \quad (2.76).$$

The series given in (2.75) and (2.76) result in the following sets of ordinary differential equations (primes denoting differentiation with respect to η):

(a) for sharp-nosed bodies,

when $j=0$

$$\left. \begin{aligned} M_0'' + S_c F M_0' &= 0 \\ T_0'' + R F_0' T_0' - A \frac{P_r}{S_c} M_0' T_0' &= 0 \\ F_0''' + F_0 F_0'' - \frac{2}{3} F_0' F_0' + \sigma_T T_0 + \sigma_M M_0 &= 0 \end{aligned} \right\} (2.77),$$

when $j=1, 2, 3, \dots$

$$\left. \begin{aligned} M_j'' + S_c F_0 M_j' - \frac{4j}{3} S_c F_0' M_j + \left(\frac{4j}{3} + 1\right) S_c F_j M_0' &= R M_j \\ R M_j &= S_c \sum_{k=1}^{j-1} \left[\frac{4k}{3} M_k F_{j-k}' - \left(\frac{4k}{3} + 1\right) F_k M_{j-k}' \right] \end{aligned} \right\}$$

$$\left. \begin{aligned}
 T_j'' + P_r F_0 T_j' - A \frac{P_r}{Sc} M_0 T_j' - \frac{4j}{3} P_r F_0' T_j + \left(\frac{4j}{3} + 1\right) P_r F_j T_0' - A \frac{P_r}{Sc} M_j' T_0' &= R_{Tj} \\
 R_{Tj} &= P_r \sum_{k=1}^{j-1} \left[\frac{4k}{3} T_k F_{j-k}' - \left(\frac{4k}{3} + 1\right) F_k T_{j-k}' + A Sc^{-1} T_k' M_{j-k}' \right] \\
 F_j''' + F_0 F_j'' - \frac{4}{3} (j+1) F_0' F_j' + \left(\frac{4j}{3} + 1\right) F_0'' F_j - \frac{4}{3} K_j F_0' F_0' + \sigma_T T_j + \sigma_M M_j &= R_{Fj} \\
 R_{Mj} &= \sum_{k=1}^{j-1} \left[\frac{4}{3} (k + \frac{1}{2}) F_k' F_{j-k}' - \left(\frac{4k}{3} + 1\right) F_k F_{j-k}'' + \frac{4}{3} K_{j-k} \sum_{i=0}^k F_i' F_{k-i}' \right]
 \end{aligned} \right\} (2.78),$$

(b) for blunt-nosed bodies,

when $j=0$

$$\left. \begin{aligned}
 M_0'' + Sc F_0 M_0' &= 0 \\
 T_0'' + P_r F_0 T_0' - A \frac{P_r}{Sc} M_0' T_0' &= 0 \\
 F_0''' + F_0 F_0'' - F_0' F_0' + \sigma_T T_0 + \sigma_M M_0 &= 0
 \end{aligned} \right\} (2.79),$$

when $j=1, 2, 3, \dots$

$$\left. \begin{aligned}
 M_j'' + Sc F_0 M_j' - 2j Sc F_0' M_j + (2j+1) Sc F_j M_0' &= R_{Mj} \\
 R_{Mj} &= Sc \sum_{k=1}^{j-1} \left[2k M_k F_{j-k}' - (2k+1) F_k M_{j-k}' \right] \\
 T_j'' + P_r F_0 T_j' - A \frac{P_r}{Sc} M_0' T_j' - 2j P_r F_0' T_j + (2j+1) P_r F_j T_0' - A \frac{P_r}{Sc} M_j' T_0' &= R_{Tj} \\
 R_{Tj} &= P_r \sum_{k=1}^{j-1} \left[2k T_k F_{j-k}' - (2k+1) F_k T_{j-k}' + A Sc^{-1} T_k' M_{j-k}' \right] \\
 F_j''' + F_0 F_j'' - 2(j+1) F_0' F_j' + (2j+1) F_0'' F_j - \frac{4}{3} K_j F_0' F_0' - \sigma_T T_j + \sigma_M M_j &= R_{Fj} \\
 R_{Fj} &= \sum_{k=1}^{j-1} \left[(2k+1) F_k' F_{j-k}' - (2k+1) F_k F_{j-k}'' + \frac{4}{3} K_{j-k} \sum_{i=0}^k F_i' F_{k-i}' \right]
 \end{aligned} \right\} (2.80).$$

The boundary conditions are:

(a) for sharp-nosed bodies,

when $\eta = 0$

$$\left. \begin{aligned} M_0(0) = T_0(0) = 1, F_0'(0) = 0, F_0(0) = B Sc^{-1} M_0'(0) \\ M_0(\infty) = T_0(\infty) = F_0(\infty) = 0 \end{aligned} \right\} \quad (2.81),$$

when $\eta = 1, 2, 3, \dots$

$$\left. \begin{aligned} M_\eta(0) = T_\eta(0) = F_\eta'(0) = M_\eta(\infty) = T_\eta(\infty) = F_\eta(\infty) = 0 \\ (1 + \frac{4\eta}{3}) F_\eta(0) = B Sc^{-1} M_\eta'(0) \end{aligned} \right\} \quad (2.82),$$

(b) for blunt-nosed bodies,

when $\eta = 0$

$$\left. \begin{aligned} M_0(0) = T_0(0) = 1, F_0'(0) = 0, F_0(\infty) = B Sc^{-1} M_0'(0) \\ M_0(\infty) = T_0(\infty) = F_0(\infty) = 0 \end{aligned} \right\} \quad (2.83),$$

when $\eta = 1, 2, 3, \dots$

$$\left. \begin{aligned} M_\eta(0) = T_\eta(0) = F_\eta'(0) = M_\eta(\infty) = T_\eta(\infty) = F_\eta(\infty) = 0 \\ (1 + 2\eta) F_\eta(0) = B Sc M_\eta'(0) \end{aligned} \right\} \quad (2.84)$$

In the absence of mass transfer Equations (2.77) and their boundary conditions comprise the same system as that investigated by Ostrach⁽²²⁾ for temperature-driven free convection in the neighborhood

of a vertical plate. Equations (2.79) and their boundary conditions, again in the absence of mass transfer, were studied by Chaing and Kaye for free convection near the stagnation point on a horizontal, circular cylinder. The succeeding systems of differential equations ($j = 1, 2, 3, \dots$) are linear systems and it is anticipated that the coefficients in the expansion of the principal function, $K(\xi)$, could be scaled out of the systems. Consider, as an example, the system describing either sharp-nosed or blunt-nosed bodies for $j=1$. If the following variables are defined,

$$M = K_1 m_1, \quad T_1 = K_1 t_1, \quad F = K_1 f_1 \quad (2.85),$$

and substituted into the differential equations for $j=1$, then the constant K_1 no longer appears in the system for $j=1$. It appears only when the series for M_1 , T_1 and F_1 are assembled. The solution of the set of equations for $j=1$ does not depend on the body contour, since the body contour enters the problem through the principal function. The same type of procedure is possible for $j=2, 3, \dots$, for blunt-nosed as well as for sharp-nosed bodies, although the algebra becomes rather tedious. Thus, it is possible to describe free convection around bodies of either class in terms of ordinary differential equations in which the particular body contour parameters are absent. As a result, the solutions can be found for a particular set of the other parameters (Sc , Pr , A , B , σ_r , σ_m) and then applied to any body contour in the class simply by assembling the series for the stream, temperature, and concentration functions. Of course,

when the series are assembled, then $S(\alpha)$, ξ , and the expansion for the principal function must be introduced for the body in question. There is another important point to be emphasized. If the series converge rapidly it may be necessary to compute only a few terms in the expansions and, as will be demonstrated in the next chapter, there are cases where only the first terms ($j=0$) need be calculated. In the latter instance the results of Ostrach⁽²²⁾ could be used for sharp-nosed bodies other than vertical plates, and those of Chaing and Kaye⁽⁷⁾ for other blunt-nosed bodies. Ostrach⁽²²⁾ presents results for a rather wide range of Prandtl numbers (.01 - 1000) while Chaing and Kaye solved the differential equations only for a Prandtl number of .7.

2.5 Special Cases of the Principal Function

The implications of a constant principal function are examined by noting that if $K(\xi)$ is constant, then taking

$$M(\xi, \eta) = \bar{M}(\eta), T(\xi, \eta) = \bar{T}(\eta), F(\xi, \eta) = \bar{F}(\eta) \quad (2.86)$$

reduces the problem to the solution of a single system of ordinary differential equations. Hence $S(\alpha)$, the sine of the angle between the normal to the surface and the body force vector, is determined for this situation by

$$\frac{M}{S} \frac{dS}{d\xi} = a \quad (2.87).$$

For $a = 0$, $S(x)$ is constant. This is the situation for a wedge.

For $a \neq 0$, since

$$\xi = \int_0^x [S(x)]^{1/3} dx, \quad (2.88),$$

then

$$b [S(x)]^{1/a} = \int_0^x [S(x)]^{1/3} dx, \quad (2.89),$$

or

$$[S(x)]^{1/3} = \frac{b}{a} [S(x)]^{1-a} \frac{dS(x)}{dx} \quad (2.90),$$

hence

$$S(x) = \left[\frac{a}{b} (x + c) \right]^{\frac{3a}{3-a}}, \quad a \neq 0, 3 \quad (2.91),$$

or

$$S(x) = c e^{\frac{3x}{b}}, \quad a = 3 \quad (2.92).$$

Four of the special cases will be examined.

S constant (a=0)

This case represents free convection near wedges of included angle $\pi - \sin^{-1}(S)$. For $S=1$ the body is a vertical plate. From Equation (2.70) it is apparent that the differential equations to be solved are the same for any wedge angle and thus the vertical-plate solution can be used to describe the situation for any wedge angle. This result could have been obtained without recourse to the various transformations.

$$\underline{S(x) = x, (a = 3/4, b = 3/4, C = 0)}$$

This represents a round-nosed body. Naturally, due to the restriction on $S(x), (0 \leq S(x) \leq 1)$, the body is of limited extent and not closed.

$$\underline{S(x) = x + C, (a = 3/4, b = 3/4, C \neq 0)}$$

Here the body has a pointed nose with an ogival shape.

$$\underline{S(x) = C e^{3x/b}, (C > 0, b < 0)}$$

This case represents sharp-nosed bodies with included angle $\pi - 2\sin^{-1}(C)$. For $C = 1$ the body has a cusped nose (ogee shape).

It is to be noted that the differential equations to be solved (for \bar{M} , \bar{T} and \bar{F}) differ according to the value of the constant a . However, all of the "special cases" can be treated with the general theory if the "correction" terms M_j , T_j and F_j are calculated.

A case which is not included in the general theory presented thus far is that for flat-nosed bodies where the expansion for the function $S(x)$ starts as

$$S(x) = Cx^3 + \dots \tag{2.93},$$

so the principal function starts as

$$K(\xi) = 1 + \dots \tag{2.94}.$$

This is not one of the two classes of body shapes for which the general theory is developed. Of course the development of the previous

section is easily carried out for this class of two-dimensional body shapes. The equations for $\beta=0$ are the same as for sharp-nosed bodies except the factor $2/3$ is changed to $4/3$ in the equation for F_0 . In Chapter 3 a single set of results for shapes in this class will be presented.

2.6 Behavior of Dependent Variables Near Stagnation Points

Before proceeding with the solution of the differential equations some of the implications of the theory, as presented up to this point, will be examined. Recall that

$$\xi = \int_0^{\alpha} [S(\alpha)]^{1/3} d\alpha, \quad \eta = \left(\frac{3}{4}\right)^{1/4} \frac{y [S(\alpha)]^{1/3}}{\xi^{1/4}} \quad (2.66).$$

The velocity components are:

(a) in the direction tangent to the surface of the body,

$$\frac{\tilde{u} L}{V_0 G r^{1/2}} = \left(\frac{4}{3}\right)^{1/2} \xi^{1/2} S^{1/3} F_{\eta} \quad (2.95),$$

(b) in the direction normal to the surface,

$$\frac{\tilde{v} L}{V_0 G r^{1/2}} = - \left[\left(\frac{3}{4}\right)^{1/4} \xi^{-1/4} S^{1/3} F + \left(\frac{4}{3}\right)^{3/4} \xi^{3/4} S^{1/3} F_{\xi} + \left(\frac{4}{3}\right)^{1/2} y \left[\frac{1}{3} \xi^{1/2} S^{-2/3} \frac{dS}{d\alpha} - \frac{1}{4} \xi^{-1/2} S^{2/3} F_{\eta} \right] \right] \quad (2.96).$$

Consider first, sharp-nosed bodies, where as α approaches zero, $S(\alpha)$ approaches a constant. First of all, it is realized that the proposed model is inapplicable in the neighborhood of the sharp nose because here the "neglected terms" in the general equations (involving derivatives with respect to α) are large, possibly of the same order of magnitude as the terms retained. Secondly, the orthogonal,

curvilinear coordinate system is inapplicable in the upstream region if the wedge angle is other than zero. Hence, the consequences of of the proposed model will not provide a valid approximation in this region. Now note that as α tends to zero for y not zero, η tends to infinity. Hence the velocity in the tangential direction, as predicted from the present theory, tends to zero. The temperature and concentration both tend to zero. The velocity in the normal direction, however, tends to infinity. Now, as α tends to zero for y equal to zero, the velocity in the normal direction is zero, in the absence of mass transfer, and increases without limit with mass transfer at the boundary. Both temperature and concentration are equal to unity. Hence, the solutions to the equations are functions which are singular at the nose. The situation is summarized in Figure 4.

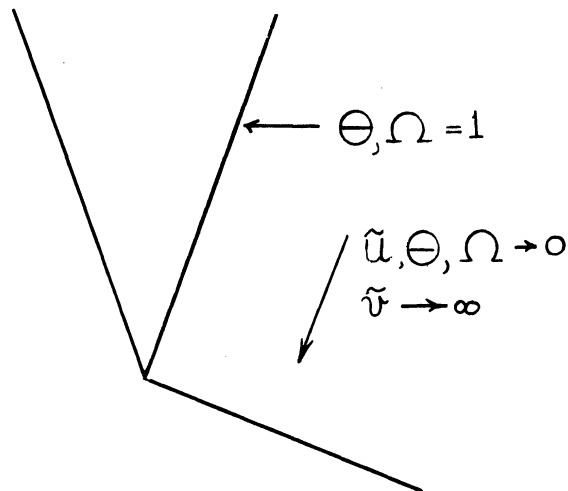


Figure 4. Dependent Variable Behavior Near a Sharp Nose

For blunt-nosed bodies the situation is different. As α tends to zero, $S(\alpha)$ approaches α and so the scaled normal distance, η , approaches y . The tangential velocity component approaches zero while the normal component is bounded, but not zero. Both the temperature and concentration are well behaved, tending to functions of y . Furthermore, due to the requirements of symmetry and the smooth behavior of the body contour near the stagnation point, the terms neglected in the boundary-layer approximation are not large. Thus for large Grashof numbers the proposed model can be expected to provide a valid approximation near the stagnation point, $\alpha=0$, and rational corrections may even be possible.

A situation similar to that at the lower stagnation point on sharp-nosed bodies prevails near the upper stagnation point on any closed body. The proposed model will break down since derivatives with respect to α become large in the region of the plume. The tangential velocity tends to zero but the normal velocity increases without bound.

Thus the best agreement between experimental results and the the proposed model would be expected for open, round-nosed bodies. For sharp-nosed bodies the agreement depends, in part, on the influence which the region near the sharp nose has on the rest of the flow and for closed bodies the agreement depends on the influence of the plume. For vertical plates the close agreement between the theory developed by Ostrach⁽²²⁾ and the experimental results of Schmidt and Beckmann⁽²⁶⁾

indicates that the effect of the sharp nose is small. The situation with respect to a horizontal circular cylinder (a closed body) will be examined in the next chapter.

CHAPTER 3

Numerical Solutions

3.1 Comparison of Theoretical and Experimental Results

The mathematical model developed in the previous chapter is useful only when: (i) the predictions of the model agree with experimental results and (ii) a small number of terms in the series are required. The first point will be examined relative to two experimental studies reported in the literature.

The first set of experimental data to be examined was reported by Jodlbauer⁽¹⁵⁾. Measurements were made of local temperatures and velocities in temperature-driven free convection around horizontal, circular cylinders. The fluid was air ($Pr = .7$) and measurements were made at Grashof numbers of 9.4×10^3 , 9.3×10^4 , 1.6×10^5 and 7.0×10^5 . The surfaces of the cylinders were approximately isothermal and ranged from 70°C to 151°C . The ambient temperatures were between 13°C and 20°C . Temperatures were measured with a thermocouple and velocities with a quartz-fiber anemometer.

The experimental data (temperatures and tangential velocity components) at angular positions of 30° , 90° and 150° , measured from the lower stagnation point, are shown on Figures 5 through 10. First, an inspection of these figures reveals that the velocity data are not in strict accord with the boundary-layer theory. Boundary-layer theory implies that at high Grashof numbers the quantity $\bar{u} L / \alpha Gr^{1/2}$ should depend only on the position in the flow, not on the Grashof number.

The temperature data do, however, conform to the theory, as $(\theta - \theta_s)/(\theta_s - \theta_\infty)$ is independent of the Grashof number. The inference is that the Grashof number should be of the order of 10^5 for the velocity field to be in the "asymptotic state" where boundary-layer theory is entirely valid.

The first two sets of differential equations, $f=0, 1$, describing temperature-driven free convection around blunt-nosed bodies were integrated for a Prandtl number of 0.7. The numerical techniques are described in the appendices. According to the development given in Chapter 2 the tangential velocity and temperature are given by

$$\frac{\bar{u} L}{v_\infty G^{1/2}} = \left(\frac{4}{3}\right)^{1/2} [\xi(x)]^{1/2} [S(x)]^{1/3} \left[F_0'(\eta) + [\xi(x)]^{3/2} F_1'(\eta) + \dots \right] \quad (3.1),$$

$$\frac{(\theta - \theta_s)}{(\theta_s - \theta_\infty)} = T_0(\eta) + [\xi(x)]^{3/2} T_1(\eta) + \dots \quad (3.2).$$

These functions are also shown on Figures 5 through 10. The term $[\xi(x)]^{3/2} F_1'(\eta)$ is generally small, for the case of the circular cylinder, although this "correction" improves the theory. The term $[\xi(x)]^{3/2} T_1(\eta)$ makes a significant contribution at 150° and improves the agreement between theory and experiment. The overall or average rates of heat transfer from the experimental measurements made by Jodlbauer⁽¹⁵⁾ are compared with the theoretical predictions in Table I.

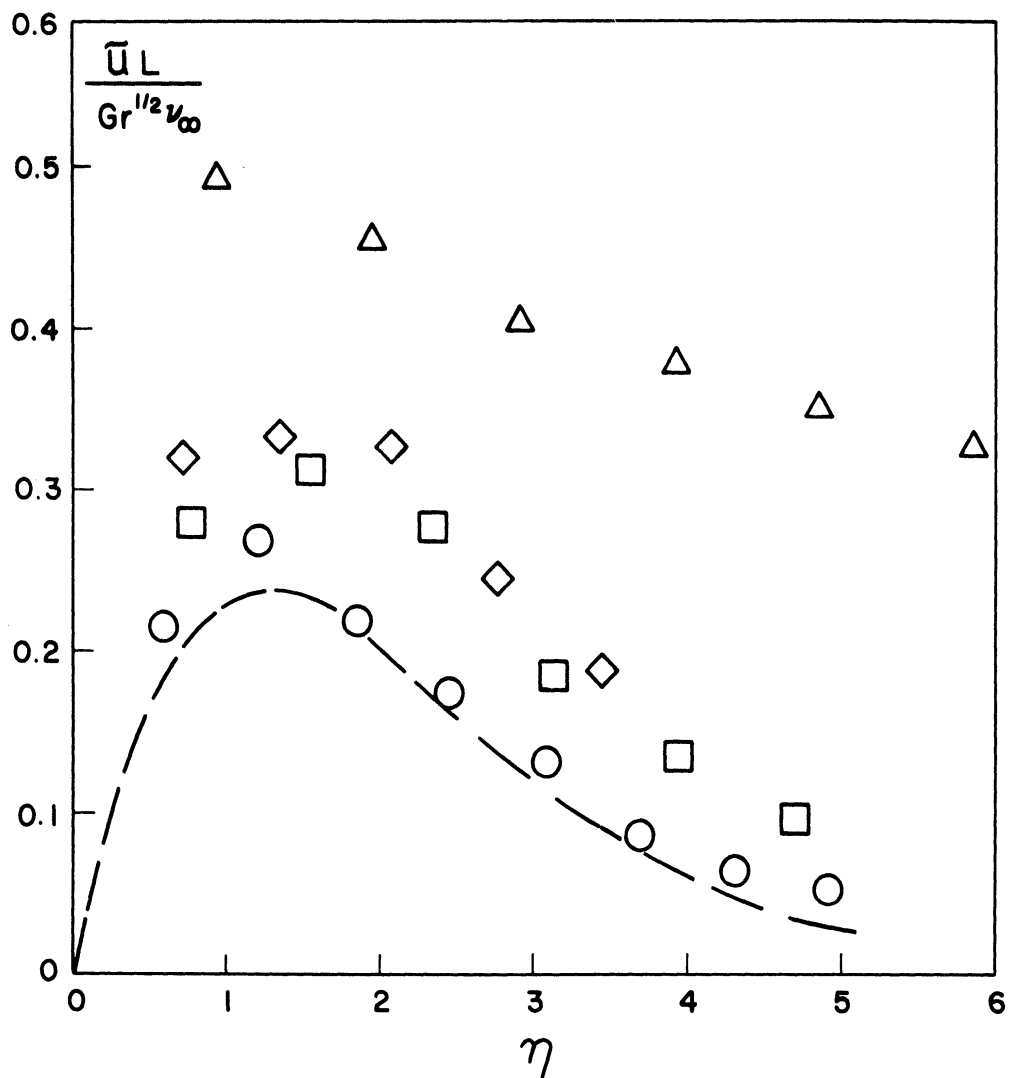


Figure 5. Temperature-Driven Free Convection Around a Horizontal, Circular Cylinder. Dimensionless Tangential Velocity-Dimensionless Normal Distance at 30° from the Lower Stagnation Point. Experimental Data of Jodlbauer: $Pr = .7$, $Gr = 7 \times 10^5$ (○), 1.6×10^5 (□), 9.3×10^4 (◇), 9.4×10^3 (△). Series Representation: one or two terms (—).

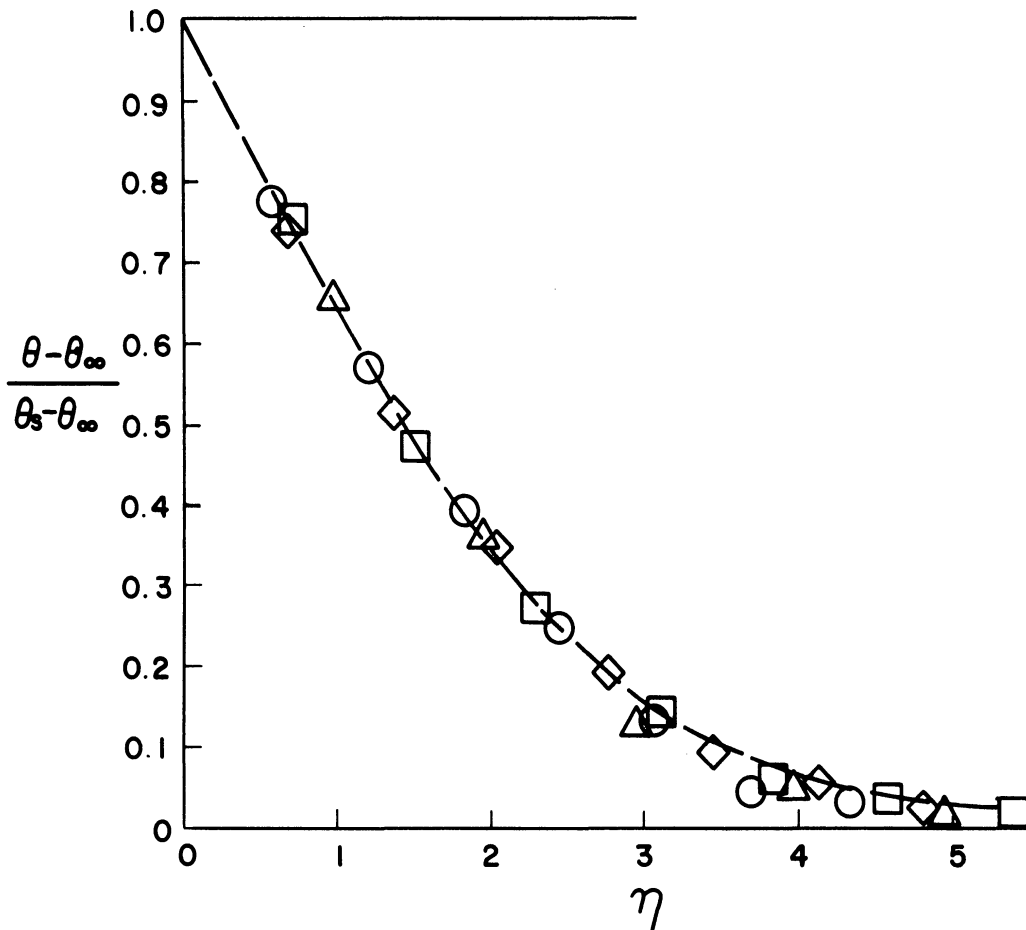


Figure 6. Temperature-Driven Free Convection Around a Horizontal, Circular Cylinder. Dimensionless Temperature - Dimensionless Normal Distance at 30° from the Lower Stagnation Point. Experimental Data of Jodlbauer: $Pr = .7$, $Gr = 7 \times 10^5$ (○), 1.6×10^5 (□), 9.3×10^4 (◇), 9.4×10^3 (△). Series Representation: one or two terms (—).

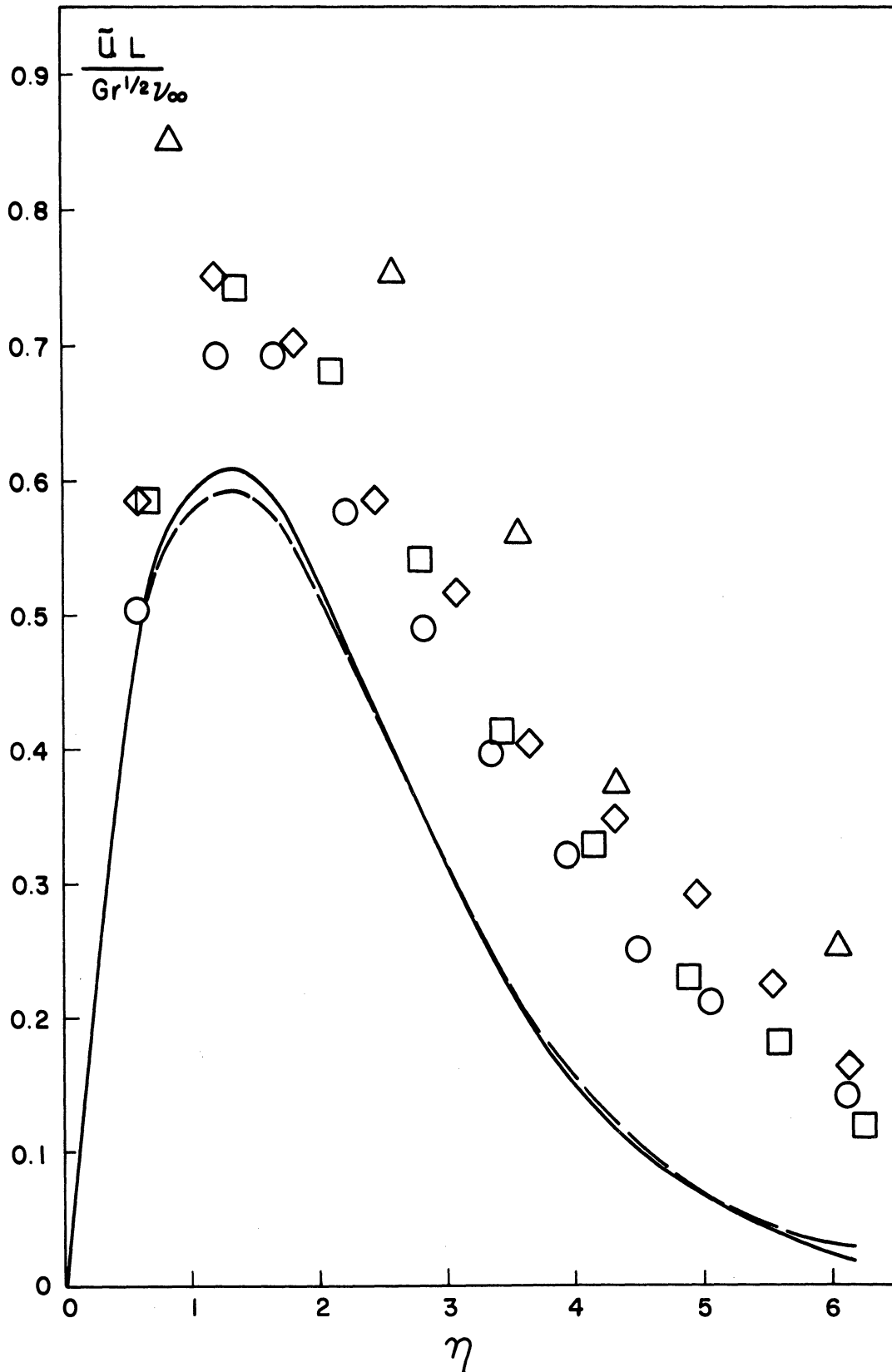


Figure 7. Temperature-Driven Free Convection Around a Horizontal, Circular Cylinder. Dimensionless Tangential Velocity - Dimensionless Normal Distance at 90° from the Lower Stagnation Point. Experimental Data of Jodlbauer: $Pr = .7$, $Gr = 7 \times 10^5$ (○), 1.6×10^5 (□), 9.3×10^4 (◇), 9.4×10^3 (△). Series Representation: one term (———), two terms (-----).

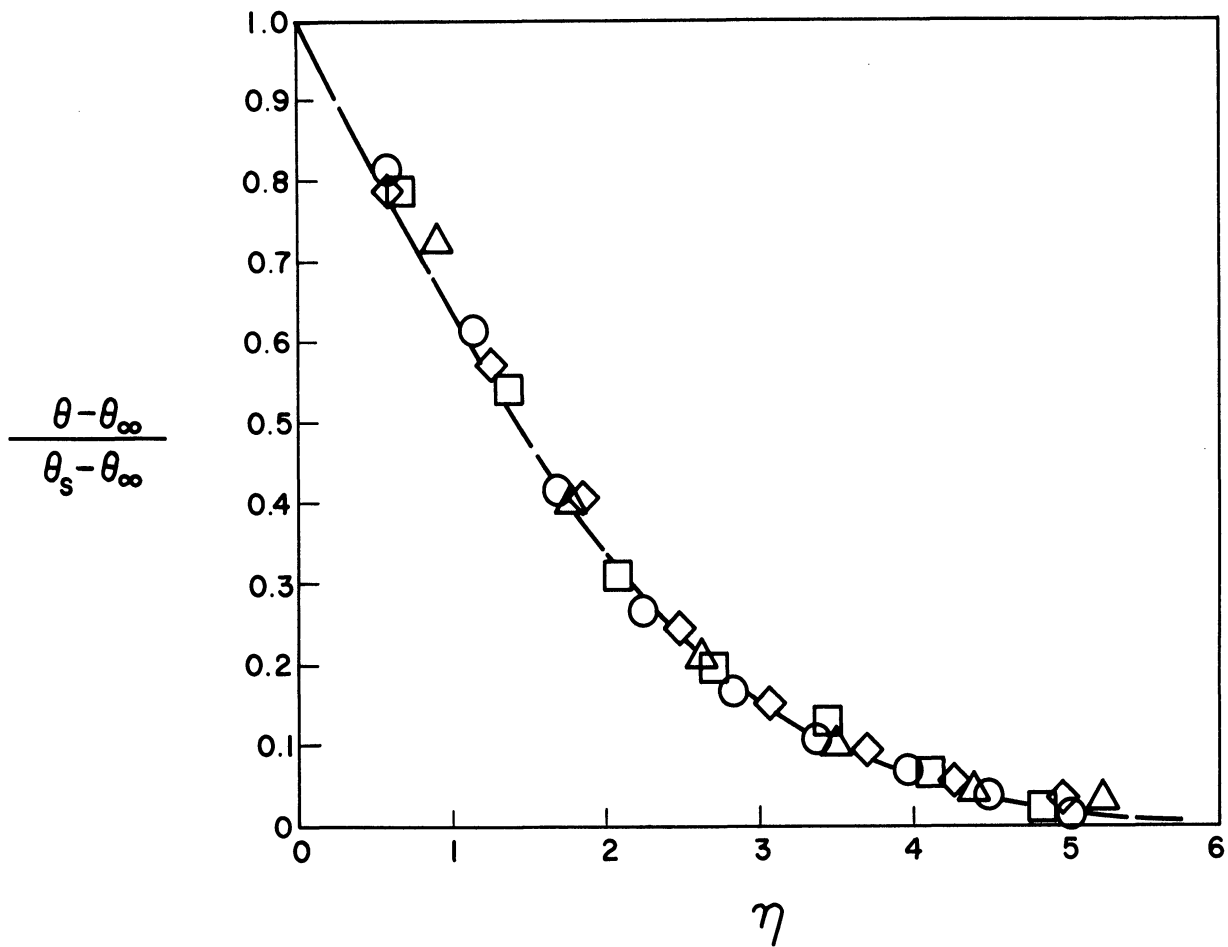


Figure 8. Temperature-Driven Free Convection Around a Horizontal, Circular Cylinder. Dimensionless Temperature - Dimensionless Normal Distance at 90° from the Lower Stagnation Point. Experimental Data of Jodlbauer: $Pr = .7$, $Gr = 7 \times 10^5$ (○), 1.6×10^5 (□), 9.3×10^4 (◇), 9.4×10^3 (△). Series Representation; one or two terms (———).

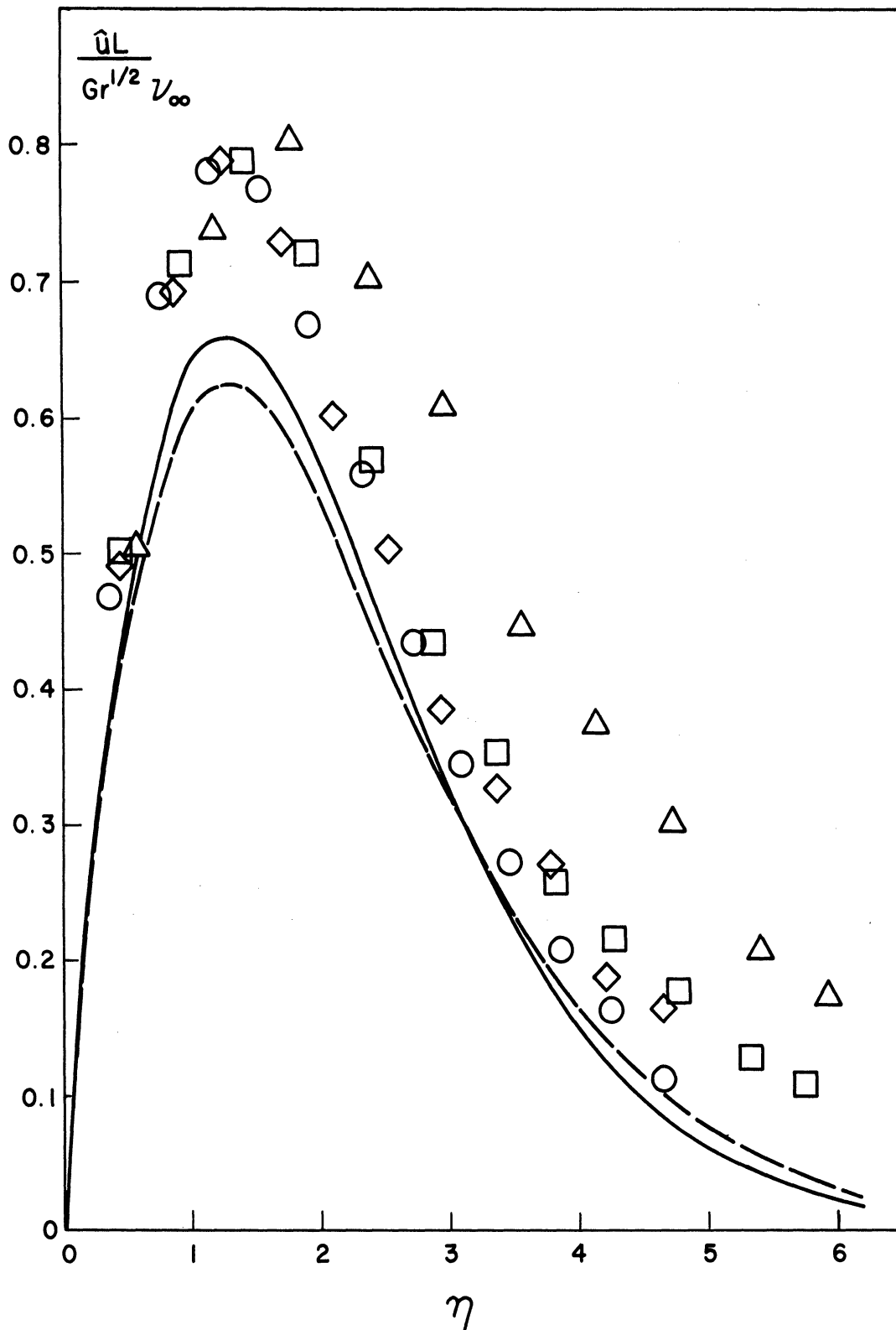


Figure 9. Temperature-Driven Free Convection Around a Horizontal, Circular Cylinder. Dimensionless Tangential Velocity - Dimensionless Normal Distance at 150° from the Lower Stagnation Point. Experimental Data of Jodlbauer: $Pr = .7$, $Gr = 7 \times 10^5$ (\circ), 1.6×10^5 (\square), 9.3×10^4 (\diamond), 9.4×10^3 (\triangle). Series Representation: one term (—), two terms (---).

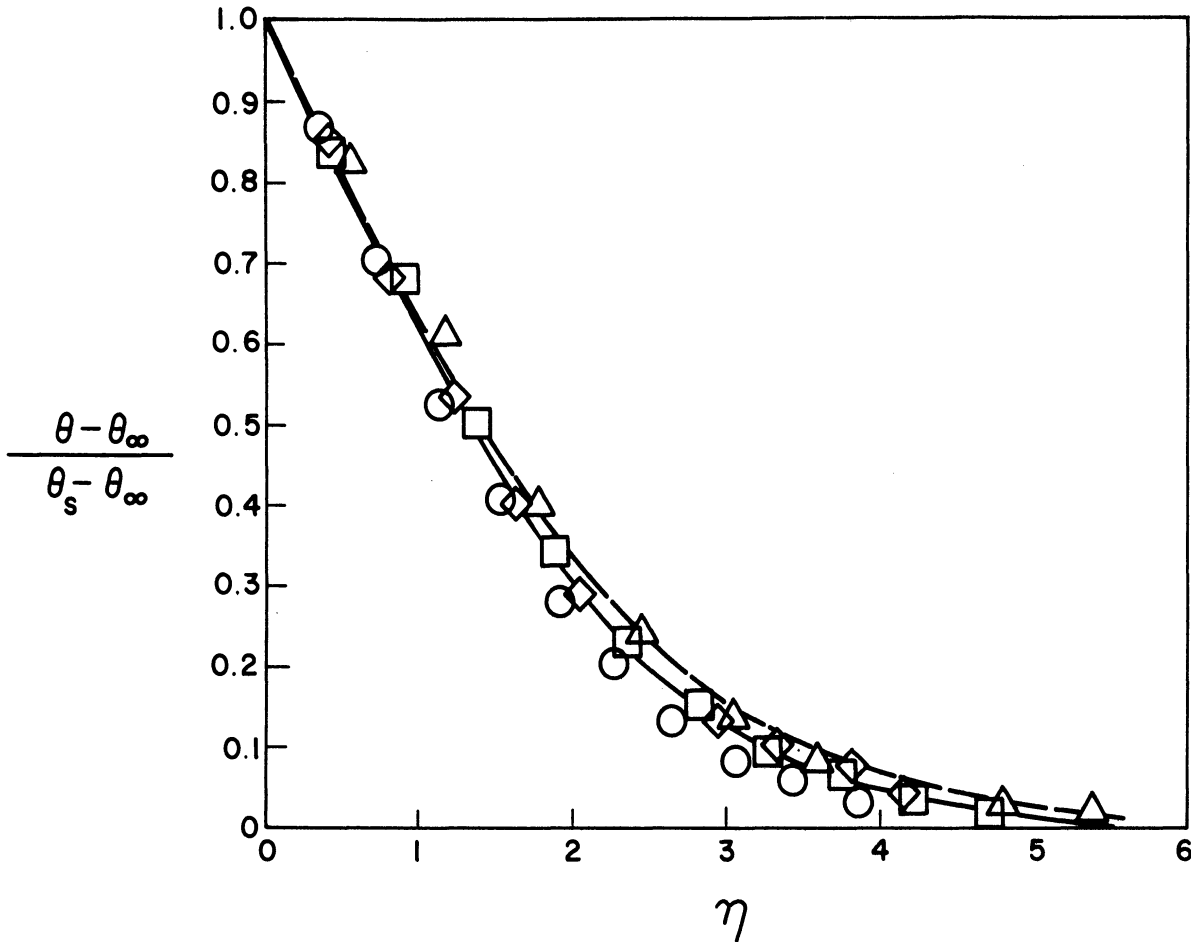


Figure 10. Temperature-Driven Free Convection Around a Horizontal, Circular Cylinder. Dimensionless Temperature - Dimensionless Normal Distance at 150° from the Lower Stagnation Point. Experimental Data of Jodlbauer: $Pr = .7$, $Gr = 7 \times 10^5$ (○), 1.6×10^5 (□), 9.3×10^4 (◇), 9.4×10^3 (△). Series Representation: one term (—), two terms (---).

TABLE I

COMPARISON OF AVERAGE NUSSELT NUMBERS DETERMINED BY JODLBAUER⁽¹⁵⁾ WITH THE PREDICTIONS OF THE BOUNDARY-LAYER THEORY (Pr=.7)

$$\overline{NuGr}^{-1/4} = -\left(\frac{3}{4}\right)^{1/4} \frac{4}{3} \frac{[\xi(\eta)]^{3/4}}{\eta} T_0'(0) - \left(\frac{3}{4}\right)^{1/4} \frac{4}{9} \frac{[\xi(\eta)]^{9/4}}{\eta} T_1'(0) \quad .298 + .004 = .302 \quad (3.3)$$

<u>Grashof Number</u>	<u>$\overline{NuGr}^{-1/4}$</u>
$.8 \times 10^4$.33
1.0×10^4	.32
6.4×10^4	.34
8.7×10^4	.35
9.2×10^4	.34
1.3×10^5	.32
1.5×10^5	.32
7.0×10^5	.31
Ave.	.33

The conclusions drawn from the figures and the table are that theory and experiment are in satisfactory agreement as far as temperature and heat-flux density are concerned. Particularly significant is the temperature field prediction at 150°, since this is near the region where the "hot plume" rises from the surface. The agreement between theory and experiment for the velocity fields is not as good as was the case for the temperature fields. The general shape and location of the maximum velocity are, however, satisfactory.

The first set of differential equations, $f=0$, describing concentration-driven free convection around blunt-nosed bodies was integrated for a Schmidt number of 1763. This corresponds to the Schmidt number obtained in an experiment reported by Schütz⁽²⁸⁾. The interfacial velocity parameter, B , was taken as zero in the numerical calculations since in the experiment $B Sc^{-1}$ was $\sim 10^{-6}$. Schütz determined local and average mass-transfer rates to a horizontal, circular cylinder immersed in a water solution of $CuSO_4$ and H_2SO_4 during electrolysis. The estimated experimental error was 5 per cent. Table II shows the local values reported by Schütz and predicted by the first term in the series for concentration. The agreement is satisfactory.

TABLE II

COMPARISON OF LOCAL SHERWOOD NUMBERS DETERMINED BY SCHÜTZ⁽²⁸⁾
WITH THE PREDICTIONS OF BOUNDARY-LAYER THEORY ($Sc=1763$)

$$Sh Gr^{-1/4} = -\left(\frac{3}{4}\right)^{1/4} [F(x)]^{-1/4} [S(x)]^{1/3} M'_1(0) \quad (3.4)$$

<u>Angular Position, ϕ</u>	<u>Local Value of $Sh Gr^{-1/4}$</u>	
	Theory	Experiment
0°	23.9	20.9
30°	25.3	23.8
60°	24.4	23.1
90°	22.4	22.6
120°	19.7	20.2
150°	15.5	16.0
180°	0	14
Average Value $\overline{Sh Gr^{-1/4}}$	20.7	20.6

It is of interest that the theory predicts a minimum in the transfer rate at the forward stagnation point, which is in accord with the experimental observation.

The independent variables and series expansions adopted in Section 2.4 were chosen with the intention of providing rapidly convergent and universal (with respect to the class of the body shape) representations of the boundary-layer variables. The generality of the representations was demonstrated in Section 2.4, where it was also emphasized that the goal was a one-term representation. The major deficiency of the method used by Chaing and Kaye⁽⁷⁾ is that at least two terms are required to give accurate heat-flux densities. Although, in the present method, two-term expansions represent the temperature fields better near the upper stagnation point on a circular cylinder (Figure 10) the present results (comparison of theory and experiment) indicate that only one term in the expansions is needed for the surface flux density of heat or mass.

3.2 The Effects Due to the Prandtl Number, the First Order Terms and the Body-Shape Class

The results presented in this section show the effects of the Prandtl number (or Schmidt number) on some free-convection phenomena. For the present the emphasis is on the zero-order terms in the series for blunt-nosed bodies. The first-order terms will be examined later in the section to estimate the magnitudes of their contributions.

Numerical results were obtained for temperature-driven free convection around blunt-nosed bodies for Prandtl numbers of .01, .7, 1., 1000 and 1763. These results also apply to concentration-driven convection if the interfacial velocity parameter, B , is taken as zero. The results are summarized in Table III and the computer output is presented in Appendix C. The results are shown in graphical form on Figures 11 and 12.

TABLE III

DERIVATIVES OF THE STREAM AND TEMPERATURE FUNCTIONS
AT THE SURFACE ($\eta=0$) FOR TEMPERATURE-DRIVEN FREE CONVECTION
AROUND BLUNT-NOSED OBJECTS

Pr	$F_0''(0)$	$-\frac{F_1''(0)}{K_1}$	$-T_0'(0)$	$-\frac{F_1''(0)}{K_1}$
.01	1.1691	(.25)*	.0593	(.02)*
.7	.8593	.09149	.3702	.03226
1.	.8039	----	.4100	----
1000.	.1954	(.01)*	3.0584	(.12)*
1763.	.1717	----	3.5328	----

Figures 11 and 12 show the expected behavior of the temperature and velocity profiles; i.e., the temperature tends to zero quite rapidly at high Prandtl numbers.

* The first-order term is estimated from a partial solution of the differential equations for $\beta=1$. See Appendix C for a discussion of this matter.

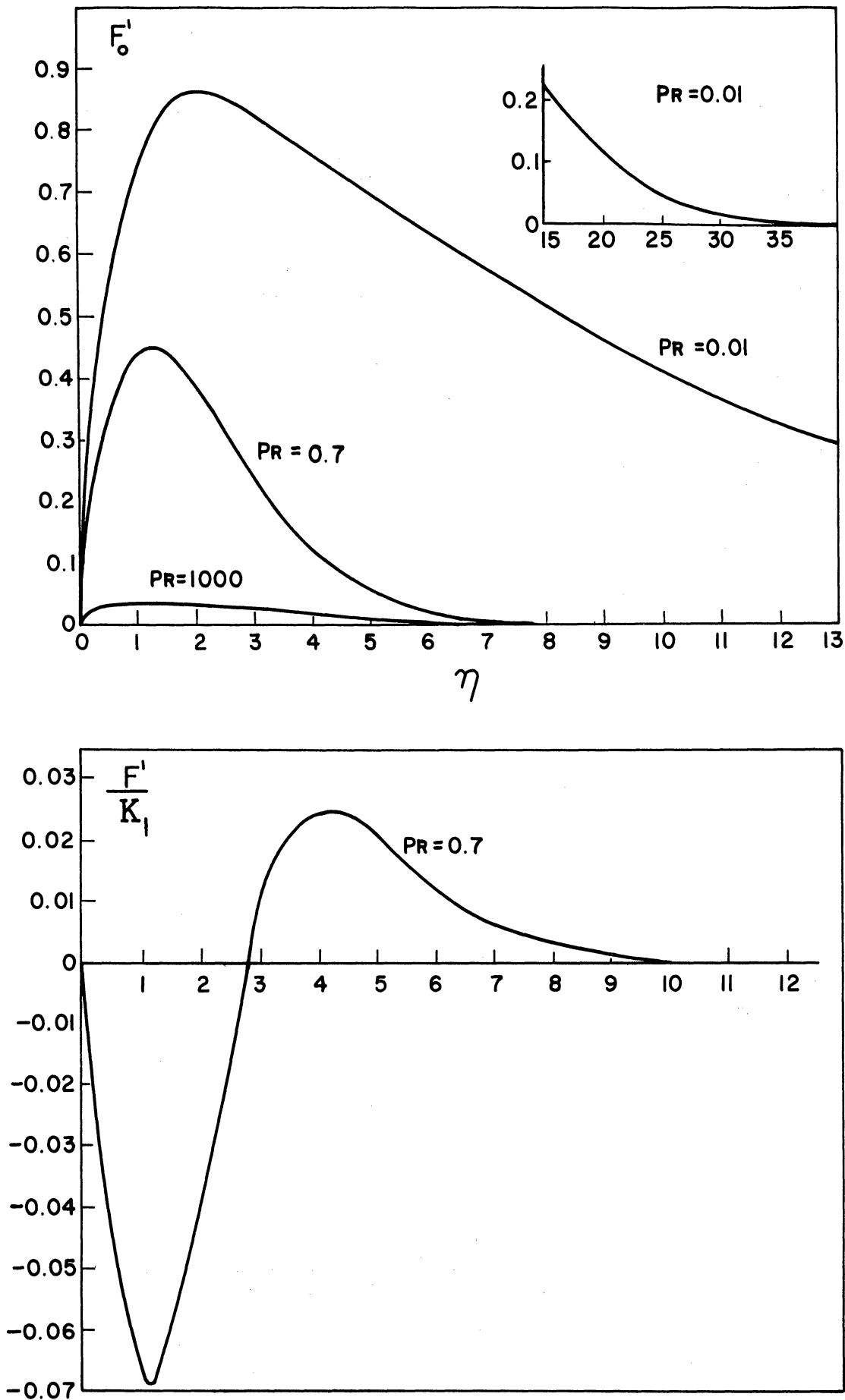


Figure 11. Derivatives of the Zero- and First-Order Stream Functions/
Blunt-Nosed Bodies

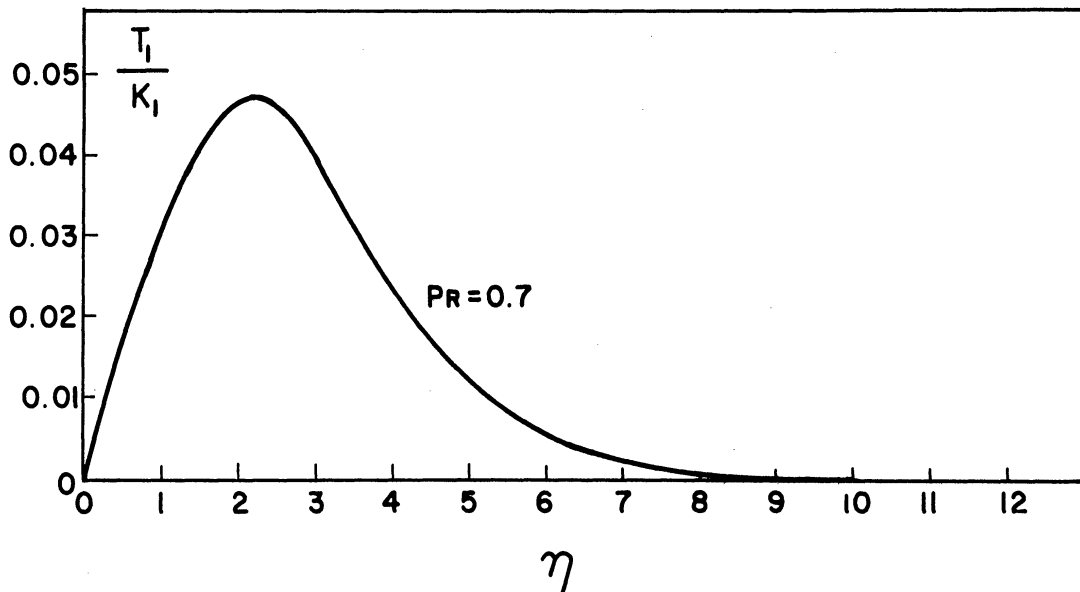
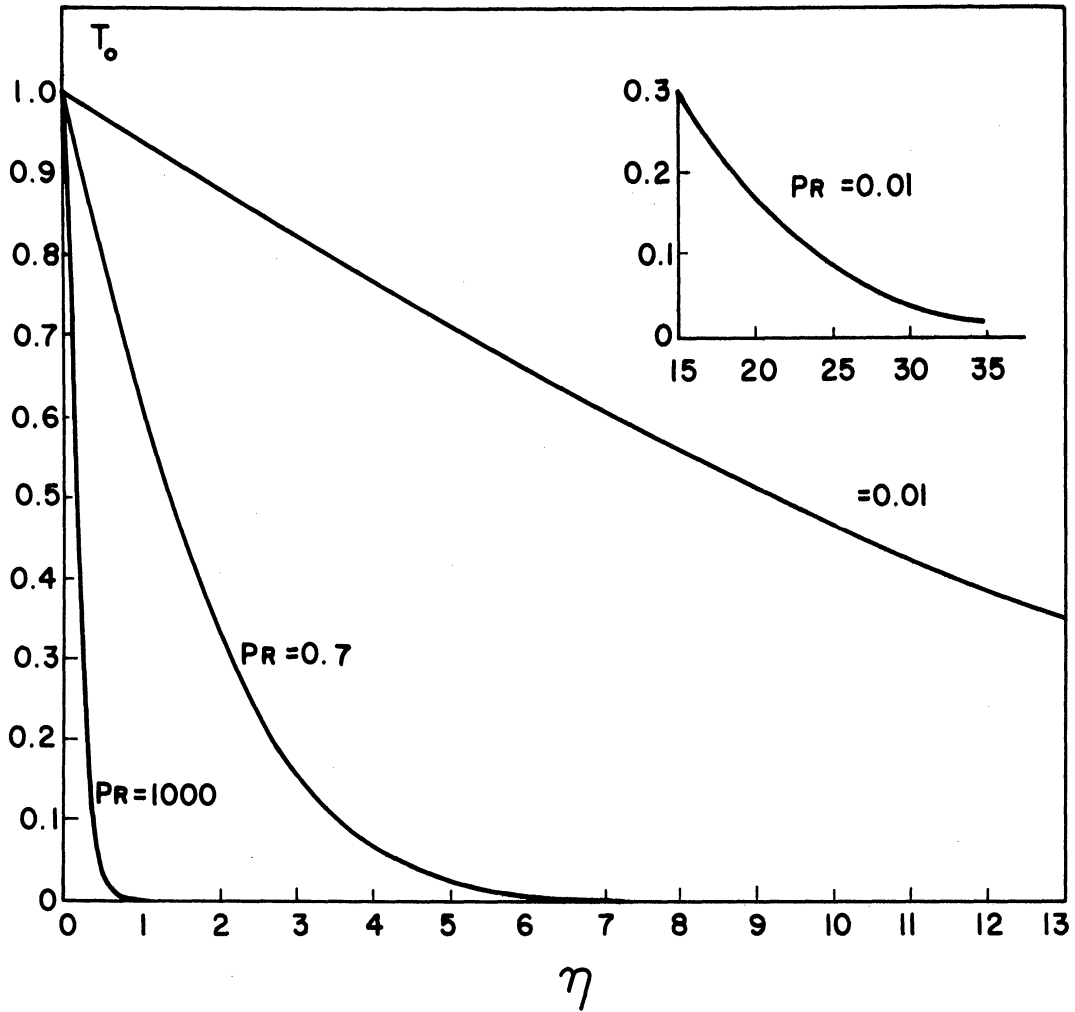


Figure 12. Zero- and First-Order Temperature Functions/Blunt-Nosed Bodies

The influence of the first-order terms will now be examined. Recall, from the previous section, that by comparing the numerical solutions with experimental data it was concluded that only the zero-order terms need be considered if the object is to calculate the derivatives of the temperature or concentration at the surface. This conclusion is now reconsidered by estimating the size of the corrections given by the first-order terms. From Equations (2.60) and (2.64) the local Nusselt number (or Sherwood number) and dimensionless shearing stress at the surface are given, in terms of the scaled variables, for blunt-nosed bodies by

$$Nu Gr^{-1/4} = -\left(\frac{3}{4}\right)^{1/4} [\xi(x)]^{-1/4} [S(x)]^{1/3} \left[T_0'(0) + [\xi(x)]^{3/2} T_1'(0) + \dots \right] \quad (3.5),$$

and

$$\mathcal{T} Gr^{-3/4} = \left(\frac{4}{3}\right)^{1/4} [\xi(x)]^{1/4} [S(x)]^{1/3} \left[E''(0) + [\xi(x)]^{3/2} F_1''(0) + \dots \right] \quad (3.6).$$

The mean values, averaged over a distance \mathcal{L} , are

$$\overline{Nu} Gr^{-1/4} = -\left(\frac{4}{3}\right)^{3/4} \frac{[\xi(\mathcal{L})]^{3/4}}{\mathcal{L}} \left[T_0'(0) + \frac{[\xi(\mathcal{L})]^{3/2}}{3} T_1'(0) + \dots \right] \quad (3.7),$$

$$\overline{\mathcal{T}} Gr^{-3/4} = \frac{4}{5} \left(\frac{4}{3}\right)^{1/4} \frac{[\xi(\mathcal{L})]^{5/4}}{\mathcal{L}} \left[E''(0) + \frac{5}{11} [\xi(\mathcal{L})]^{3/2} F_1''(0) + \dots \right] \quad (3.8).$$

To place a numerical value on the size of the correction due to the first-order terms consider a circular cylinder ($K \doteq -.115$, Appendix A). The maximum correction would be for $\chi = \pi$, ($\xi \doteq 2.59$). The corrections, expressed as (first-order term/zero-order term) 100, are shown in Table IV.

TABLE IV

"FIRST-ORDER CORRECTIONS" TO THE NUSSELT NUMBER AND SURFACE,
SHEAR STRESS (CIRCULAR CYLINDER)

\overline{Pr}	Nu	\overline{Nu}	$\overline{\mathcal{T}}$	$\overline{\overline{\mathcal{T}}}$
.01	16. %	5.4%	7.1%	3.2%
.7	4.2%	1.4%	5.1%	2.3%
1000.	1.6%	.5%	2.5%	1.1%

The results shown in this table, derived from the numerical solutions summarized in Table III, demonstrate that the zero-order terms provide reasonable approximations to the derivatives of the temperature (or concentration) and stream functions. It is true, as was shown on Figure 10, that the first-order terms tend to improve the predictions of local values of the dependent variables. Furthermore, for body contours where the K_j 's are large these corrections may be necessary for accurate predictions of the surface flux densities. This matter must be decided with reference to the body contour in question.

The fact that the importance of the higher order terms increases as the Prandtl number decreases is indicated by an inspection of the differential equation for F (Equation (2.70)). Adopt, for the moment, the scaling which will be used in the next chapter for high Prandtl numbers (i.e., $F \rightarrow \overline{Pr}^{-3/4} F$, $\eta \rightarrow \overline{Pr}^{-1/4} \eta$). The effects of the non-linear terms, which necessitate the series expansion of F , are seen to be "damped" by the large Prandtl number. For small Prandtl

numbers (adopting $F \rightarrow R^{-1/2} F$, $\eta \rightarrow R^{-1/2} \eta$) it is the linear term which is "damped." This supports the observation that as the Prandtl number decreases higher-order terms are necessary for accurate representations of the boundary-layer variables F and T .

The conclusions which are drawn relative to the present method of describing free convection are as follows:

(a) For blunt-nosed bodies the Nusselt number-Prandtl number relation and the surface shear stress-Prandtl number relation can be determined by solving the differential equations for the zero-order terms. This conclusion is expected to apply for other classes of two-dimensional bodies (e.g., sharp-nosed or flat-nosed) and for free convection driven by both temperature and concentration differences.

(b) For those cases where the higher-order terms are necessary, due to the body contour and/or the size of the Prandtl number, then these corrections can be found once and for all (for given values of the parameters Sc , Pr , A , B , σ_T , σ_m) without reference to the body contour in the solution of the differential equations, only the class of the body needs to be considered.

That matter of differences due to the body class is now examined. The numerical results presented thus far have emphasized the class of blunt-nosed bodies. Fortunately, the zero-order terms for the class of sharp-nosed bodies can be derived, in terms of the variables used in this research, from the numerical solutions of Ostrach⁽²²⁾. Although Ostrach studied free convection near a vertical plate, the present work indicates that these results will provide

a reasonable approximation for sharp-nosed bodies, when the results are interpreted in terms of the present variables. The zero-order equations were solved for the class of flat-nosed bodies (see Section 2.5) for a Prandtl number of 1. The results are summarized in Table V, where the results for sharp-nosed and blunt-nosed bodies are given for comparison.

TABLE V
THE EFFECTS OF THE BODY SHAPE CLASS

$Pr =$	<u>.01</u>		<u>1.</u>		<u>1000.</u>	
	<u>$F_0''(\omega)$</u>	<u>$-T_0'(\omega)$</u>	<u>$F_0''(\omega)$</u>	<u>$-T_0'(\omega)$</u>	<u>$F_0''(\omega)$</u>	<u>$-T_0'(\omega)$</u>
Sharp Nosed						
Ostrach ⁽²²⁾	1.297	.0617	.845	.431	.191	3.05
Blunt Nosed	1.169	.0595	.817	.421	.196	3.05
Flat Nosed	---	---	.793	.413	---	---

The differences are surprisingly small. However, the Nusselt number and the dimensionless shear stress are also dependent on the body contour (Equations (3.5) and (3.6)), so these small differences may be changed by the body contours.

3.3 The Effects of the Interfacial Velocity Parameter, B , and the Ackermann Parameter, A , on Simultaneous Heat and Mass Transfer

In the numerical results presented thus far the free convection has been driven by either temperature or concentration effects. The effects of the interfacial velocity parameter, B , and the Ackermann

parameter, A , have been ignored. The argument is that since A and B are both dependent on the characteristic concentration difference (Equation (2.36)) they are, by definition, small in a model which ignores the variations in fluid properties due to concentration. To assess the effect of choosing small but finite values of these parameters the equations for the zero-order terms were integrated for the parameter values shown in Table VI. The tabulated solutions are in Appendix C.

TABLE VI

THE EFFECTS OF THE INTERFACIAL VELOCITY PARAMETER, B , AND THE ACKERMANN PARAMETER, A , FOR FREE CONVECTION AROUND BLUNT-NOSED BODIES ($P_r = S_c = 1.$)

A	B	$F_0''(0)$	$-T_0'(0)$	$-M_0'(0)$	$-\left[T_0'(0) + \frac{P_r}{S_c}(A+B)M_0'(0)\right]$
0	0	1.374	.501	.501	.501
0	.1	1.372	.476	.476	.524
0	-.1	1.376	.530	.530	.477
-.1	.1	1.378	.454	.478	.454

The local Nusselt number, Sherwood number and the dimensionless shear stress at the surface are given by

$$Nu Gr^{-1/4} = -\left(\frac{3}{4}\right)^{1/4} [\xi(x)]^{-1/4} [S(x)]^{1/3} [T_0'(0) + (A+B)M_0'(0)] \quad (3.9),$$

$$Sh Gr^{-1/4} = -\left(\frac{3}{4}\right)^{1/4} [\xi(x)]^{-1/4} [S(x)]^{1/3} M_0'(0) \quad (3.10),$$

$$\tau Gr^{-3/4} = \left(\frac{4}{3}\right)^{1/4} [\xi(x)]^{1/4} [S(x)]^{1/3} F_0''(0) \quad (3.11),$$

in terms of the zero-order solutions. The first observation is that the local surface shear stress is relatively constant. For $B > 0$, the interfacial velocity is directed from the object to the fluid and this flow tends to increase the concentration gradient at the surface, lowering the Sherwood number. The situation is reversed for $B < 0$. This state of affairs is in contrast to the behavior of the Nusselt number where, due to the energy transported by the flow normal to the surface, the Nusselt number increases for $B > 0$ and decreases for $B < 0$. Finally, if the heat capacity of the material undergoing transfer is lower than the heat capacity of the fluid ($A < 0$), the rate of heat transfer is lower than the case where the heat capacities are identical ($A = 0$). In all of these cases the errors which would have been introduced if the parameters A and B had been taken as zero are less than 10 per cent.

CHAPTER 4

Asymptotic Solutions

4.1 General Observations

In the previous chapter it was shown that free convection in two dimensions around submerged objects could be described rather closely by the solutions to three, coupled, ordinary differential equations. Even then the description contains five dimensionless parameters (Pr , Sc , A , B , σ_T and σ_m). The objective of the work reported in this chapter is to ascertain the manner in which changes in the Schmidt and Prandtl numbers affect the rates of transfer from the submerged object to the fluid. One approach might be to correlate the results of numerical solutions for a set of values of the parameters in question. There are two arguments which make this approach rather unappealing. Firstly, a large number of solutions may be needed and secondly, the solutions are difficult to obtain. Numerical solutions were attempted for $Pr = .01, Sc = 1000$ (approximating the properties of a liquid metal) and for $Pr = 10, Sc = 1000$ (a viscous fluid). In both cases the attempts were unsuccessful. The temperature tends toward zero much slower than the concentration in both these situations and "errors," apparently due to the size of the integration steps, caused the stream, temperature and concentration functions to take on unacceptable values. The velocity in the tangential direction became negative in some regions and positive in other regions of the range of the independent variable.

Both temperature and concentration took on negative values. The step sizes used were those suggested from the numerical solutions wherein only one driving force was present (see Appendix C) and, apparently, much smaller step sizes must be used. In view of the amount of computing time involved (the order of hours) were this approach to have been continued it was decided to stop work along these lines.

Another method of describing the effects due to changes in the parameters would be to use one of the approximate methods of solution, such as that described by Meksyn⁽¹⁹⁾. Brindley⁽⁴⁾ used Meksyn's technique for temperature-driven free convection near a vertical plate. The difficulty associated with Brindley's series representations is in the interpretation of the results. Due to the rather cumbersome series expansions it is not at all apparent that, as $Pr \rightarrow \infty$, $Nu \rightarrow (\text{constant})(Gr Pr)^{1/4}$. This result is readily apparent if (say) the numerical solutions or experimental data are examined.

The approach adopted here is to examine the forms of the differential equations as the parameters take on extreme values. As will be demonstrated, this offers reliable information about the effects due to changes in the parameters. Interest is to be centered on the effects of the Schmidt and Prandtl numbers. Within the framework of the constant property assumption the parameters A and B must be small (and will be taken as zero), since both are proportional to the characteristic concentration difference. Some numerical studies

of the effects due to non-zero values of A and B were mentioned in the previous chapter. Acrivos⁽¹⁾ has studied the effect of the interfacial-velocity parameter, B , when it assumes large positive values or values near -1 . The author is not aware of a systematic investigation of the effects of the Ackermann parameter, A . Possibly its effects may be investigated as perturbations on the $A=0$ case. Two body-shape classes are to be considered, sharp- and blunt-nosed. The methods can easily be applied to other classes; e.g., flat-nosed.

In the following sections, rather liberal use will be made of the order symbol " o " (little "oh"). Its meaning is as follows:

$$f(\epsilon) = o(g(\epsilon)) \text{ if, } \lim_{\epsilon \rightarrow 0} \frac{f(\epsilon)}{g(\epsilon)} = 0 \quad (4.1).$$

4.2 Asymptotic Solutions for Lewis Number

The case of the Lewis number (P_r / S_c) equal to unity with A and B both zero will be treated in this section. This is the case for some binary gas mixtures; e.g., for water vapor in air $P_r = .7$ and $S_c = .6$. Fortunately, numerical solutions are available to check the results. The differential equations to be solved are (dropping the subscript zero)

$$\left. \begin{aligned} F''' + FF'' - \left(\frac{2}{3}\right)^6 F'F' + \sigma_r T + \sigma_m M &= 0 \\ T'' + P_r F T' &= 0 \\ M'' + S_c F M' &= 0 \end{aligned} \right\} (4.2),$$

with boundary conditions

$$F(0) = F'(0) = F''(0) = T(\infty) = M(\infty) = 0, T(0) = M(0) = 1 \quad (4.3),$$

where $\delta = 1$ for blunt-nosed bodies while $\delta = 0$ for sharp-nosed bodies. Since the Schmidt and Prandtl numbers are equal $T=M$ and the scaling

$$\left. \begin{aligned} F &= (\sigma_T + \sigma_m)^{1/4} \bar{F} \\ \bar{\eta} &= (\sigma_T + \sigma_m)^{1/4} \eta \end{aligned} \right\} \quad (4.4)$$

reduces the problem to temperature (or concentration) driven free convection. The equations are now (dropping the "over bars")

$$\left. \begin{aligned} F''' + FF'' - \left(\frac{2}{3}\right)^\delta F'F' + T &= 0 \\ T'' + Pr F T' &= 0 \\ F(0) = F'(0) = F''(0) = T(\infty) = 0, T(0) &= 1 \end{aligned} \right\} \quad (4.5).$$

The case of small Prandtl numbers will be examined first. Now, let

$F = Pr^{-1/2} \tilde{F}$, $T = \tilde{T}$ and $\xi = Pr^{1/2} \eta$ so that

$$\left. \begin{aligned} Pr \tilde{F}''' + \tilde{F}\tilde{F}'' - \left(\frac{2}{3}\right)^\delta \tilde{F}'\tilde{F}' + \tilde{T} &= 0 \\ \tilde{T}'' + \tilde{F}\tilde{T}' &= 0 \end{aligned} \right\} \quad (4.6)$$

with the boundary conditions unchanged. Suppose that interest is in

the solution for small Prandtl numbers. If the Prandtl number tends to zero in the equations as they stand, then the highest derivative is lost, and a solution of the equations in this form cannot satisfy all of the boundary conditions. This is the classical indication of what are termed singular perturbation problems. It is now assumed that the equations written without the highest derivative represent the situation in some region away from the origin and another set of equations, wherein the highest derivative is retained, describe the situation near the origin. The former region will be termed the outer region, the latter, the inner region. Two limits are now defined.

The outer limit

$$Pr \rightarrow 0 \quad \text{with} \quad 0 \leq K < \zeta < \infty$$

and the inner limit

$$Pr \rightarrow 0 \quad \text{with} \quad 0 \leq \zeta^* \leq k < \infty, \quad \zeta = \zeta^* Pr^{1/2}$$

The temperature and stream functions are now assumed to take on the forms:

(i) the outer expansions for $Pr \rightarrow 0, 0 \leq K < \zeta < \infty$

$$\tilde{F} \sim \overset{(0)}{f}_0(\zeta) + o(Pr^{1/2})$$

$$\tilde{T} \sim \overset{(0)}{t}_0(\zeta) + o(Pr^{1/2})$$

} (4.7),

(ii) the inner expansions for

$$\left. \begin{aligned} \tilde{F} &\sim Pr^{1/2} f_i^{(0)}(\zeta^*) + o(Pr^{1/2}) \\ \tilde{T} &\sim t_i^{(0)}(\zeta^*) + o(Pr^{1/2}) \end{aligned} \right\} \quad (4.8),$$

where the higher order terms are taken as being small as $Pr \rightarrow 0$.

Now, upon substituting the outer expansions into the differential equations and taking the outer limit one finds

$$\left. \begin{aligned} f_0'' f_0'' - \left(\frac{2}{3}\right) f_0' f_0' + t_0 &= 0 \\ t_0'' + f_0' t_0' &= 0 \end{aligned} \right\} \quad (4.9),$$

while following a similar procedure with the inner expansions and the inner limit results in

$$\left. \begin{aligned} f_i''' + f_i' f_i'' - \left(\frac{2}{3}\right) f_i'' f_i' + t_i &= 0 \\ t_i'' &= 0 \end{aligned} \right\} \quad (4.10).$$

The boundary conditions at the origin are to be used with the "inner equations" and those at infinity with the "outer equations." There are undetermined constants to be evaluated since there are an insufficient number of boundary conditions for either set of equations. These constants are determined by requiring that the inner and outer expansions match to terms of the same order in the Prandtl number, since they are assumed to represent the same function. Fortunately

the equations can be solved explicitly for temperature to give

$$\left. \begin{aligned} \bar{t}_0^{(0)}(\zeta) &= a + b \int_0^\zeta \exp\left(-\int_0^{x_2} \bar{f}_0^{(0)}(x_1) dx_1\right) dx_2 \\ (-b)^{-1} &= \bar{a}^{-1} \int_0^\infty \exp\left(-\int_0^{x_1} \bar{f}_0^{(0)}(x_2) dx_2\right) dx_1 \end{aligned} \right\} \quad (4.11),$$

$$\bar{t}_i^{(0)}(\zeta^*) = 1 + C \zeta^* \quad (4.12).$$

Now, in order to determine the constants "a" and "C," the outer solution is written in terms of the inner variables and the inner limit process applied to give

$$\bar{T} \sim a + b \zeta^* P_r^{1/2}, \quad P_r \rightarrow 0, \quad 0 \leq \zeta^* \leq K < \infty \quad (4.13).$$

The analogous process applied to the inner solution gives

$$\bar{T} \sim 1 + C \zeta P_r^{-1/2}, \quad P_r \rightarrow 0, \quad 0 \leq K < \zeta < \infty \quad (4.14).$$

So, if both series are to match to terms of order $o(P_r^{1/2})$, then

$$a = 1, \quad C = 0 \quad (4.15).$$

Now, the differential equations for the stream functions are

$$\bar{f}_0'' \bar{f}_0'' - \left(\frac{2}{3}\right) \bar{f}_0' \bar{f}_0' + \bar{t}_0 = 0 \quad (4.16),$$

$$\bar{f}_i''' + \bar{f}_i' \bar{f}_i'' - \left(\frac{2}{3}\right) \bar{f}_i' \bar{f}_i' + 1 = 0 \quad (4.17),$$

where $\bar{t}_0^{(0)}(\zeta)$ is given by Equation (4.11). Closed expressions for $\bar{f}_i^{(0)}$ and $\bar{f}_0^{(0)}$ are not known, but each expression would contain one

undetermined constant, so the argument is as follows. The inner expansion for the stream function under the outer limit process is

$$\tilde{F} \sim P_r^{1/2} f_i^{(0)}(\infty) \quad (4.18),$$

while if the function $f_o^{(0)}(\zeta)$ has a series expansion

$$f_o^{(0)}(\zeta) = f_o^{(0)} + f_o^{(0)'} \zeta + \dots \quad (4.19),$$

than under the inner limit it takes the form

$$\tilde{F} \sim f_o^{(0)} + f_o^{(0)'} P_r^{1/2} \zeta^* + \dots \quad (4.20).$$

Now if the perturbation series are to match to terms of order $o(P_r^{1/2})$ then

$$f_o^{(0)} = 0, \quad f_i^{(0)}(\infty) = f_o^{(0)'} \zeta^* \quad (4.21).$$

The function $f_o^{(0)'} \zeta^*$ is a solution for Equation (4.17), if, for $\delta = 0$,

$$f_o^{(0)'} = 1 \quad (4.22)$$

and if, for $\delta = 1$,

$$f_o^{(0)'} = \left(\frac{3}{2}\right)^{1/2} \quad (4.23).$$

In summary, the inner problem is:

for $\delta = 0$,

$$\left. \begin{aligned} f_i^{(0)''''} + f_i^{(0)'} f_i^{(0)''} - f_i^{(0)'} f_i^{(0)'} + 1 &= 0 \\ f_i^{(0)} = f_i^{(0)'} &= 0, \quad f_i^{(0)'}(\infty) = 1 \end{aligned} \right\} \quad (4.24),$$

and for $\delta = 1$,

$$\left. \begin{aligned} \phi_i'''' + \phi_i' \phi_i'' - \frac{2}{3} \phi_i' \phi_i' + 1 &= 0 \\ \phi_i(0) = \phi_i'(0) = 0, \quad \phi_i'(\infty) &= \left(\frac{3}{2}\right)^{1/2} \end{aligned} \right\} (4.25).$$

The problem given by Equation (4.24) is the same as that for the boundary-layer flow past a wedge of included angle π , (where the mainstream velocity is $U = U_0 x$ i.e., stagnation or Hiemenz flow⁽²⁵⁾).

On the other hand, if one makes the substitutions

$$\left. \begin{aligned} \phi_i(\zeta) &= \left(\frac{3}{2}\right)^{1/4} h(y) \\ y &= \left(\frac{3}{2}\right)^{1/4} \zeta^* \end{aligned} \right\} (4.26),$$

Equations (4.25) become

$$\left. \begin{aligned} h'''' + h h'' + \frac{2}{3} (1 - h' h) &= 0 \\ h(0) = h'(0) = 0, \quad h'(\infty) &= 1 \end{aligned} \right\} (4.27).$$

However, this is the same differential equation and boundary conditions as that for the boundary-layer flow past a wedge of included angle $2\pi/3$, (where the mainstream velocity is $U = U_0 x^{1/2}$). The numerical solutions for both of the inner-flow problems, sometimes called the Falkner-Skan equations, are available (Schlichting⁽²⁵⁾, p. 144)*.

* The author is indebted to Professor J. D. Goddard for pointing out the correspondence between the inner flow problems and the Falkner-Skan equations.

Thus, the inner-flow problems can be regarded as solved, to the order of the terms retained.

The outer problem is

$$\left. \begin{aligned} \frac{\partial^2 \theta_0^{(0)}}{\partial \eta^2} - \left(\frac{2}{3}\right) \frac{\partial \theta_0^{(0)}}{\partial \eta} \frac{\partial \theta_0^{(0)}}{\partial \xi} + \theta_0^{(0)} &= 0 \\ \theta_0^{(0)} + \frac{\partial \theta_0^{(0)}}{\partial \xi} &= 0 \end{aligned} \right\} \quad (4.28),$$

with $\theta_0^{(0)} = 1$, $\frac{\partial \theta_0^{(0)}}{\partial \eta}(0) = \frac{\partial \theta_0^{(0)}}{\partial \eta}(\infty) = \theta_0^{(0)}(\infty) = 0$

For $\delta = 0$, these equations have already been solved numerically by LeFevre⁽¹⁶⁾, who reports $\theta_0^{(0)}(0) = -.645$

The dimensionless shear stress at the surface, \mathcal{T} , is given by

$$\mathcal{T} = Gr^{3/4} \left[\Psi_{,yy} \right]_{y=0} \quad (2.64).$$

Taking all of the various changes of variables into account, one finds that the dimensionless shear stress is

$$\mathcal{T} = Gr^{3/4} (\sigma_r + \sigma_m)^{3/4} \left(\frac{4}{3}\right)^{1/4} [S(x)]^{2/3} [\xi(x)]^{1/4} \theta_0^{(0)} \quad (4.29),$$

to terms of order $o(P_r^{1/2})$, within the framework of the boundary-layer theory developed in the previous chapter. Hence, as the Prandtl number tends to zero the description of free convection tends to approach that of a forced-convection problem in the region near the surface of the object. Accordingly, the shear stress approaches a limit independent of the Prandtl number.

The dimensionless flux densities for heat or mass transfer, i.e., the Nusselt or Sherwood numbers, are not found easily. First of all, according to the inner expansion for the temperature function, the gradient of the temperature is zero at the surface of the object. To obtain an approximation to the heat-flux density, (or the mass-flux density since $T = M$), note that from Equations (4.6)

$$-\tilde{T}'(0) = \int_0^{\infty} \tilde{F} \tilde{T}' d\alpha_1 \quad (4.30).$$

Now applying the outer limit process and assuming that the limit and integration processes can be interchanged one finds

$$-\tilde{T}'(0) = \lim_{P_r \rightarrow 0} \int_0^{\infty} \tilde{F} \tilde{T}' d\alpha_1 = \int_0^{\infty} \tilde{F}_0^{(0)} \tilde{T}'_0 d\alpha_1 + o(P_r^{1/2}) \quad (4.31).$$

This may also be shown by writing Equation (4.30) as

$$-\tilde{T}'(0) = \int_0^{\infty} (\tilde{F} \tilde{T}' - \tilde{F}_0^{(0)} \tilde{T}'_0) d\alpha_1 + \int_0^{\infty} \tilde{F}_0^{(0)} \tilde{T}'_0 d\alpha_1 \quad (4.32).$$

Now, writing the first integral in Equation (4.32) as

$$\int_0^{mP_r^{1/2}} (\tilde{F} \tilde{T}' - \tilde{F}_0^{(0)} \tilde{T}'_0) d\alpha_1 + \int_{mP_r^{1/2}}^{\infty} (\tilde{F} \tilde{T}' - \tilde{F}_0^{(0)} \tilde{T}'_0) d\alpha_1 \quad (4.33),$$

with $0 < m < \infty$, one notes that in the second term in (4.33), α_1 is restricted to the domain called the outer region as $P_r \rightarrow 0$. Hence the limit of the second term of (4.33) as $P_r \rightarrow 0$ is order $o(P_r^{1/2})$, according to the series postulated for \tilde{F} and \tilde{T} (Equations (4.7)). From the mean-value theorem of calculus the first term in (4.33) is also indicated as order $o(P_r^{1/2})$. So, once again, as $P_r \rightarrow 0$

$$-\tilde{T}'(0) = \int_0^{\infty} \frac{\partial}{\partial x_1} t_0^{(0)} dx_1 + o(P_r^{1/2}) \quad (4.34).$$

Then, from Equations (4.28),

$$\int_0^{\infty} \frac{\partial}{\partial x_1} t_0^{(0)} dx_1 = - \int_0^{\infty} \frac{\partial}{\partial x_1} t_0^{(0)} dx_1 = -t_0^{(0)}(0) \quad (4.35)$$

and so

$$\tilde{T}'(0) = t_0^{(0)}(0), \quad P_r \rightarrow 0 \quad (4.36).$$

Now, returning to the original variables, one finds that

$$Nu = Sh = G_r^{1/4} (\alpha_T + \alpha_M)^{1/4} P_r^{1/2} \left(\frac{3}{4}\right)^{1/4} [S(x)]^{1/4} [\Xi(x)]^{-1/4} [-t_0^{(0)}] \quad (4.37).$$

The number $-t_0^{(0)}(0)$ is given by the solution of the appropriate equations and, as has been mentioned, is 0.645 for $\delta = 1$. In the case where $\delta = 1$ a very good approximation can also be obtained from the numerical solution of Ostrach⁽²²⁾ for $P_r = .01$ since

$$\tilde{T}'(0) = \tilde{T}'(0) P_r^{1/2} \sim t_0^{(0)}(0) P_r^{1/2}, \quad P_r \rightarrow 0 \quad (4.38).$$

For $P_r = .01$, Ostrach reports $\tilde{T}'(0) = -.0616$, in terms of the problem as stated by Equations (4.5), hence, $t_0^{(0)}(0) = -.616$. This result differs from the value obtained by LeFevre⁽¹⁶⁾ by less than 5 per cent. For $\delta = 0$, the approximate value obtained from the numerical results reported in Chapter 3 is $t_0^{(0)}(0) = -.593$.

The case wherein the Prandtl number is large will now be examined. The writer has been unable to develop a formal, but systematic, treatment of this case which utilizes the concept of matched

expansions. As an alternative, a scaling is sought which simplifies the problem.

Let the transformation of variables be

$$\left. \begin{aligned} \bar{F}(\bar{\eta}) &= P_r^{-3/4} \tilde{F}(\zeta) \\ \bar{T}(\bar{\eta}) &= \tilde{T}(\zeta) \\ \zeta &= P_r^{1/4} \bar{\eta} \end{aligned} \right\} (4.39).$$

Then the problem, as stated in Equations (4.5), is

$$\left. \begin{aligned} \tilde{F}''' + P_r^{-1} (\tilde{F} \tilde{F}'' - \tilde{F}' \tilde{F}') + \tilde{T} &= 0 \\ \tilde{T}'' + \tilde{F} \tilde{T}' &= 0 \end{aligned} \right\} (4.40)$$

with the boundary conditions unchanged. Now, since the Prandtl number is large the "inertial" or non-linear terms are neglected and the result is

$$\left. \begin{aligned} \tilde{F}''' + \tilde{T} &= 0 \\ \tilde{T}'' + \tilde{F} \tilde{T}' &= 0 \end{aligned} \right\} (4.41).$$

The boundary condition on \tilde{F}' as $\zeta \rightarrow \infty$ must be discarded, since, as will become apparent, it cannot be satisfied. The solution to this set of equations, with the appropriate boundary conditions is

$$\left. \begin{aligned}
 \tilde{F}(\zeta) &= - \int_0^{\zeta} \int_0^{x_3} \int_0^{x_2} \tilde{T} dx_1 dx_2 dx_3 + \tilde{F}''(\omega) \zeta^2 / 2 \\
 \tilde{T}(\zeta) &= 1 + \tilde{T}'(\omega) \int_0^{\zeta} \exp(-\int_0^{x_2} \tilde{F} dx_1) dx_2 \\
 [-T(\omega)]^{-1} &= \int_0^{\infty} \exp(-\int_0^{x_2} \tilde{F} dx_1) dx_2
 \end{aligned} \right\} (4.42).$$

From this solution it can be readily shown, from an integration by parts, that

$$\tilde{F}'(\zeta) = \tilde{T}'(\omega) \frac{\zeta^2}{2} \int_0^{\infty} \tilde{q}(x_1) dx_1 + \left[\tilde{F}''(\omega) + \tilde{T}'(\omega) \int_0^{\zeta} x_1 \tilde{q}(x_1) dx_1 \right] \zeta + \int_0^{\zeta} \frac{x_1^2}{2} \tilde{q}(x_1) dx_1, \quad (4.43),$$

where

$$\tilde{q}(x_1) = \exp(-\int_0^{x_1} \tilde{F} dx_1) \quad (4.44).$$

So, for large ζ , $\tilde{F}'(\zeta)$ is proportional to ζ unless the second term on the right in Equation (4.43) is made to vanish as ζ tends to infinity. In this case, $\tilde{F}'(\zeta)$ approaches a constant. Requiring that the second term vanish is equivalent to setting $\tilde{F}''(\omega)$ equal to zero. Now, returning to the original variables, one finds that

$$\begin{aligned}
 \bar{F}'(\bar{\eta}) &= \tilde{T}'(\omega) \frac{\bar{\eta}^2}{2} \int_0^{\infty} \tilde{q}(x_1) dx_1 + \left[\tilde{F}''(\omega) + \tilde{T}'(\omega) \int_0^{\bar{\eta} P_T^{1/4}} x_1 \tilde{q}(x_1) dx_1 \right] \bar{\eta} P_T^{-1/4} + \\
 &\quad P_T^{-1/2} \int_0^{\bar{\eta} P_T^{1/4}} \frac{x_1^2}{2} \tilde{q}(x_1) dx_1
 \end{aligned} \quad (4.45).$$

So with $\bar{\eta}$ fixed as $0 < k \leq \bar{\eta}$, the limit of $\bar{F}'(\bar{\eta})$ as the Prandtl number becomes large is

$$\lim_{Pr \rightarrow \infty} \bar{F}(\bar{\eta}) = o(Pr^{-1/4}) \quad (4.46),$$

when the condition $\tilde{F}''(\infty) = 0$ is used. Thus, the boundary condition on \bar{F}' is satisfied to the order $o(Pr^{-1/4})$.

The problem given by Equations (4.41) with the boundary condition $\tilde{F}''(\infty) = 0$ was solved numerically by LeFevre,⁽¹⁶⁾ who found $\tilde{F}''(0) = 1.08$ and $\tilde{T}'(0) = -.540$. Numerical methods, however, are not necessary for obtaining rather accurate approximations to these derivatives.

The problem is to evaluate the integrals

$$-\tilde{F}''(0) = \tilde{T}'(0) \int_0^{\infty} x \tilde{g}(x) dx, \quad (4.47)$$

and

$$[-\tilde{T}'(0)]^2 = \int_0^{\infty} \tilde{g}(x) dx, \quad (4.48),$$

when $\tilde{g}(x)$ is given by Equation (4.44). The Laplace method, as described by Erdelyi,⁽¹⁰⁾ will be used. The first two terms in a power series for $\tilde{F}(x)$ are used as an approximation, viz.,

$$\tilde{F}(x) = \tilde{F}(0) \frac{x^2}{2} - \frac{\chi_1^3}{6} + \dots \quad (4.49).$$

Now, if the integrand is expanded by using the expansion for $\tilde{F}(x)$ and then the integration carried out, one has

$$-\tilde{F}''(0) = \tilde{T}'(0) \left[2 \cdot 6^{-1/3} \Gamma(2/3) [\tilde{F}''(0)]^{-2/3} + 2^{-1} [\tilde{F}''(0)]^{-2} \right] \quad (4.50),$$

$$[-\tilde{T}'(0)] = 2 \cdot 6^{-2/3} \Gamma(1/3) [\tilde{F}''(0)]^{-1/3} + 2^{-1} \cdot 6^{-1/3} \Gamma(5/3) [\tilde{F}''(0)]^{-5/3} \quad (4.51),$$

where $\Gamma(\rho)$ denotes the "gamma function." The solution to this set of Equations is $\tilde{F}''(0) = 1.04$ and $\tilde{T}'(0) = -0.546$. This technique will be employed later for the simultaneous heat and mass transfer when the Schmidt and Prandtl numbers are not equal.

Thus, for large Prandtl numbers, the dimensionless shear stress at the surface is

$$\tau = G_F^{3/4} (\sigma_T + \sigma_m)^{3/4} P_F^{-1/4} \left(\frac{4}{3}\right)^{1/4} [S(x)]^{1/3} [\xi(x)]^{1/4} \tilde{F}''(0) \quad (4.52).$$

The Nusselt number is

$$Nu = G_F^{1/4} (\sigma_T + \sigma_m)^{1/4} P_F^{1/4} \left(\frac{3}{4}\right)^{1/4} [S(x)]^{1/3} [\xi(x)]^{-1/4} [-\tilde{T}'(0)] \quad (4.53).$$

It should be noted that in this approximation, for large Prandtl numbers, there is no distinction as to the class of the two-dimensional body.

The results given in this section show that for equal Schmidt and Prandtl numbers the effects of heat and mass transport are additive (in the absence of heat capacity effects and for small interfacial velocities; i.e., $A = B = 0$). Thus an "effective" Grashof number may be written as

$$G_F^* = G_F (\sigma_T + \sigma_m) = \frac{g \beta \Delta \theta L^3}{\nu_\infty^2} + \frac{g \chi \Delta \omega L^3}{\nu_\infty^2} \quad (4.54).$$

So, many of the experimental and theoretical analyses for a single "driving force" may be taken to apply for situations where both temperature and concentration contribute to the density differences within the fluid. Apparently, this result was first noted by Nusselt⁽²¹⁾ in 1930. The one-quarter power dependence on the Prandtl number was given by Lorenz⁽¹⁷⁾ in 1881, based, however, on some rather questionable assumptions. LeFevre⁽¹⁶⁾, in 1956, showed that the high and low Prandtl number behavior could be obtained from a scaling of the differential equations. The boundary conditions were obtained from "physical arguments" rather than by the more systematic method employed here.

4.3 Asymptotic Solutions for Large Schmidt Numbers and Small Prandtl Numbers

This situation is expected to obtain in liquid metal systems where, although the kinematic viscosity may be of the same order of magnitude as for other viscous liquids, the high thermal diffusivity leads to a small Prandtl number. The Schmidt number is high due to a low molecular diffusivity, which is a characteristic of liquids. If the scalings $F = Pr^{-1/2} \tilde{F}$, $T = \tilde{T}$, $M = \tilde{M}$ and $\zeta = Pr^{1/2} \eta$, along with Equations (4.2) and the boundary conditions, Equations (4.3), are adopted, then

$$\left. \begin{aligned} \tilde{F}''' + \tilde{F} \tilde{F}'' - \left(\frac{2}{3}\right) \tilde{F}' \tilde{F}' + \alpha_T \tilde{T} + \alpha_m \tilde{M} &= 0 \\ \tilde{T}'' + \tilde{F} \tilde{T}' &= 0 \\ \tilde{M}' + \frac{Sc}{Pr} F \tilde{M}' &= 0 \end{aligned} \right\} (4.55),$$

along with

$$\tilde{F}(0) = \tilde{F}'(0) = \tilde{F}'(\infty) = \tilde{T}(\infty) = \tilde{M}(\infty) = 0, \tilde{T}(0) = \tilde{M}(0) = 1 \quad (4.56).$$

Now, on assuming out and inner expansions, along with the appropriate limits, as was done before in Section 4.2, one finds that the outer and inner equations are

$$\left. \begin{aligned} f_0^{(0)} f_0'' - \left(\frac{2}{3}\right) f_0^{(0)} f_0' + \sigma_T t_0^{(0)} &= 0 \\ t_0'' + f_0^{(0)} t_0' &= 0 \end{aligned} \right\} \quad (4.57),$$

and

$$\left. \begin{aligned} f_i''' + f_i^{(0)} f_i'' - \left(\frac{2}{3}\right) f_i^{(0)} f_i' + \sigma_T + \sigma_m m_i^{(0)} &= 0 \\ m_i'' + S_c f_i^{(0)} m_i' &= 0 \end{aligned} \right\} \quad (4.58).$$

The correct solutions for $m_0^{(0)}$ and $t_i^{(0)}$ are zero and unity respectively. For $|\beta \Delta \theta| \geq |\delta \Delta \omega|, \sigma_T = 1$ (see Equation (2.56)). In this event $\sigma_m \leq 1$ and the effect of concentration (mass transfer) is to be treated as a perturbation on forced convection in the inner region. The first approximation is as follows. In the inner and outer regions the temperature problem is the same as that treated in Section 4.2 and, therefore, the shear stress and heat transfer rate are given by Equations (4.29) and (4.37). If, to a first approximation, the stream function is assumed to be independent of mass transfer effects the

Laplace method can, once again, be used to evaluate the mass flux density at the surface. From the equation for $\overline{m}_i^{(o)}$ it follows that

$$[-\overline{m}_i^{(o)}]^{-1} = \int_0^\infty \exp(-Sc \int_0^{x_2^{(o)}} f_i' dx_1) dx_2 \quad (4.59).$$

Here, the fact that the Schmidt number is large can be used to advantage, since only the first term in the expansion for $f_i^{(o)}$ needs to be used. The result is

$$[-\overline{m}_i^{(o)}]^{-1} = 2 \cdot 6^{-2/3} \Gamma(1/3) [f_i^{(o)''}]^{1/3} Sc^{-1/3} \quad (4.60),$$

where $f_i^{(o)''}$ is obtained from the proper solution to the Falkner-Skan equations (see Section 4.2). Finally, the dimensionless mass-flux density is

$$Sh = Gr^{1/4} Pr^{1/2} Sc^{1/3} 2^{-1} 6^{-2/3} \left(\frac{3}{4}\right)^{1/4} [\Gamma(1/3)]^{-1} [S(x)]^{1/3} [\xi(x)]^{-1/4} [f_i^{(o)''}]^{1/3} \quad (4.61).$$

Free convection superimposed on a forced-convection and vice versa have been studied by Brindley⁽⁴⁾, using the Meksyn method which was mentioned in Section 4.1. For those situations where mass transfer effects are large, $|\delta \Delta \omega| > |\beta \Delta \theta|$, Brindley's approach should also be used in the present problem. For sharp-nosed bodies Brindley's results, in the form of asymptotic series, also indicate the one-third power dependence on the Schmidt number, for large Schmidt numbers. Brindley's method is a much more involved process than the technique used here, but it appears that such a method would have to be used to develop corrections to the present results.

4.4 Asymptotic Solutions for Large Schmidt and Prandtl Numbers

Heat and mass transfer in viscous fluids, such as water or oil, are characterized by large Schmidt and Prandtl numbers (relative to unity). The Schmidt number is usually much greater than the Prandtl number since the molecular diffusivity of binary liquid systems is $\sim 10^{-5} \text{cm}^2/\text{sec}$. For example, simultaneous heat and mass transfer in systems where water is the solvent would be characterized by Prandtl numbers of ~ 10 and Schmidt numbers of ~ 1000 . To analyze this situation a procedure similar to that of Section 4.2 is adopted. Equations (4.2) and the boundary conditions, Equations (4.3), are scaled according to

$$\left. \begin{aligned} F(\eta) &= Pr^{-3/4} \tilde{F}(\zeta) \\ T(\eta) &= \tilde{T}(\zeta) \\ M(\eta) &= \tilde{M}(\zeta) \\ \zeta &= Pr^{1/4} \eta \end{aligned} \right\} (4.62),$$

and the boundary condition $\tilde{F}''(\infty) = 0$ is used. Thus, the differential equations become, for large Schmidt and Prandtl numbers,

$$\left. \begin{aligned} \tilde{F}''' + \sigma_T \tilde{T} + \sigma_M \tilde{M} &= 0 \\ \tilde{T}'' + \tilde{F} \tilde{T}' &= 0 \\ \tilde{M}'' + \frac{Sc}{Pr} \tilde{F} \tilde{M}' &= 0 \end{aligned} \right\} (4.63),$$

with boundary conditions

$$\tilde{F}(0) = \tilde{F}'(0) = \tilde{F}'(\infty) = \tilde{T}(\infty) = \tilde{M}(\infty) = 0, \quad \tilde{T}(0) = \tilde{M}(0) = 1 \quad (4.64).$$

Now, the first two terms in a series expansion for \tilde{F} , viz.,

$$\tilde{F}(\xi) = \tilde{F}''(0) \frac{\xi^2}{2} - (\sigma_T + \sigma_M) \frac{\xi^3}{6} + \dots \quad (4.65),$$

are used with the Laplace method to evaluate the following integrals, which are obtained in the manner outlined in Section 4.2,

$$-\tilde{F}''(0) = \tilde{T}(0) \sigma_T \int_0^\infty x_1 \tilde{g}(x_1) dx_1 + \tilde{M}(0) \sigma_M \int_0^\infty x_1 \tilde{h}(x_1) dx_1 \quad (4.66),$$

$$[\tilde{T}(0)]^{-1} = \int_0^\infty \tilde{g}(x_1) dx_1 \quad (4.67),$$

$$[\tilde{M}(0)]^{-1} = \int_0^\infty \tilde{h}(x_1) dx_1 \quad (4.68),$$

where,

$$g(x_1) = \exp\left(-\int_0^{x_1} \tilde{F} dx\right) \quad (4.69),$$

and

$$h(x_1) = \exp\left(-\frac{Sc}{Pr} \int_0^{x_1} \tilde{F} dx\right) \quad (4.70).$$

The following results are found:

$$-\tilde{F}''(o) = \tilde{T}'(o)\sigma_T \left[2 \cdot \bar{c}^{-1/3} \Gamma(2/3) [\tilde{F}''(o)]^{-2/3} + (\sigma_T + \sigma_M) \bar{z}^{-1} [\tilde{F}''(o)]^{-2} \right] + \quad (4.71),$$

$$\tilde{M}'(o)\sigma_M \left[2 \cdot \bar{c}^{-1/3} \Gamma(2/3) [\tilde{F}''(o)]^{-2/3} \left(\frac{S_C}{P_T} \right)^{-2/3} + (\sigma_T + \sigma_M) \bar{z}^{-1} [\tilde{F}''(o)]^{-2} \left(\frac{S_C}{P_T} \right)^{-2} \right]$$

$$[-\tilde{T}'(o)]^{-1} = 2 \cdot \bar{c}^{-2/3} \Gamma(1/3) [\tilde{F}''(o)]^{-1/3} + (\sigma_T + \sigma_M) \bar{z}^{-1} \bar{c}^{-1/3} \Gamma(5/3) [\tilde{F}''(o)]^{-5/3} \quad (4.72),$$

$$[-\tilde{M}'(o)]^{-1} = 2 \cdot \bar{c}^{-2/3} \Gamma(1/3) [\tilde{F}''(o)]^{-1/3} \left(\frac{S_C}{P_T} \right)^{-1/3} + (\sigma_T + \sigma_M) \bar{z}^{-1} \bar{c}^{-1/3} \Gamma(5/3) [\tilde{F}''(o)]^{-5/3} \left(\frac{S_C}{P_T} \right)^{-5/3} \quad (4.73).$$

Defining, now, a_1, a_2, b_1, b_2 , as

$$\begin{aligned} a_1 &\triangleq 2 \cdot \bar{c}^{-1/3} \Gamma(1/3), & a_2 &\triangleq (\sigma_T + \sigma_M) \bar{z}^{-1} \\ b_1 &\triangleq 2 \cdot \bar{c}^{-2/3} \Gamma(2/3), & b_2 &\triangleq (\sigma_T + \sigma_M) \bar{z}^{-1} \bar{c}^{-1/3} \Gamma(5/3) \end{aligned} \quad (4.74),$$

one obtains the equation for $\tilde{F}''(o), (=X)$,

$$\begin{aligned} &b_1^2 X^{12/3} + [b_1 b_2 (1 + \left(\frac{S_C}{P_T} \right)^{-4/3}) - a_1 b_1 (\sigma_T + \sigma_M \left(\frac{S_C}{P_T} \right)^{-1/3})] X^{8/3} + \\ &[b_2^2 \left(\frac{S_C}{P_T} \right)^{-4/3} - a_1 b_2 (\sigma_T \left(\frac{S_C}{P_T} \right)^{-4/3} + \sigma_M \left(\frac{S_C}{P_T} \right)^{-1/3}) - a_2 b_1 (\sigma_T + \sigma_M \left(\frac{S_C}{P_T} \right)^{-5/3})] X^{4/3} \\ &- a_2 b_2 \left(\frac{S_C}{P_T} \right)^{-4/3} (\sigma_T + \sigma_M \left(\frac{S_C}{P_T} \right)^{-1/3}) = 0 \end{aligned} \quad (4.75).$$

This is a cubic equation in $X^{4/3}$ which can be solved to evaluate $\tilde{F}''(o)$ and hence, $\tilde{T}'(o)$ and $\tilde{M}'(o)$. The results for three specific cases are shown in Table VII. Mathers, Madden and Piret⁽¹⁸⁾ used an analog

computer to solve the same set of differential equations (Equations (4.63)) for the cases noted in the table and their results are shown for comparison.

TABLE VII.

APPROXIMATE SOLUTIONS FOR LARGE SCHMIDT AND PRANDTL NUMBERS

σ_T	σ_m	Sc/Pr	Approximate Solution		Mathers, et al ⁽¹⁸⁾	
			$-\tilde{T}'(0)$	$-\tilde{M}'(0)$	$-\tilde{T}'(0)$	$-\tilde{M}'(0)$
1	1	2	.614	.847	.616	.812
1	.5	2	.585	.804	.585	.760
1	1	4	.594	1.08	.594	1.01

Mathers, Madden and Piret correlated their results, using forms suggested by Somers⁽²⁸⁾. Somers, as was mentioned in Chapter 1, investigated the simultaneous transfer processes from a vertical plate using the "integral method." The correlations found are

$$-\tilde{T}'(0) = \text{constant} \left[\sigma_T + \sigma_m \left(\frac{Pr}{Sc} \right)^{1/2} \right]^{1/4} \quad (4.76),$$

$$-\tilde{M}'(0) = \text{constant} \left[\sigma_T + \sigma_m \left(\frac{Pr}{Sc} \right)^{1/2} \right]^{1/4} \left(\frac{Sc}{Pr} \right)^{3/8} \quad (4.77),$$

where the constant is approximately 0.54 in both cases. The results from the approximate method, used in this section, can be treated in the same manner, although the constant in Equation (4.77) is slightly different (0.575).

Equation (4.75) indicates that as the ratio Pr/Sc approaches zero, $\tilde{F}''(0)$ and $\tilde{T}'(0)$ approach constant values while $\tilde{M}'(0)$ is proportional to the ratio Sc/Pr raised to the one-third power. For $\sigma_T = \sigma_M = 1$, $\tilde{F}''(0) = 1.11$, $-\tilde{T}'(0) = .504$ and $-\tilde{M}'(0) = .638 (Sc/Pr)^{1/3}$.

In Section 4.2, where the Schmidt and Prandtl numbers were treated as being equal, the effects of the heat and mass transfer processes were indicated to be additive. That this is not the case for unequal Schmidt and Prandtl numbers is indicated by Equations (4.76) and (4.77). Returning now to the boundary-layer variables one deduces that the local shear stress and the local Nusselt and Sherwood numbers are given by

$$\tau = Gr^{3/4} Pr^{1/4} \left(\frac{4}{3}\right)^{1/4} [S(x)]^{1/3} [\xi(x)]^{1/4} [\tilde{F}''(0)] \quad (4.78),$$

$$Nu = Gr^{1/4} Pr^{1/4} \left(\frac{3}{4}\right)^{1/4} [S(x)]^{1/3} [\xi(x)]^{1/4} [-\tilde{T}'(0)] \quad (4.79),$$

$$Sh = Gr^{1/4} Pr^{1/4} \left(\frac{3}{4}\right)^{1/4} [S(x)]^{1/3} [\xi(x)]^{1/4} [-\tilde{M}'(0)] \quad (4.80),$$

where $\tilde{F}''(0)$, $\tilde{T}'(0)$ and $\tilde{M}'(0)$ still depend on σ_T , σ_M , Pr and Sc . The derivatives can be calculated (approximately) from Equations (4.72), (4.73) and (4.75). For Schmidt and Prandtl numbers of the same order of magnitude Equations (4.75) and (4.77) indicate the dependence of $\tilde{T}'(0)$ and $\tilde{M}'(0)$ on the Schmidt and Prandtl numbers, while for $Pr/Sc \rightarrow 0$, $\tilde{M}'(0)$ is proportional to the one-third power of the quantity Sc/Pr . This last result is to be expected since, in

this case, the region in which the major variation in the concentration occurs is very near the surface. Near the surface the flow appears as forced convection, "driven by temperature," with superimposed free convection.

The results of the study of the asymptotic forms of the differential equations for the zero-order terms in the series expansions are summarized in Table VIII, for $A=B=0$. The table gives the functional dependence of the dimensionless quantities \mathcal{T} , Nu and Sh on the Schmidt and Prandtl numbers, the Grashof number and the expansion coefficient ratios σ_T and σ_M . When interpreting Table VIII it must be remembered, Equations (2.56) and (2.57), that for $|\beta\Delta\theta| \geq |\gamma\Delta\omega|$, $Gr \triangleq g\beta\Delta\theta L^3/\nu_\infty^2$ and for $|\beta\Delta\theta| < |\gamma\Delta\omega|$, $Gr \triangleq g\gamma\Delta\omega L^3/\nu_\infty^2$.

TABLE VIII.

FUNCTIONAL BEHAVIOR OF THE SHEAR STRESS, \mathcal{T} , THE NUSSELT NUMBER, Nu AND THE SHERWOOD NUMBER, Sh .

	\mathcal{T}	Nu	Sh
(a) $P_r = Sc, P_r \rightarrow 0$	$[Gr(\sigma_T + \sigma_M)]^{3/4}$	$[Gr(\sigma_T + \sigma_M)]^{1/4} P_r^{1/2}$	$[Gr(\sigma_T + \sigma_M)]^{1/4} P_r^{1/2}$
(b) $P_r = Sc, P_r \rightarrow \infty$	$[Gr(\sigma_T + \sigma_M)]^{3/4} P_r^{-1/4}$	$[Gr(\sigma_T + \sigma_M)]^{1/4} P_r^{1/4}$	$[Gr(\sigma_T + \sigma_M)]^{1/4} P_r^{1/4}$
(c) $P_r \rightarrow 0, Sc \rightarrow \infty$	$[Gr(\sigma_T + \sigma_M)]^{3/4}$	$[Gr(\sigma_T + \sigma_M)]^{1/4} P_r^{1/2}$	$Gr^{1/4} P_r^{1/2} Sc^{1/3}$

(d) $P_r \rightarrow \infty, Sc \rightarrow \infty$
with Sc/P_r constant

$$1 < Sc/P_r < 4 \quad \left[Gr \left[\sigma_T + \sigma_M \left(\frac{P_r}{Sc} \right)^{1/2} \right] P_r \right]^{1/4} \left[Gr \left[\sigma_M + \sigma \left(\frac{Sc}{P_r} \right)^{1/3} \right] Sc \right]^{1/4}$$

$$1 \ll Sc/P_r \quad Gr^{1/4} P_r^{1/4} \quad Gr^{1/4} P_r^{1/4} \left(\frac{Sc}{P_r} \right)^{1/3}$$

The equations which indicate these functional behaviors are: Case (a)-(4.29), (4.37); Case (b)-(4.52), (4.53); Case (c)-(4.29), (4.37); and Case (d)-for $1 < Sc/P_r < 4$, (4.76), (4.77); for $Sc/P_r \gg 1$, (4.75), (4.79), (4.80).

CHAPTER 5

Final Remarks

A laminar boundary-layer theory of free convection around plane, two-dimensional bodies has been developed here for arbitrary body shapes. The flow is a result of a combination of temperature and concentration differences between the surface of the object and the fluid. Dilute, binary fluid mixtures were studied. For a body maintained at a uniform temperature and concentration of the species undergoing transfer it was possible to treat a number of combinations of "driving forces" (characteristic temperature and concentration differences) and coefficients of expansion (Sec. 2.2).

By means of transformations suggested by analogy with the work of Goertler⁽¹²⁾ on forced convection, new series representations of the boundary-layer variables were developed (Sec. 2.4). The functional coefficients in these series are universal, and are determined by the solutions of ordinary differential equations which are independent of the body contour for a given class of body shapes (e.g., sharp-nosed, blunt-nosed, or flat-nosed). The class of the body shape fixes certain numerical coefficients in the differential equations. As a consequence, numerical solutions for a particular class of body shapes may be obtained once and for all, for a given set of the dimensionless parameters appearing in the problem. Hence, the particular body contour in question is taken into account only when the series are assembled to represent the dependent variables.

The series developed here were found to converge rapidly for the class of blunt-nosed bodies (one term was sufficient to determine the flux densities and shear stress at the surface. The rates of convergence of the series were verified by comparing the numerical results for the zero-order terms with experimental data and also by determining the corrections given by the first order terms (Secs. 3.1, 3.2).

For blunt-nosed bodies the zero-order terms were calculated for several Prandtl numbers between .01 and 1763. On the other hand, it was indicated that for sharp-nosed bodies the zero-order terms are presently available from the tabulated solutions of Ostrach⁽²²⁾, when his results for the vertical plate are interpreted in terms of the new dependent and independent variables.

Next, the effects due to the class of the body shape were examined by obtaining the zero-order numerical solution for the class of flat-nosed bodies at a Prandtl number of 1 and then comparing this result with the solutions for sharp- and blunt-nosed bodies. Sharp- and blunt-nosed bodies were also compared at Prandtl numbers of .01 and 1000. The differences due to the class of the body shape were found to be small (Sec. 3.2).

In addition, the influences of interfacial velocities and of differences between the heat capacities of the "diffusing" and "stagnant" species were briefly examined by comparing the numerical solutions for cases when both temperature and concentration effects were present (Sec. 3.2).

Finally, several asymptotic forms of the differential equations for the zero-order terms were used to describe the dependence of the flux

densities and shear stress at the surface on the Prandtl and Schmidt numbers. For equal Schmidt and Prandtl numbers the "effective" Grashof number is, as expected, the sum of the Grashof numbers for the temperature and concentration effects (Sec. 4.1). In the cases of (a) low Prandtl numbers but high Schmidt numbers (liquid metals) or (b) high Schmidt and Prandtl numbers (viscous liquids), the effective Grashof number is not a sum. Explicit formulas were developed for these cases and, in some instances, checked with numerical solutions available in the literature (Sec. 4.2, 4.3).

There are several other problems to which the techniques developed in this research can be applied. One is the description of free convection around axisymmetric bodies and another is the problem involving a three-dimensional body with two orthogonal planes of symmetry. The latter problem has been studied by Poots⁽²⁴⁾, whose solutions are restricted to the region near the stagnation point. The results of the present research indicate that Poots' solutions could be expected to apply over a much larger region of the surface when interpreted in terms of the present theory. The techniques developed here could be used to analyse problems involving combined free and forced convection and also for problems in which the flux density of heat or mass is specified at the surface, rather than the temperature or composition.

Another aspect of the theory of free convection around submerged objects which warrants study is the extension of boundary-layer theory to lower Grashof numbers. The systematic development of corrections to free-convection boundary-layer theory, using the techniques of matched asymptotic expansions, has received only slight attention. The only published research on this topic, to the writers knowledge, is the paper by Yang and Jergers.⁽³²⁾

APPENDICES

APPENDIX A

EXPANSIONS FOR THE SCALED TANGENTIAL COORDINATE
AND THE PRINCIPAL FUNCTION

Case 1 - Sharp-Nosed Bodies

The sine of the angle between the body force vector and the normal to the surface, $S(\chi)$, is assumed to be an analytic function of χ , the distance along the surface, with non-zero $S(0)$ and $S'(0)$.

(a) ξ in terms of χ and χ in terms of ξ

Since $[S(z)]^{1/3}$ is analytic in a neighborhood of $z=0$, ($z=\chi+i\eta$),

$$S^{1/3} = a_1 + a_2 z + a_3 z^2 + \dots \quad (\text{A.1}),$$

where the a 's are found in the usual fashion. Hence

$$\xi = a_1 z + \frac{a_2}{2} z^2 + \dots \quad (\text{A.2}).$$

Since ξ is analytic near $z=0$, and $\xi'(0) \neq 0$, ξ has an inverse (Churchill⁽⁶⁾),

$$z = b_1 \xi + b_2 \xi^2 + \dots \quad (\text{A.3}).$$

Now to find the b 's write

$$dz = \sum_{j=1}^{\infty} b_j \xi^{j-1} d\xi \quad (\text{A.4}),$$

so that

$$\xi^{-m} dz = \sum_{j=1}^{\infty} b_j \xi^{j-m-1} d\xi \quad (\text{A.5})$$

and a circuit around the origin in the z plane yields, then,

$$\oint \frac{dz}{\xi^m} = \sum_{j=1}^{\infty} b_j \oint \xi^{j-m-1} d\xi = 2\pi i b_m \quad (\text{A.6}).$$

According to the Cauchy integral formula and the residue theorem,

b_m is the coefficient of z^{-1} in the expansion of ξ^{-m} in powers of z ; e.g., $b_1 = 1/a_1$.

(b) The Principal Function, $K(\xi)$

$$K(\xi) = \frac{1}{2} + \frac{1}{3} \frac{\xi}{S^{4/3}} \frac{dS}{d\alpha} \quad (\text{A.7})$$

Suppose

$$S(z) = s_0 + s_1 z + \dots \quad (\text{A.8}),$$

then

$$\frac{1}{S} \frac{dS}{d\alpha} = \frac{s_1}{s_0} \left[\frac{1 + 2(s_2/s_1)z + 3(s_3/s_2)z^2 + \dots}{1 + (s_1/s_0)z + (s_2/s_0)z^2 + \dots} \right] \quad (\text{A.9}),$$

or

$$\frac{1}{S} \frac{dS}{d\alpha} = \frac{s_1}{s_0} \left[1 + \frac{2s_2 s_0 - s_1^2}{s_1 s_0} z + \dots \right] \quad (\text{A.10}).$$

Now writing z in terms of ξ one finds

$$\frac{1}{2} + \frac{1}{3} \frac{\xi}{S^{4/3}} \frac{dS}{d\alpha} = \frac{1}{2} + \frac{1}{3} \frac{\frac{s_1}{s_0} \xi + b_1 \frac{2s_2 s_0 - s_1^2}{s_1 s_0} \xi^2 + \dots}{a_1 + a_2 \xi + \dots} \quad (\text{A.11}).$$

Hence,

$$K(\xi) = \frac{1}{2} + K_1 \xi + \dots \quad (\text{A.12}).$$

Case 2 - Blunt-Nosed Bodies

Since the body is symmetrical and $S(\alpha)$ is assumed to be analytic with $S'(0) \neq 0$,

$$S(z) = z + s_3 z^3 + \dots \quad (\text{A.13}).$$

(a) ξ in terms of α and α in terms of ξ

Write

$$[S(\alpha)]^{1/3} d\alpha = [S(\alpha)]^{1/3} \frac{d\alpha}{dS} dS \quad (\text{A.14}).$$

Since $S(z)$ is analytic and $S'(0) \neq 0$,

$$\alpha(S) = \alpha_1 S + \frac{\alpha_3}{6} S^3 + \dots \quad (\text{A.15}),$$

and using the same argument to find α 's as was used for the b 's in Case 1, one finds that α_m is the coefficient of α^{-1} in the expansion of S^{-m} in powers of α . Hence,

$$\xi = \sum_{d=1}^{\infty} \int_0^S S^{1/3} \alpha_d S^{d-1} dS = \frac{3}{4} \alpha_1 S^{4/3} + \frac{3}{10} \alpha_3 S^{10/3} \quad (\text{A.16}).$$

So

$$\frac{\xi}{S^{1/3}} = \frac{3}{4} \alpha_1 S + \frac{3}{10} \alpha_3 S^3 + \dots \quad (\text{A.17}),$$

$$\frac{\xi^3}{S} = a_1 S^3 + a_2 S^5 + \dots \quad (\text{A.18}),$$

and, finally,

$$\xi^3 = d_1 z^4 + d_2 z^6 + \dots \quad (\text{A.19}).$$

Now

$$(\xi^3)^{1/4} = a_1^{1/4} S (1 + g(S))^{1/4} \quad (\text{A.20})$$

where $g(S)$ is a power series in S , so by expanding with the binomial theorem one finds that

$$(\xi^3)^{1/4} = b_1 S + b_2 S^2 + \dots \quad (\text{A.21}).$$

Since $d[(\xi^3)^{1/4}]/dS \neq 0$ at $S=0$ the series can be inverted to give

$$S = c_1 \xi^{3/4} + c_2 \xi^{9/4} + \dots \quad (\text{A.22}).$$

The c 's are calculated from

$$\oint \frac{dS}{(\xi^{3/4})^m} = 2\pi i c_m \quad (\text{A.23}).$$

From Equation (A.21) the result is that

$$z = e_1 \xi^{3/4} + e_2 \xi^{9/4} + \dots \quad (\text{A.24}),$$

where the e 's are calculated in the same manner as the c 's.

(b) The Principal Function, $K(\xi)$

$$\begin{aligned} K(\xi) &= \frac{1}{2} + \frac{1}{3} \left(\frac{3}{4} \alpha_1 + \frac{3}{10} \alpha_3 S + \dots \right) (S_1 + 2S_2 \chi_1 + \dots) \\ &= \frac{1}{2} + \frac{1}{3} \frac{3}{4} \alpha_1 S_1 + K_1 \xi^{6/4} + \dots \\ &= \frac{3}{4} + K_1 \xi^{3/2} + \dots \end{aligned} \quad (\text{A.25})$$

K(ξ) for $S(x) = \sin(x)$

(a) ξ in terms of x and x in terms of ξ

$$S(x) = x - \frac{1}{6} x^3 + \frac{1}{120} x^5 + \dots \quad (\text{A.26})$$

From the previous section,

$$\xi = \frac{3}{4} \alpha_1 S^{4/3} + \frac{3}{10} \alpha_3 S^{10/3} + \dots \quad (\text{A.27}).$$

Here, α_j is the coefficient of z^{-j} in the expansion of S^{-j} in powers of z . So, for α_1 ,

$$\left(z - \frac{1}{6} z^3 + \dots \right)^{-1} = z^{-1} + \dots, \quad \alpha_1 = 1 \quad (\text{A.28}),$$

and for α_3

$$\left(z - \frac{1}{6} z^3 + \dots \right)^{-3} = z^{-3} + \frac{1}{2} z^{-1} + \dots, \quad \alpha_3 = \frac{1}{2} \quad (\text{A.29}),$$

hence,

$$\frac{\xi}{S^{1/3}} = \frac{3}{4} S + \frac{3}{20} S^3 + \dots \quad (\text{A.30}).$$

Now

$$\frac{\xi^3}{S} = \frac{27}{64} S^3 + \frac{81}{320} S^5 + \dots \quad (\text{A.31}),$$

so that

$$(\xi^3)^{1/4} = \left(\frac{27}{64} \right)^{1/4} S \left(1 + \frac{3}{5} S^2 + \dots \right)^{1/4} \quad (\text{A.32}),$$

and

$$\xi^{3/4} = \left(\frac{27}{64}\right)^{1/4} \left(S + \frac{3}{20} S^3 + \dots \right) \quad (\text{A.33}).$$

Finally

$$S = C_1 \xi^{3/4} + C_2 \xi^{9/4} + \dots \quad (\text{A.34})$$

and, in the manner outlined above,

$$S = \left(\frac{64}{27}\right)^{1/4} \xi^{3/4} + \dots \quad (\text{A.35}),$$

which yields

$$\chi = \left(\frac{64}{27}\right)^{1/4} \xi^{3/4} + \dots \quad (\text{A.36}).$$

(b) Principal Function, $K(\xi)$

$$\begin{aligned} K(\xi) &= \frac{1}{2} + \frac{1}{3} \left[\frac{3}{4} + \frac{3}{20} S^2 + \dots \right] \left[1 - \frac{1}{2} \chi^2 + \frac{1}{24} \chi^5 - \dots \right] \\ &= \frac{1}{2} + \frac{1}{3} \left[\frac{3}{4} + \frac{3}{20} \left(\frac{64}{27}\right)^{1/4} (\xi^{6/4} - \dots) \right] \left[1 - \frac{1}{2} \left(\frac{64}{27}\right)^{1/2} \xi^{6/4} - \dots \right] \\ &= \frac{3}{4} - \frac{3}{40} \left(\frac{64}{27}\right)^{1/2} \xi^{6/4} + \dots \end{aligned} \quad (\text{A.37})$$

Therefore, $K_1 \doteq -.115$

The scaled tangential coordinate, ξ , was calculated and the results are shown in Table IX. Simpson's rule was used to evaluate the integral.

TABLE IX.

SCALED TANGENTIAL COORDINATE, ξ , FOR $S(x) = \text{Si}(x)$
(EVALUATED BY SIMPSON'S RULE INTEGRATION WITH A STEP SIZE = $\pi/2000$)

$x \cdot \frac{360}{2\pi}$	ξ	$x \cdot \frac{360}{2\pi}$	ξ
0	0		
10	.073092	100	1.467780
20	.183823	110	1.640231
30	.314572	120	1.809052
40	.4594400	130	1.972265
50	.614822	140	2.127646
60	.778035	150	2.272514
70	.946855	160	2.403264
80	1.119306	170	2.513995
90	1.293545	180	2.587089

APPENDIX B

NUMERICAL TECHNIQUES AND COMPUTER PROGRAMS

The problem, stated in terms of ordinary differential equations by Equations (2.77) through (2.84), is of the two-point, boundary-value type. The zero-order equations are non-linear, while the succeeding equations are linear. The higher-order equations have variable coefficients, which are the solutions to the lower-order equations. Closed form solutions are not known for any of these equations and numerical or "approximate" methods must be used. A variety of methods may be used to treat initial-value problems, some of the more popular types are the Runge-Kutta methods (Carnahan, Luther and Wilkes⁽⁵⁾). The two basic difficulties associated with the application of initial value methods to the present problem are the lack of sufficient information at the starting point and the meaning of the boundary conditions at infinity. These "conditions at infinity" are statements about the asymptotic form which the solution assumes as the independent variable increases without bound. As a consequence, a decision must be made as to a reasonable point at which to terminate the calculations when a numerical method is used. A third difficulty, or "error," is associated with the method of integration. This error, due to the approximate nature of the method of solution, is called the discretization error. Usually the discretization error can be reduced by reductions in the step size.

The method adopted is to treat the problem as an initial value problem. A step size, a maximum value of the independent variable ("infinity"), and the missing initial conditions are chosen. For the zero-order problem the system of differential equations is a seventh order system, when the effects of temperature and concentration are both included. Four conditions are known at the origin and three are unknown. Hereinafter these unknown derivatives will be called the characteristic values. These are the conditions at the origin which determine that solution which has the desired asymptotic character. The differential equations are integrated out to the maximum value of the independent variable and the asymptotic character of the solution is checked. The requirement that the derivative of the stream function (a velocity), the temperature and the concentration all vanish is impossible to satisfy with a numerical method. Hence, the approximate condition used is that the sum of the squares of: (a) the derivative of the stream function, (b) the temperature, and (c), the concentration be as small as possible. The integration procedure is repeated with successive sets of initial values until a minimum in the sum of squares is found. The effects due to step size and the location of infinity can be ascertained by repeating the whole process. The numerical results obtained in a study of these parameters are discussed in Appendix C.

The systematic location of the characteristic values, the three missing initial conditions in the general case, is not a simple matter. The first difficulty is associated with the non-linear

character of the equations. If initial values are chosen which are not near the characteristic values then the "solution" may "oscillate" and generate numbers which are too large for the computer to handle. Thus, the first problem is to find a region, in the domain of the initial values, in which the solution is "bounded." The second problem is to converge to the characteristic values.

The selection of a sequence of initial values which converges to the characteristic values is accomplished with a program which implements the "pattern search" procedure. This is a frequently used technique in optimization problems (Wilde⁽³³⁾) and is basically a method of successive trials with a strategy. The procedure requires an initial value of an "object function," calculated on the basis of a set of values for the independent variables in the optimization. In the present case the independent variables are the missing initial values. Then, small changes are made in each of the variables in turn. The value of the object function is calculated after each change. Improvements in the value of the object function near the initial point determine a direction in the space of the independent variables. A move is then made in this direction and the procedure is repeated. The strategy is that moves made in a "successful direction" are amplified. Suppose then, that at a point, \vec{Y}_i , small changes in the independent variables disclose that a nearby point, \vec{Y}_{i+1} , is "better", according to some criterion established with the object function. Then, instead of continuing with local changes in the independent variables

around \vec{Y}_{i+1} , the behavior of the object function is investigated near \vec{Y}_{i+2} , where $\vec{Y}_{i+2} = 2\vec{Y}_{i+1} - \vec{Y}_i$. This procedure accelerates the convergence process. For the details of the method the reader is referred to the book by Wilde.

Three types of object functions are used. In the initial stage, where bounded solutions are sought, the object function is simply the value of the distance, η , at which the solution becomes "unbounded." This object function is maximized. The second stage is the minimization of the sum of squares at the value of η chosen to approximate infinity. In some cases the minimum in the sum of squares resulted in a small (in magnitude) negative value of the derivative of the stream function, of the temperature or of the concentration. In those cases the object function was modified to force these quantities to be small and positive.

Several computer programs were written and used in this work. Only three of the programs will be mentioned here, as the others are only simple modifications of these. The main difference is the deletion of certain effects; e.g., those due to mass transfer in the study of temperature-driven convection.

The two major programs are BLUNTO. and BLUNTL.. BLUNTO. is used to solve the zero-order problem and BLUNTL. for the first-order problem, for free convection around blunt-nosed bodies. Both programs call on the library subroutine for the Runge-Kutta integration and on the pattern search procedure, PSER., written by the author. The

object function is a separate subroutine FN.. All of the programs were written in the MAD language⁽²⁾. The programs BLUNTO., BLUNT1., PSER. and FN. are reproduced next, along with the input variable lists.

Input Variables for BLUNTO.

<u>Symbol</u>	<u>Definition</u>
A	Ackermann effect parameter, Equation (2.36)
B	interfacial velocity parameter, Equation (2.36)
CONST	a scale factor for FN.
DX	array of increment values for the initial changes in the estimates of the characteristic values
DY	step size for the integration
EIGEN	array for the initial estimates of the characteristic values
EPSI	final tolerance on the characteristic values
FPRNT	printing counter for PSER.
FREQ	printing counter for the output
M	total number of steps
PR	Prandtl Number
SC	Schmidt Number
SIGMAT	σ_T parameter, Equations (2.56) and (2.57)
SIGMAM	σ_m parameter, Equations (2.56) and (2.57)

Input Variables for BLUNTL.

In addition to those listed for BLUNTO., they are

EVAL	characteristic values for the zero-order equations
------	--

```

$ COMPILE MAD,EXECUTE,DUMP,PRINT OBJECT,PUNCH OBJECT          BLNT0.01
R   PROGRAM TO INTEGRATE THE ODE DESCRIBING NATURAL
R   CONVECTION DRIVEN BY NON-UNIFORM TEMPERATURE AND
R   COMPOSITION FIELDS AROUND BLUNT NOSED OBJECTS
R   ZERO ORDER TERMS
EXECUTE FTRAP.
EXECUTE SETRKD.(7,F(0),G(0),Q(0),Y,DY)
START PRINT COMMENT $1$
READ AND PRINT DATA PR,SC,SIGMAT,SIGMAM,A,B,DY,M,EIGEN,DX,
1EPSI,STEPSM,FPRNT,FREQ,CONST
SWTCH=1B
YMAX=M*DY
R.....CALCULATION OF EIGEN VALUES.....
EXECUTE PSER.(3,EIGEN,DX,EPSI,OBJ.,FPRNT,STEPSM,BAD)
R.....INTEGRATION USING EIGEN VALUES.....
COUNT=0
PRINT COMMENT $1 TEMPERATURE AND CONCENTRATION DRIVEN NATURAL
1 CONVECTION AROUND TWO DIMENSIONAL BLUNT NOSED OBJECTS $
PRINT COMMENT $0 ZERO ORDER TERMS$
PRINT RESULTS PR,SC,SIGMAT,SIGMAM,A,B,DY,M
PRINT FORMAT OUT1
PRINT FORMAT OUT2,0.,B*EIGEN(3)/SC,0.,EIGEN(1),1.,EIGEN(2),
11.,EIGEN(3)
SWTCH=0B
EXECUTE OBJ.(EIGEN)
TRANSFER TO DONE
BAD PRINT COMMENT $0.....STEPSM EXCEEDED.....$
DONE TRANSFER TO START
DIMENSION F(6),G(6),Q(6),EIGEN(3),DX(3)
INTEGER STEPSM,FPRNT,FREQ,COUNT,M
BOOLEAN SWITCH,GO
VECTOR VALUES OUT1=$1H0,S14,H*Y*,S12,H*(F0)*,S11,H*(F0)***,S10
1,H*(F0)***,S12,H*(T0)*,S11,H*(T0)***,S12,H*(M0)*,S11,H*(M0)***
2$
VECTOR VALUES OUT2=$8(E16.6)*$
INTERNAL FUNCTION (EGEN)
ENTRY TO OBJ.
COUNT=0
GO=0B
M=0
Y=0.
F(0)=B*EGEN(3)/SC
F(1)=0.
F(2)=EGEN(1)
F(3)=1.
F(4)=EGEN(2)
F(5)=1.
ONE F(6)=EGEN(3)
S=RKDEQ.(0)
WHENEVER S.E.1.
G(0)=F(1)
G(1)=F(2)
G(2)=-SIGMAT*F(3)-SIGMAM*F(5)-F(0)*F(2)+F(1)*F(1)
G(3)=F(4)
G(4)=-PR*F(0)*F(4)+A*F(4)*F(6)
G(5)=F(6)
G(6)=-SC*F(0)*F(6)
TRANSFER TO ONE
OTHERWISE
M=M+1
COUNT=COUNT+1
WHENEVER SWITCH,EXECUTE FN.(F,EGEN,DY,YMAX,M,CONST,VAL,GO,
1START)
WHENEVER GO,FUNCTION RETURN VAL
WHENEVER .NOT.SWTCH.AND.Y.LE.YMAX+DY/2..AND.COUNT.E.FREQ
COUNT=0
PRINT FORMAT OUT2, Y,F(0),F(1),F(2),F(3),F(4),F(5),F(6)
END OF CONDITIONAL
WHENEVER Y.GE.YMAX.AND..NOT.SWTCH,FUNCTION RETURN
TRANSFER TO ONE
END OF CONDITIONAL
END OF FUNCTION
END OF PROGRAM

$ COMPILE MAD,EXECUTE,DUMP,PRINT OBJECT,PUNCH OBJECT          BLNT1.01
R   PROGRAM TO INTEGRATE THE ODE DESCRIBING NATURAL
R   CONVECTION DRIVEN BY NON-UNIFORM TEMPERATURE AND
R   COMPOSITION FIELDS AROUND BLUNT NOSED OBJECTS
R   FIRST ORDER TERMS
EXECUTE FTRAP.
EXECUTE SETRKD.(14,F(0),G(0),Q(0),Y,DY)
START READ AND PRINT DATA PR,SC,SIGMAT,SIGMAM,A,B,DY,M,EIGEN,EVAL,
1DX,EPSI,STEPSM,FPRNT,FREQ,CONST
SWTCH=1B
YMAX=M*DY
C=4./3.

```

```

R.....CALCULATION OF EIGEN VALUES.....
EXECUTE PSER.(3,EIGEN,DX,EPSI,OBJ.,FPRNT,STEPSP,BAD)
R.....INTEGRATION USING EIGEN VALUES.....
PRINT COMMENT $1 TEMPERATURE AND CONCENTRATION DRIVEN NATURAL
1 CONVECTION AROUND TWO DIMENSIONAL BLUNT NOSED OBJECTS $
PRINT COMMENT $0 FIRST ORDER TERMS$
PRINT RESULTS PR,SC,SIGMAT,SIGMAM,A,B,DY,M,EVAL(1)...EVAL(3)
PRINT FORMAT OUT1
PRINT FORMAT OUT2,0.,B*EIGEN(3)/SC/3.,0.,EIGEN(1),0.,
1EIGEN(2),0.,EIGEN(3)
SWTCH=0B
EXECUTE OBJ.(EIGEN)
TRANSFER TO DONE
BAD
DONE
PRINT COMMENT $0.....STEPSP EXCEEDED.....$
TRANSFER TO START
DIMENSION F(13),G(13),Q(13),EIGEN(3),DX(3),EVAL(3)
INTEGER STEPSP,FPRNT,M
BOOLEAN SWTCH,GO
VECTOR VALUES OUT1=$1H0,S14,H*Y*,S12,H*(F1)*,S11,H*(F1)**,S10
1,H*(F1)***,S12,H*(T1)*,S11,H*(T1)***,S12,H*(M1)*,S11,H*(M1)**
2$
VECTOR VALUES OUT2=$8(E16.6)*$
INTERNAL FUNCTION (EGEN)
ENTRY TO OBJ.
M=0
COUNT=0
GO=0B
Y=0.
F(0)=B*EVAL(3)/SC
F(1)=0.
F(2)=EVAL(1)
F(3)=1.
F(4)=EVAL(2)
F(5)=1.
F(6)=EVAL(3)
F(7)=B*EGEN(3)/SC/3.
F(8)=0.
F(9)=EGEN(1)
F(10)=0.
F(11)=EGEN(2)
F(12)=0.
F(13)=EGEN(3)
S=RKDEQ.(0)
WHENEVER S.E.1.
ONE
G(0)=F(1)
G(1)=F(2)
G(2)=-SIGMAT*F(3)-SIGMAM*F(5)-F(0)*F(2)+F(1)*F(1)
G(3)=F(4)
G(4)=-PR*F(0)*F(4)+A*F(4)*F(6)
G(5)=F(6)
G(6)=-SC*F(0)*F(6)
G(7)=F(8)
G(8)=F(9)
G(9)=-SIGMAT*F(10)-SIGMAM*F(12)-F(0)*F(9)+4.*F(1)*F(8)-3.*F(2)
1)*F(7)+C*F(1)*F(1)
G(10)=F(11)
G(11)=PR*(-F(0)*F(11)+2.*F(1)*F(10)-3.*F(4)*F(7))+A*(F(4)*F(1)
13)+F(11)*F(6))
G(12)=F(13)
G(13)=SC*(-F(0)*F(13)+2.*F(1)*F(12)-3.*F(6)*F(7))
TRANSFER TO ONE
OTHERWISE
M=M+1
COUNT=COUNT+1
WHENEVER SWTCH,EXECUTE FN.(F,EGEN,DY,YMAX,M,CONST,VAL,GO,
1START)
WHENEVER GO,FUNCTION RETURN VAL
WHENEVER .NOT.SWTCH.AND.Y.LE.YMAX+DY/2..AND.COUNT.E.FREQ
COUNT=0
PRINT FORMAT OUT2, Y,F(7),F(8),F(9),F(10),F(11),F(12),F(13)
END OF CONDITIONAL
WHENEVER Y.GE.YMAX.AND..NOT.SWTCH,FUNCTION RETURN
TRANSFER TO ONE
END OF CONDITIONAL
END OF FUNCTION
END OF PROGRAM
$ COMPILE MAD,PRINT OBJECT,PUNCH OBJECT PSER.001
R PROGRAM TO MAXIMIZE AN OBJECT FUNCTION,F.,
R THE PATTERN SEARCH PROCEDURE DESCRIBED BY WILDE-
R OPTIMUM SEEKING METHODS IS USED.
EXTERNAL FUNCTION (N,X,DX,EPSI,F.,FPRNT,STEPSP,BAD)
STATEMENT LABEL BAD
INTEGER I,J,N,FPRNT,STEPSP,STEPS,PRNT
BOOLEAN K,L
DIMENSION B(3),T(3),TT(3)
ENTRY TO PSER.
THROUGH ONE,FOR I=1,1,I.G.N
B(I)=X(I)
TT(I)=X(I)
ONE
T(I)=X(I)

```

```

R.....CALCULATE INITIAL VALUE OF FUNCTION.....
BOBJ=F.(B)
TOBJ=BOBJ
PRINT RESULTS B(1)...B(N),BOBJ
STEPS=0
PRNT=0
J=0
K=0B
L=0B
TRANSFER TO START
R.....CALCULATE OBJ AT TEMPORARY HEAD.....
GO   WHENEVER J.NE.0,TOBJ=F.(T)
R.....RETURN TO OLD TEMPORARY HEAD IF NEW HEAD UNSATISFACTORY.
    WHENEVER TOBJ.LE.BOBJ
    TOBJ=BOBJ
    THROUGH REPEAT, FOR I=1,1,I.G.N
REPEAT TT(I)=B(I)
      T(I)=B(I)
      J=0
    END OF CONDITIONAL
R.....LOCAL EXCURSIONS.....
START THROUGH TWO, FOR I=1,1,I.G.N
      TT(I)=T(I)+DX(I)
      TTOBJ=F.(TT)
      WHENEVER TTOBJ.G.TOBJ
      TOBJ=TTOBJ
      L=1B
      OTHERWISE
      TT(I)=T(I)-DX(I)
      TTOBJ=F.(TT)
      END OF CONDITIONAL
      WHENEVER L,TRANSFER TO TWO
      WHENEVER TTOBJ.G.TOBJ
      TOBJ=TTOBJ
      OTHERWISE
      J=J+1
      TT(I)=T(I)
      END OF CONDITIONAL
TWO  L=0B
R.....MOVE TO A NEW TEMPORARY HEAD.....
    WHENEVER J.NE.N,TRANSFER TO MOVE
R.....CHANGE STEP SIZE.....
    THROUGH THREE, FOR I=1,1,I.G.N
    DX(I)=DX(I)/2.
    T(I)=B(I)
    TT(I)=B(I)
    WHENEVER DX(I).L.EPSI,K=1B
THREE CONTINUE
      WHENEVER K,TRANSFER TO DONE
      TOBJ=BOBJ
      J=0
      TRANSFER TO GO
MOVE R.....CALCULATE COORDINATES OF NEW TEMPORARY HEAD.....
      THROUGH FIVE, FOR I=1,1,I.G.N
      T(I)=2.*TT(I)-B(I)
      B(I)=TT(I)
      TT(I)=T(I)
      BOBJ=TOBJ
      J=5
FIVE R.....CHECK FOR PRINTING OR MAXIMUM STEPS.....
      STEPS=STEPS+1
      PRNT=PRNT+1
      WHENEVER PRNT.E.FPRNT
      PRNT=0
      PRINT RESULTS B(1)...B(N),BOBJ
      END OF CONDITIONAL
      WHENEVER STEPS.G.STEPSM
      PRINT RESULTS B(1)...B(N),BOBJ
      TRANSFER TO BAD
      END OF CONDITIONAL
      TRANSFER TO GO
DONE R.....EIGEN VALUES RETURNED TO MAIN PROGRAM.....
      PRINT RESULTS B(1)...B(N),BOBJ
      THROUGH SIX, FOR I=1,1,I.G.N
SIX  X(I)=B(I)
      FUNCTION RETURN
      END OF FUNCTION
$ COMPILE MAD,PRINT OBJECT,PUNCH OBJECT FN.50001
      EXTERNAL FUNCTION (F,EGEN,DY,YMAX,M,CONST,VAL,GO,START)
      ENTRY TO FN.
      BOOLEAN GO
      STATEMENT LABEL START
      INTEGER M
      WHENEVER M*DY.LE.YMAX
      WHENEVER F(1).L.0..OR.F(3).L.0..OR.F(5).L.0.
      GO=1B
      VAL=-ELOG.(1.+F(1)*F(1)*CONST+F(3)*F(3)*CONST+F(5)*F(5)*
      1CONST+((YMAX-M*DY)*CONST).P.2)
      END OF CONDITIONAL
      END OF CONDITIONAL
      WHENEVER M*DY.GE.YMAX
      GO=1B
      VAL=-ELOG.(1.+F(1)*F(1)*CONST+F(3)*F(3)*CONST+F(5)*F(5)*CONST
      1)
      END OF CONDITIONAL
      FUNCTION RETURN
      END OF FUNCTION

```

APPENDIX C

Numerical Results

The numerical values for the zero- and first-order terms in the expansions of the dependent variables in the boundary-layer equations are given in this section.

The effects of the step size in the integration (ΔY) and the value chosen for "infinity" ($M \cdot \Delta Y$) were investigated for a range of Prandtl numbers. Only the zero-order equations for blunt-nosed bodies were used. The results are shown in Table X. An inspection of the table indicates that further decreases in step size and increases in "infinity" would not result in substantial changes in the derivatives at the origin (characteristic values).

The effects of step size and "infinity" were not investigated for the first-order terms. The point in question is the magnitude of the derivatives at the surface of the object (to determine the flux densities and shear stress). Therefore, the calculations for the first-order terms were carried out only to the extent of estimating these derivatives. The determination of these quantities for temperature-driven free convection involves the solution of a system of ten, simultaneous, first order differential equations (for combined heat and mass transfer the system is of the fourteenth order). To obtain one significant figure for a Prandtl number of 1000 required 11 minutes of computing time. For a Prandtl number of .7 the first-order characteristic values were determined to four significant figures so that an accurate comparison could be made between the numerical results and the experimental data of Jodlbauer⁽¹⁵⁾.

TABLE X.

THE EFFECTS OF STEP SIZE AND "INFINITY" ON THE CHARACTERISTIC VALUES FOR THE ZERO-ORDER TERMS

<u>P_r</u>	<u>DY</u>	<u>M DY</u>	<u>F₀'(0)</u>	<u>-T₀'(0)</u>
.01	.25	25	1.16356	.06359
.01	.25	35	1.16906	.05934
.01	.25	40	1.16911	.05953
.01	.025	40	1.16912	.05934
.7	.25	12.5	.85933	.37024
.7	.25	20.	.85935	.37025
.7	.1	12.5	.85934	.37023
1000.	.01	4.	.197	3.053
1000.	.01	6.	.19575	3.05359
1000.	.005	6.	.19575	3.05359
1000.	.025	20.	.19544	3.05843

The parameter values for the tabulated results are shown in Table XI.

The results for a Prandtl number of 1000 are not entirely satisfactory. An inspection of the tabulated results reveals that, although the first derivative of the stream function, F_0' , is tending towards zero, the temperature has leveled off at a constant, but non-zero value for large values of the independent variable. Thus for large values of the independent variable the differential equation being solved is

$$F_0'' + F_0 F_0'' - F_0' F_0' + \text{constant} = 0 \quad (\text{C.1}).$$

TABLE XI

SUMMARY OF PARAMETER VALUES IN THE TABULATED RESULTS

<u>Pr</u>	<u>Sc</u>	<u>A</u>	<u>B</u>	<u>σ_T</u>	<u>σ_m</u>	<u>DY</u>	<u>MDY</u>	<u>"order"</u>
0.01	---	---	---	---	---	.25	35.0	Zero
0.7	---	---	---	---	---	.25	12.5	"
0.7	---	---	---	---	---	.25	12.5	First
1.0	---	---	---	---	---	.25	12.5	Zero
1.0	---	---	---	---	---	.25	12.5	"
1000.0	---	---	---	---	---	.025	20.0	"
1.0	1.0	0.0	0.0	1.0	1.0	.5	12.5	"
1.0	1.0	0.0	0.1	1.0	1.0	.1	12.5	"
1.0	1.0	0.0	-1.1	1.0	1.0	.1	12.5	"
1.0	1.0	-0.1	0.1	1.0	1.0	.1	12.5	"

As a consequence, since F_0' is being forced towards zero, the second derivative of F_0 does not approach zero, as it should. In all of the other calculations made, at lower Prandtl numbers, the stream function and temperature behaved in the expected fashion with F_0' , F_0'' , T_0 and T_0' all tending towards zero. This unsatisfactory behavior is the result of "truncation errors." The computer can carry only a finite number of significant figures in the arithmetic operations (about eight for floating point arithmetic). Hence, when the derivative of temperature is much smaller than the temperature,

then no change is made in the temperature across an integration step. This difficulty could be remedied by using a numerical procedure which would carry a larger number of significant figures; e.g., "double precision arithmetic." However, in the present study, this difficulty is of little consequence since accurate analytic methods were developed in Chapter 4 for the high Prandtl number region and, even with this "error," the numerical results for the characteristic values are very close to those given by Ostrach. (22)

In all of the cases reported, the iteration process, described in Appendix B, was continued until there was no change in the fourth decimal place of the characteristic values. However, in some cases the process was carried out further. The notation used in the printed results is the same as that used in the text, except for:

- (a) the independent variable η is denoted by Y ,
- (b) subscripts are denoted by upper case numericals,
(e.g.) T_0 appears as $(T0)$,
- (c) in the first order solution for a Prandtl number of .7 the tabulated values are scaled by a factor $1/K_1$,
(see Equation (2.85)).

The "E field" notation is used so that a number appearing as (e.g.) $1.01 E -01$ is to be interpreted as $1.01 \times 10^{-1} = 0.101$. The computing time for the last run shown in Table XI was 7.9 minutes which is typical for the calculation of the zero-order solutions. Naturally this depends on the initial estimate for the characteristic values. The runs for a single transport process (heat or mass) took about 5 minutes each to establish four significant figures of the characteristic values.

TEMPERATURE DRIVEN NATURAL CONVECTION AROUND TWO DIMENSIONAL, BLUNT NOSED OBJECTS. ZERO ORDER TERMS

PR = .010000, DY = .250000, M = 140

Y	(FO)	(FO)'	(FO)''	(TO)	(TO)'
.000000E 01	.000000E 00	.000000E 00	.116911E 01	.100000E 01	-.595260E-01
.100000E 01	.428945E 00	.719086E 00	.344708E 00	.940498E 00	-.594337E-01
.200000E 01	.124645E 01	.860825E 00	.930063E-02	.861269E 00	-.589445E-01
.300000E 01	.209493E 01	.825354E 00	-.586414E-01	.822773E 00	-.579661E-01
.400000E 01	.288925E 01	.762480E 00	-.640503E-01	.765487E 00	-.565364E-01
.500000E 01	.362000E 01	.699411E 00	-.617773E-01	.709828E 00	-.547231E-01
.600000E 01	.428904E 01	.639223E 00	-.585212E-01	.656144E 00	-.525987E-01
.700000E 01	.489959E 01	.582479E 00	-.549267E-01	.604711E 00	-.502344E-01
.800000E 01	.545523E 01	.529417E 00	-.511838E-01	.555733E 00	-.476978E-01
.900000E 01	.595968E 01	.480118E 00	-.474162E-01	.509352E 00	-.450497E-01
.100000E 02	.641871E 01	.434563E 00	-.437080E-01	.465652E 00	-.423448E-01
.110000E 02	.683003E 01	.392662E 00	-.401168E-01	.424668E 00	-.396296E-01
.120000E 02	.720321E 01	.354277E 00	-.366807E-01	.386383E 00	-.369431E-01
.130000E 02	.753969E 01	.319240E 00	-.334239E-01	.350760E 00	-.343168E-01
.140000E 02	.784274E 01	.287364E 00	-.303601E-01	.317721E 00	-.317755E-01
.150000E 02	.811541E 01	.258453E 00	-.274957E-01	.287174E 00	-.293379E-01
.160000E 02	.836057E 01	.232306E 00	-.248314E-01	.259006E 00	-.270174E-01
.170000E 02	.858087E 01	.208724E 00	-.223639E-01	.233097E 00	-.248226E-01
.180000E 02	.877880E 01	.187514E 00	-.200870E-01	.209318E 00	-.227585E-01
.190000E 02	.895663E 01	.168489E 00	-.179927E-01	.187536E 00	-.208269E-01
.200000E 02	.911645E 01	.151471E 00	-.160715E-01	.167620E 00	-.190271E-01
.210000E 02	.926018E 01	.136292E 00	-.143133E-01	.149439E 00	-.173565E-01
.220000E 02	.938959E 01	.122794E 00	-.127077E-01	.132865E 00	-.158116E-01
.230000E 02	.950628E 01	.110829E 00	-.112442E-01	.117777E 00	-.143855E-01
.240000E 02	.961171E 01	.100262E 00	-.991231E-02	.104056E 00	-.130739E-01
.250000E 02	.970722E 01	.909644E-01	-.870201E-02	.915928E-01	-.118700E-01
.260000E 02	.979402E 01	.828207E-01	-.760362E-02	.802824E-01	-.107672E-01
.270000E 02	.987321E 01	.757232E-01	-.660795E-02	.700270E-01	-.975873E-02
.280000E 02	.994579E 01	.695737E-01	-.570633E-02	.607356E-01	-.883801E-02
.290000E 02	.100126E 02	.642822E-01	-.489066E-02	.523239E-01	-.799859E-02
.300000E 02	.100746E 02	.597666E-01	-.415336E-02	.447134E-01	-.723424E-02
.310000E 02	.101324E 02	.559520E-01	-.348740E-02	.378323E-01	-.653901E-02
.320000E 02	.101867E 02	.527705E-01	-.288629E-02	.316142E-01	-.590730E-02
.330000E 02	.102381E 02	.501601E-01	-.234404E-02	.259993E-01	-.533279E-02
.340000E 02	.102872E 02	.480649E-01	-.185514E-02	.209289E-01	-.481354E-02
.350000E 02	.103344E 02	.464340E-01	-.141454E-02	.163550E-01	-.434195E-02

PR=.01,DY=.25,M=140,EIGEN(1)=1.16911,-.099526,DX(1)=1.E-4,1.E-4,

EPSI=1.E-7,FPRNT=1,FREQ=4,STEP=100,CONST=1000.*

TEMPERATURE DRIVEN NATURAL CONVECTION AROUND TWO DIMENSIONAL, BLUNT NOSED OBJECTS. ZERO ORDER TERMS

PR = .700000, DY = .250000, M = 50

Y	(FO)	(FO)'	(FO)''	(TO)	(TO)'
.000000E 00	.000000E 00	.000000E 00	.859329E 00	.100000E 01	-.370236E 00
.250000E 00	.243252E-01	.184650E 00	.622567E 00	.907477E 00	-.369698E 00
.500000E 00	.877226E-01	.313891E 00	.417036E 00	.815399E 00	-.366266E 00
.750000E 00	.177366E 00	.396077E 00	.246416E 00	.724756E 00	-.357976E 00
.100000E 01	.282591E 00	.440016E 00	.110850E 00	.636899E 00	-.343912E 00
.125000E 01	.394913E 00	.454228E 00	.808279E-02	.553281E 00	-.324135E 00
.150000E 01	.507890E 00	.446470E 00	-.656189E-01	.475239E 00	-.299507E 00
.175000E 01	.616891E 00	.423456E 00	-.114751E 00	.403818E 00	-.271412E 00
.200000E 01	.718822E 00	.390740E 00	-.144017E 00	.339689E 00	-.241446E 00
.225000E 01	.811830E 00	.352717E 00	-.157921E 00	.283122E 00	-.211151E 00
.250000E 01	.895025E 00	.312712E 00	-.160514E 00	.234031E 00	-.181832E 00
.275000E 01	.968227E 00	.273107E 00	-.155242E 00	.192044E 00	-.154455E 00
.300000E 01	.103175E 01	.235505E 00	-.144904E 00	.156589E 00	-.129641E 00
.325000E 01	.108623E 01	.200890E 00	-.131670E 00	.126984E 00	-.107697E 00
.350000E 01	.113249E 01	.169773E 00	-.117150E 00	.102497E 00	-.886832E-01
.375000E 01	.117143E 01	.142324E 00	-.102475E 00	.824073E-01	-.724850E-01
.400000E 01	.120396E 01	.118482E 00	-.883966E-01	.660384E-01	-.588770E-01
.425000E 01	.123095E 01	.980359E-01	-.753713E-01	.527769E-01	-.475759E-01
.450000E 01	.125323E 01	.806874E-01	-.636393E-01	.420839E-01	-.382790E-01
.475000E 01	.127153E 01	.661001E-01	-.532885E-01	.334955E-01	-.306900E-01
.500000E 01	.128648E 01	.539286E-01	-.443051E-01	.266198E-01	-.245343E-01
.525000E 01	.129866E 01	.438397E-01	-.366114E-01	.211297E-01	-.195669E-01
.550000E 01	.130855E 01	.355246E-01	-.300940E-01	.167554E-01	-.155753E-01
.575000E 01	.131655E 01	.287053E-01	-.246235E-01	.132761E-01	-.123786E-01
.600000E 01	.132301E 01	.231367E-01	-.200670E-01	.105127E-01	-.982562E-02
.625000E 01	.132821E 01	.186064E-01	-.162965E-01	.832031E-02	-.779125E-02
.650000E 01	.133238E 01	.149329E-01	-.131940E-01	.658255E-02	-.617306E-02
.675000E 01	.133573E 01	.119627E-01	-.106534E-01	.520617E-02	-.488774E-02
.700000E 01	.133841E 01	.956722E-02	-.858161E-02	.411666E-02	-.386901E-02
.725000E 01	.134055E 01	.763959E-02	-.689833E-02	.325463E-02	-.305975E-02
.750000E 01	.134226E 01	.609147E-02	-.553501E-02	.257285E-02	-.241956E-02
.775000E 01	.134362E 01	.485030E-02	-.443392E-02	.203379E-02	-.191281E-02
.800000E 01	.134471E 01	.385674E-02	-.354677E-02	.160767E-02	-.151187E-02
.825000E 01	.134557E 01	.306247E-02	-.283355E-02	.127090E-02	-.119477E-02
.850000E 01	.134625E 01	.242827E-02	-.226124E-02	.100478E-02	-.944052E-03
.875000E 01	.134679E 01	.192240E-02	-.180277E-02	.794517E-03	-.745865E-03
.900000E 01	.134722E 01	.151927E-02	-.143606E-02	.628402E-03	-.589235E-03
.925000E 01	.134756E 01	.119825E-02	-.114311E-02	.497175E-03	-.465465E-03
.950000E 01	.134783E 01	.942797E-03	-.909378E-03	.393516E-03	-.367674E-03
.975000E 01	.134804E 01	.739627E-03	-.723081E-03	.311636E-03	-.290417E-03
.100000E 02	.134820E 01	.578109E-03	-.574733E-03	.246963E-03	-.229385E-03
.102500E 02	.134833E 01	.449745E-03	-.456702E-03	.195881E-03	-.181175E-03
.105000E 02	.134843E 01	.347751E-03	-.362864E-03	.155535E-03	-.143094E-03
.107500E 02	.134850E 01	.266714E-03	-.288308E-03	.123670E-03	-.113016E-03
.110000E 02	.134856E 01	.202323E-03	-.229108E-03	.985032E-04	-.892592E-04
.112500E 02	.134860E 01	.151147E-03	-.182128E-03	.786266E-04	-.704956E-04
.115000E 02	.134864E 01	.110544E-03	-.144861E-03	.629285E-04	-.556760E-04
.117500E 02	.134866E 01	.870759E-04	-.115313E-03	.505304E-04	-.439715E-04
.120000E 02	.134868E 01	.522890E-04	-.918946E-04	.407388E-04	-.347275E-04
.122500E 02	.134869E 01	.317253E-04	-.733399E-04	.330050E-04	-.274268E-04
.125000E 02	.134869E 01	.152991E-04	-.586438E-04	.268981E-04	-.216609E-04

PR=.7,DY=.25,M=50,EIGEN(1)=.859348,-.370234,DX(1)=1.E-4,1.E-4,

EPSI=1.E-6,FPRNT=1,FREQ=1,STEP=100,CONST=01*

TEMPERATURE DRIVEN NATURAL CONVECTION AROUND TWO DIMENSIONAL, BLUNT NOSED OBJECTS, FIRST ORDER TERMS

Table with columns Y, (F1), (F1)', (F1)'', (T1), (T1)'. Rows range from 0.00000E 00 to 1.25000E 02. Includes parameters R=70000, M=250000, M=50.

PR=.7,DY=.25,M=50,EVAL(1)=.8593292,-.3702356,EIGEN(1)=.C92125,.C3225,

DX(1)=1.E-3,1.E-3,EPSI=1.E-6,STEPSP=100,FREQ=1,FPRAT=1,

CONST=1.0

TEMPERATURE DRIVEN NATURAL CONVECTION AROUND TWO DIMENSIONAL, BLUNT NOSED OBJECTS, ZERO ORDER TERMS

Table with columns Y, (F0), (F0)', (F0)'', (T0), (T0)'. Rows range from 0.00000E 00 to 1.25000E 02. Includes parameters PR=1.000000, DY=.250000, M=50.

PR=1.0,DY=.25,EIGEN(1)=.8,-.4,DX(1)=.01,.01,M=50,EPSI=1.E-5,FPRAT=1,

PR=1.0,STEPSP=100,CONST=1.0

TEMPERATURE DRIVEN NATURAL CONVECTION AROUND TWO DIMENSIONAL, FLAT NOSED OBJECTS. ZERO ORDER TERMS

PR = 1.000000, DY = .250000, M = 50

Y	(FO)	(FO)*	(FO)**	(TO)	(TO)*
.00000E 00	.00000E 00	.00000E 00	.793325E 00	.100000E 01	-.413137E 00
.25000E 00	.222715E-01	.168302E 00	.358901E 00	.896769E 00	-.412352E 00
.50000E 00	.796384E-01	.282274E 00	.359782E 00	.794184E 00	-.407377E 00
.75000E 00	.159695E 00	.351463E 00	.200270E 00	.693665E 00	-.395516E 00
.10000E 01	.252461E 00	.385525E 00	.782030E-01	.597097E 00	-.375724E 00
.12500E 01	.350286E 00	.393318E 00	-.107193E-01	.506432E 00	-.348471E 00
.15000E 01	.447583E 00	.382473E 00	-.718229E-01	.423352E 00	-.315377E 00
.17500E 01	.540506E 00	.359259E 00	-.110559E 00	.349044E 00	-.278701E 00
.20000E 01	.626607E 00	.328623E 00	-.132005E 00	.284101E 00	-.240830E 00
.22500E 01	.704522E 00	.294316E 00	-.140612E 00	.228551E 00	-.203879E 00
.25000E 01	.773694E 00	.259067E 00	-.140113E 00	.181950E 00	-.169451E 00
.27500E 01	.834140E 00	.224759E 00	-.133521E 00	.143528E 00	-.138575E 00
.30000E 01	.886259E 00	.192612E 00	-.123182E 00	.112325E 00	-.111742E 00
.32500E 01	.930689E 00	.163328E 00	-.110857E 00	.873135E-01	-.890262E-01
.35000E 01	.968192E 00	.137239E 00	-.978135E-01	.674874E-01	-.702065E-01
.37500E 01	.999581E 00	.114406E 00	-.849222E-01	.519188E-01	-.548915E-01
.40000E 01	.102566E 01	.947156E-01	-.727439E-01	.397895E-01	-.426109E-01
.42500E 01	.104718E 01	.779451E-01	-.616058E-01	.304015E-01	-.328821E-01
.45000E 01	.106485E 01	.638115E-01	-.516664E-01	.231744E-01	-.252510E-01
.47500E 01	.107928E 01	.520077E-01	-.429671E-01	.176356E-01	-.193134E-01
.50000E 01	.109102E 01	.422270E-01	-.354717E-01	.134060E-01	-.147239E-01
.52500E 01	.110054E 01	.341781E-01	-.290973E-01	.101858E-01	-.111954E-01
.55000E 01	.110823E 01	.275938E-01	-.237353E-01	.773981E-02	-.849424E-02
.57500E 01	.111444E 01	.222359E-01	-.192470E-01	.588561E-02	-.643366E-02
.60000E 01	.111944E 01	.178957E-01	-.155734E-01	.448218E-02	-.486615E-02
.62500E 01	.112346E 01	.143941E-01	-.125415E-01	.342127E-02	-.367643E-02
.65000E 01	.112669E 01	.115785E-01	-.100683E-01	.262011E-02	-.277507E-02
.67500E 01	.112929E 01	.932112E-02	-.806160E-02	.201558E-02	-.209318E-02
.70000E 01	.113139E 01	.751556E-02	-.644139E-02	.155973E-02	-.157792E-02
.72500E 01	.113308E 01	.607402E-02	-.513886E-02	.121618E-02	-.118894E-02
.75000E 01	.113445E 01	.492458E-02	-.409577E-02	.957362E-03	-.895507E-03
.77500E 01	.113556E 01	.400864E-02	-.326337E-02	.762453E-03	-.674285E-03
.80000E 01	.113647E 01	.327876E-02	-.260120E-02	.615711E-03	-.507585E-03
.82500E 01	.113721E 01	.269647E-02	-.207596E-02	.505259E-03	-.382019E-03
.85000E 01	.113783E 01	.223167E-02	-.166043E-02	.422137E-03	-.287467E-03
.87500E 01	.113834E 01	.185919E-02	-.133247E-02	.359593E-03	-.216287E-03
.90000E 01	.113876E 01	.155966E-02	-.107420E-02	.312538E-03	-.162713E-03
.92500E 01	.113912E 01	.131751E-02	-.871216E-03	.277140E-03	-.122397E-03
.95000E 01	.113943E 01	.112042E-02	-.711984E-03	.250514E-03	-.920626E-04
.97500E 01	.113968E 01	.958652E-03	-.587286E-03	.230488E-03	-.692414E-04
.10000E 02	.113991E 01	.824522E-03	-.489790E-03	.215426E-03	-.520742E-04
.10250E 02	.114010E 01	.711985E-03	-.413674E-03	.204099E-03	-.391513E-04
.10500E 02	.114026E 01	.616294E-03	-.354332E-03	.195581E-03	-.294491E-04
.10750E 02	.114041E 01	.533730E-03	-.308127E-03	.189175E-03	-.221447E-04
.11000E 02	.114053E 01	.461379E-03	-.272194E-03	.184359E-03	-.166515E-04
.11250E 02	.114064E 01	.396968E-03	-.244281E-03	.180737E-03	-.125206E-04
.11500E 02	.114073E 01	.338721E-03	-.222622E-03	.178014E-03	-.941422E-05
.11750E 02	.114081E 01	.285254E-03	-.205831E-03	.175966E-03	-.707840E-05
.12000E 02	.114087E 01	.235491E-03	-.192827E-03	.174427E-03	-.532205E-05
.12250E 02	.114093E 01	.188597E-03	-.182765E-03	.173269E-03	-.400143E-05
.12500E 02	.114097E 01	.143920E-03	-.174985E-03	.172399E-03	-.306848E-05

PR=1.,DY=.25,M=50,EIGEN(1)=.803875,-.41,DX(1)=1.E-4,1.E-4,EP51=1.E-5,

STEP5M=100,FREQ=1,FPRINT=1,CONST=1.*

TEMPERATURE DRIVEN NATURAL CONVECTION AROUND TWO DIMENSIONAL, BLUNT NOSED OBJECTS. ZERO ORDER TERM

PR = 1000.000000, DY = .025000, M = 800

Y	(FO)	(FO)*	(FO)**	(TO)	(TO)*
.00000E 00	.000000E 00	.000000E 00	.195437E 00	.100000E 01	-.305843E 01
.50000E 00	.110020E-01	.294013E-01	.576291E-02	.273404E-01	-.330116E 00
1.00000E 00	.262306E-01	.313834E-01	.347001E-02	.199360E-02	-.314492E-04
.15000E 01	.423335E-01	.329840E-01	.293805E-02	.199245E-02	-.142344E-11
.20000E 01	.591717E-01	.343273E-01	.244120E-02	.199245E-02	-.786988E-22
.25000E 01	.766208E-01	.354310E-01	.197942E-02	.199245E-02	-.669928E-33
.30000E 01	.945555E-01	.363124E-01	.155216E-02	.199245E-02	-.113677E-37
.35000E 01	.112899E 00	.369847E-01	.115835E-02	.199245E-02	-.113677E-37
.40000E 01	.131523E 00	.374761E-01	.796547E-03	.199245E-02	-5.226785E-39
.45000E 01	.150346E 00	.377902E-01	.464962E-03	.199245E-02	-5.226785E-39
.50000E 01	.169286E 00	.379457E-01	.161596E-03	.199245E-02	-5.226785E-39
.55000E 01	.188267E 00	.379561E-01	-.115700E-03	.199245E-02	-5.226785E-39
.599999E 01	.207220E 00	.378399E-01	-.369150E-03	.199245E-02	-5.226785E-39
.649999E 01	.226081E 00	.375905E-01	-.600987E-03	.199245E-02	-5.226785E-39
.699999E 01	.244792E 00	.372361E-01	-.813396E-03	.199245E-02	-5.226785E-39
.749999E 01	.263300E 00	.367800E-01	-.100847E-02	.199245E-02	-5.226785E-39
.799999E 01	.281556E 00	.362302E-01	-.118818E-02	.199245E-02	.000000E 00
.849999E 01	.299516E 00	.355940E-01	-.135433E-02	.199245E-02	.000000E 00
.899999E 01	.317137E 00	.348778E-01	-.150857E-02	.199245E-02	.000000E 00
.949999E 01	.334381E 00	.340871E-01	-.165235E-02	.199245E-02	.000000E 00
.999999E 01	.351212E 00	.332269E-01	-.178696E-02	.199245E-02	.000000E 00
.105000E 02	.367596E 00	.323015E-01	-.191391E-02	.199245E-02	.000000E 00
.110000E 02	.383503E 00	.313146E-01	-.203291E-02	.199245E-02	.000000E 00
.115000E 02	.398901E 00	.302696E-01	-.214596E-02	.199245E-02	.000000E 00
.120000E 02	.413763E 00	.291695E-01	-.225327E-02	.199245E-02	.000000E 00
.125000E 02	.428062E 00	.280172E-01	-.235537E-02	.199245E-02	.000000E 00
.130000E 02	.441772E 00	.268149E-01	-.245263E-02	.199245E-02	.000000E 00
.135000E 02	.454889E 00	.255653E-01	-.254535E-02	.199245E-02	.000000E 00
.140000E 02	.467329E 00	.242703E-01	-.263375E-02	.199245E-02	.000000E 00
.145000E 02	.479131E 00	.229322E-01	-.271796E-02	.199245E-02	.000000E 00
.150000E 02	.490254E 00	.215530E-01	-.279807E-02	.199245E-02	.000000E 00
.155000E 02	.500678E 00	.201348E-01	-.287412E-02	.199245E-02	.000000E 00
.159999E 02	.510382E 00	.186795E-01	-.294610E-02	.199245E-02	.000000E 00
.164999E 02	.519351E 00	.171893E-01	-.301399E-02	.199245E-02	.000000E 00
.169999E 02	.527566E 00	.156662E-01	-.307773E-02	.199245E-02	.000000E 00
.174999E 02	.535012E 00	.141123E-01	-.313727E-02	.199245E-02	.000000E 00
.179999E 02	.541673E 00	.125296E-01	-.319252E-02	.199245E-02	.000000E 00
.184999E 02	.547536E 00	.109205E-01	-.324339E-02	.199245E-02	.000000E 00
.189999E 02	.552589E 00	.928679E-02	-.328980E-02	.199245E-02	.000000E 00
.194999E 02	.556819E 00	.763142E-02	-.333165E-02	.199245E-02	.000000E 00
.199999E 02	.560217E 00	.595610E-02	-.336885E-02	.199245E-02	.000000E 00

PR=1000.,DY=.025,M=800,EIGEN(1)=.19575,-3.05984,DX(1)=.01,.01,

EP51=1.E-4,STEP5M=100,FREQ=20,FPRINT=1,CONST=1000.*

TEMPERATURE AND CONCENTRATION DRIVEN NATURAL CONVECTION AROUND TWO DIMENSIONAL BLUNT NOSED OBJECTS

ZERO ORDER TERMS

Table with columns: PR, SC, SIGMAT, SIGMA, A, B, DY, M, Y, (FO), (FO)', (FO)'', (TO), (TO)', (MO), (MO)'. Contains numerical data for various parameters and indices.

SC=1.,PR=1.,SIGMAT=1.,SIGMA=1.,A=0.,B=0.,DY=.5,M=25,EIGEN(1)=1.38,-.5,
-.50,DX(1)=1.F-2,1.F-2,1.E-2,EPSI=1.E-5,STEPSP=100,FPRINT=1,FREQ=1,
CCNST=1.E3

TEMPERATURE AND CONCENTRATION DRIVEN NATURAL CONVECTION AROUND TWO DIMENSIONAL BLUNT NOSED OBJECTS

ZERO ORDER TERMS

Table with columns: PR, SC, SIGMAT, SIGMA, A, B, DY, M, Y, (FO), (FO)', (FO)'', (TO), (TO)', (MO), (MO)'. Contains numerical data for various parameters and indices.

PR=1.,SC=1.,DY=.1,M=25,SIGMAT=1.,SIGMA=1.,DX(1)=1.E-4,1.E-4,1.E-4,
EIGEN(1)=1.372505,-.476189,-.4765149,EPSI=1.E-5,FREQ=3,FPRINT=1,
CCNST=1.E3,STEPSP=100,A=0.,B=0.

TEMPERATURE AND CONCENTRATION DRIVEN NATURAL CONVECTION AROUND TWO DIMENSIONAL BLUNT NOSED OBJECTS

ZERO ORDER TERMS

Table with 8 columns: Y, (FO), (FO)', (FO)'', (TO), (TO)', (MO), (MO)'. Rows range from 0.00000E 00 to 1.23000E 02. Parameters: PR=1.000000, SC=1.000000, SIGMAT=1.000000, SIGMAM=1.000000, A=.000000, B=-.100000, DY=.100000, M=125.

PR=1.,SC=1.,DY=.1,M=125,SIGMAT=1.,SIGMAM=1.,DX(1)=1.E-4,1.E-4,1.E-4,

EIGEN(1)=1.37684,-.529363,-.5306889,EPSI=1.E-5,FREQ=3,FPRNT=1,

CONST=1.E3,STEPSP=100,A=0.,B=-.1*

TEMPERATURE AND CONCENTRATION DRIVEN NATURAL CONVECTION AROUND TWO DIMENSIONAL BLUNT NOSED OBJECTS

ZERO ORDER TERMS

Table with 8 columns: Y, (FO), (FO)', (FO)'', (TO), (TO)', (MO), (MO)'. Rows range from 0.00000E 00 to 1.23000E 02. Parameters: PR=1.000000, SC=1.000000, SIGMAT=1.000000, SIGMAM=1.000000, A=-.100000, B=.100000, DY=.100000, M=125.

PR=1.,SC=1.,DY=.1,M=125,SIGMAT=1.,SIGMAM=1.,DX(1)=1.E-4,1.E-4,1.E-4,

EIGEN(1)=1.379998,-.4755832,-.4769022,EPSI=1.E-5,FREQ=3,FPRNT=1,

CONST=1.E3,STEPSP=100,A=-.1,B=.1*

BIBLIOGRAPHY

- (1) Acrivos, Andreas, "The Asymptotic Form of the Laminar Boundary-Layer Mass-Transfer Rate for Large Interfacial Velocities," J. Fluid Mech., 12, 337 (1962).
- (2) Arden, B., Galler, B., and Graham, R., The Michigan Algorithm Decoder, Univ. of Michigan Computing Center, (Jan. 1963).
- (3) Bird, R. B., Stewart, W. E., and Lightfoot, E. N., Transport Phenomena, John Wiley and Sons, Inc., New York (1960).
- (4) Brindley, J., "An Approximation Technique for Natural Convection in a Boundary Layer," Int. J. Heat Mass Transfer, 6, 1035 (1963).
- (5) Carnahan, Brice, Luther, H. A., and Wilkes, J. O., Applied Numerical Methods, Volume II (preliminary edition), John Wiley and Sons, Inc., New York (1964).
- (6) Churchill, R. V., Complex Variables and Applications, 2nd ed., McGraw-Hill Book Company, Inc., New York (1960).
- (7) Chaing, T., and Kaye, J., On Laminar Free Convection From a Horizontal Cylinder, Proc. 4th Nat'l Congr. of Appl. Mech. (Berkeley), June 1962, pp. 1213-1219.
- (8) Denbigh, K., The Principles of Chemical Equilibrium, Cambridge University Press, Cambridge (1961).
- (9) Ede, A. J., Natural Convection on Vertical Surfaces, (Heat 141), Department of Scientific and Industrial Research, Mechanical Engineering Laboratory, Glasgow, (1956).
- (10) Erdelyi, A., Asymptotic Expansions, Dover Publications, Inc. (1956).
- (11) Gill, W. N., del Casal, E., and Zeh, D. W., "Binary Diffusion and Heat Transfer in Laminar Free Convection Boundary Layers on a Vertical Plate," Int. J. Heat Mass Transfer, 8, 1135 (1965).
- (12) Goertler, H., "A New Series for the Calculations of Steady Laminar Boundary Layer Flows," J. of Math. and Mech., 6, 1 (1957).
- (13) Hellums, J. D., and Churchill, S. W., "Dimensional Analysis and Natural Convection," Chem. Eng. Progr. Symposium Ser., No. 32, 57, 75 (1969).

- (14) Hermann, R., "Wärmeübergang bei freier Strömung am wagrechten Zylinder in zweiatomigen Gasen," VDI Forschungsheft No. 379 (1936). (Also NACA TM 1366).
- (15) Jodlbauer, K., "Das Temperaten-und Geschwindigkeitsfeld um ein geheiztes Rohr bei freier Konvektion," Forsch. Ing.-Wes., 4, 157 (1933).
- (16) LeFevre, E. J., "Laminar Free Convection from a Vertical Plane Surface," Proc. 9th International Congr. of Appl. Mech. (Brussels), 4, 168 (1957).
- (17) Lorenz, L., "On the Conductivity of Metals for Heat and Electricity," Ann. Phys. Chem., 13, 582 (1881).
- (18) Mathers, W. G., Madden, A. J., and Piret, E. L., "Simultaneous Heat and Mass Transfer in Free Convection," IEC, 49, 961 (1957).
- (19) Meksyn, D., New Methods in Laminar Boundary-Layer Theory, Pergamon Press, New York (1961).
- (20) Merk, H. J., "The Macroscopic Equations for Simultaneous Heat and Mass Transfer in Isotropic, Continuous and Closed Systems," Appl. Sci. Res., Sec. A, 8, 73 (1958).
- (21) Nusselt, W., "Wärmeübergang, Diffusion and Verdunstung," ZaMM, 10, 105 (1930). (Also NACA TM 1367.)
- (22) Ostrach, S., "An Analysis of Laminar Free-Convection Flow and Heat Transfer About a Flat Plate Parallel to the Direction of the Generating Body Force," NACA Report 1111 (1953).
- (23) Ostrach, S., "Laminar Flows with Body Forces," in Theory of Laminar Flows; ed. by F. K. Moore, Princeton University Press, Princeton, New Jersey (1964).
- (24) Poots, G., "Laminar Free Convection Near the Lower Stagnation Point on an Isothermal Curved Surface," Int. J. Heat Mass Transfer, 7, 863 (1964).
- (25) Schlichting, H., Boundary Layer Theory, 4th ed., McGraw-Hill Book Company, Inc., New York (1960).
- (26) Schmidt, E. and Beckmann, W., "Das Temperatur-und Geschwindigkeitsfeld vor einer Wärme abgebenden senkrechten Platte bei natürlicher Konvektion," Tech. Mech. u. Thermodynamik, 1, 341, 391 (1930).



- (27) Schmidt, E., "Heat Transfer by Natural Convection," presented as a lecture at the International Heat Transfer Conference, Univ. of Colorado (1961).
- (28) Schutz, G., "Natural Convection Mass-Transfer Measurements on Spheres and Horizontal Cylinders by an Electrochemical Method," Int. J. Heat Mass Transfer, 6, 873 (1963).
- (29) Somers, E. V., "Theoretical Considerations of Combined Thermal and Mass Transfer From a Vertical Plate," J. Appl. Mech., 23, 295 (1956).
- (30) Sparrow, E. M., Minkowycz, W. J., and Eckert, E. R. G., "Transpiration-Induced Buoyancy and Thermal Diffusion-Diffusion-Thermo in a Helium-air Free-Convection Boundary Layer," J. Heat Transfer, C86, 508 (1964).
- (31) van Dyke, M., Perturbation Methods in Fluid Mechanics, Academic Press, New York (1964).
- (32) Yang, K. T., and Jergers, E. W., "First Order Perturbations of Laminar Free Convection Boundary Layers on a Vertical Plate," J. Heat Transfer, C86, 107 (1964).
- (33) Wilde, D. J., Optimum Seeking Methods, Prentice-Hall, Inc., Englewood Cliffs, New Jersey (1964).